

RESTRICTED

COPY NO.  
RM No. E8D23

8



24 AUG 1948

NACA

# RESEARCH MEMORANDUM

PERFORMANCE OF SEVERAL AIR EJECTORS WITH CONICAL MIXING

SECTIONS AND SMALL SECONDARY FLOW RATES

By S. C. Huddleston, H. D. Wilsted, and C. W. Ellis

Flight Propulsion Research Laboratory  
Cleveland, Ohio

CLASSIFICATION CANCELLED

Authority *J. W. Cromley* Date *12/14/53*  
*E010571*  
By *MDA 2/1/54* See *MDA*  
*R7 1991*

CLASSIFIED DOCUMENT

This document contains classified information affecting the National Defense of the United States within the meaning of the Espionage Act, USC 5031 and 5041. Its transmission or the revelation of its contents in any manner to an unauthorized person is prohibited by law. Information so classified may be imparted only to persons in the military and naval services of the United States, appropriate civilian officers and employees of the Federal Government who have a legitimate interest therein, and to United States citizens of known loyalty and discretion who of necessity must be informed thereof.

TECHNICAL  
EDITING  
WAIVED

## NATIONAL ADVISORY COMMITTEE FOR AERONAUTICS

WASHINGTON

July 19, 1948

N A C A LIBRARY

LANGLEY MEMORIAL AERONAUTICAL  
LABORATORY

Langley Field, Va.

RESTRICTED

UNCLASSIFIED

UNCLASSIFIED

NACA RM No. ESD23

~~RESTRICTED~~

NATIONAL ADVISORY COMMITTEE FOR AERONAUTICS

RESEARCH MEMORANDUM

PERFORMANCE OF SEVERAL AIR EJECTORS WITH CONICAL MIXING

SECTIONS AND SMALL SECONDARY FLOW RATES

By S. C. Huddleston, H. D. Wilsted, and C. W. Ellis

SUMMARY

Several ejector configurations were investigated to determine the ability to handle the air required for engine cooling. The results presented are limited to investigations of conical-type mixing-section ejectors at ratios of mixing-section minimum diameter to primary-jet-nozzle diameter of 1.21, 1.10, and 1.00 using unheated air. Results were cross-plotted in charts to show the performance of ejectors with configurations within the range of those investigated.

The experimental results showed that for diameter ratios of 1.21 and 1.10 the spacing giving maximum air flow varied with diameter ratio but did not vary with primary and secondary pressure ratios. Ejector operation at a diameter ratio of 1.00 was comparatively critical and use of diameter ratios close to 1.00 should be avoided. The ejectors investigated conducted secondary air flows of less than 15 percent of the primary air flow when the secondary pressure ratio was less than or equal to 1.0; in general, the thrust obtained by use of a conical-mixing-section ejector varied only slightly from that developed by the primary jet alone but a small decrease in thrust was noted with configurations having a large spacing between the primary-jet exit and the mixing-section exit.

INTRODUCTION

Temperature limitations in the development of high-performance turbojet engines and in the development of thrust augmentation by such means as tail-pipe burning are of concern at the present stage of jet-engine development. The air ejector as a simple, light-weight unit for pumping cooling air is promising as a solution to high-temperature problems. The ejector as a pumping device and as a thrust augmentor has been the subject of numerous investigations, both theoretical and experimental.

~~RESTRICTED~~

UNCLASSIFIED

Methods of theoretical analysis of ejectors are developed in references 1 and 2; reference 1 also presents results of investigations of ejectors having ratios of mixing-section minimum diameter to primary-jet-nozzle diameter  $D_s/D_p$  from approximately 15.5 to 23.5 with straight mixing sections after the conical mixing section. Other investigations have been made with conical-mixing-section ejectors having smaller diameter ratios. In general, however, the available ejector data apply to ejectors having diameter ratios too large to make them applicable to turbojet cooling problems.

In order to extend the range of existing performance data and to determine means of applying model-ejector data to the design of full-scale ejectors, the NACA Cleveland laboratory is conducting an experimental and analytical investigation of cooling-air ejectors. The purpose of this investigation is to establish the performance of various ejector configurations capable of pumping small quantities of secondary air (from 5 to 30 percent of the quantity discharged by the primary-jet nozzle) and to correlate the results with ejector theory. Experimental performance data obtained with model ejectors having conical mixing sections and diameter ratios of 1.21, 1.10, and 1.00 over a range of primary pressure ratios  $P_p/P_0$  and secondary pressure ratios  $P_s/P_0$  are presented. In order to minimize the scale effect, the model ejectors were made as large as possible (primary-jet diameter, 4.0 in.), being limited only by the available air capacity. This type of ejector, although somewhat less efficient in performance than some configurations, is of interest in that it is simple to construct, is more durable than many other configurations, and adapts itself well to nacelle and to rear-fuselage installations. The investigation was conducted with a conical primary-jet nozzle having a discharge diameter of 4 inches. The air was unheated. The ejector nomenclature used herein is defined in figure 1.

#### APPARATUS

The apparatus used for the model-ejector investigation is schematically shown in figure 2. The high-velocity air of the primary jet discharges into the mixing section and induces secondary flow through the concentric mixing section. The performance of an ejector can be evaluated by measuring the amount of secondary air flow induced and the increase in thrust due to the secondary flow at various combinations of primary-total-pressure ratio and secondary-pressure ratio.

986  
The primary and secondary systems are so separated as to permit measurement of the flow through each and to control independently the total pressures. In both systems, air flow is measured by standard A.S.M.E. sharp-edged orifices. Temperatures are measured by iron-constantan thermocouples and a potentiometer. For the primary-jet nozzle, the temperature and total-pressure measuring station is located 4 diameters upstream of the primary-nozzle exit and the secondary measuring station is fixed 17 inches upstream of the primary-jet-nozzle exit. The temperatures of both the primary  $T_p$  and secondary  $T_s$  air supply were approximately  $80^\circ$  F during these investigations. Thrust is measured by a balanced-diaphragm-type measuring device.

The model air ejectors are made as large as the available air capacity will allow in order to minimize the scale effect. The primary-jet nozzle is a conical section with a  $15^\circ$  half-cone angle  $\alpha$ , an exit diameter of 4.0 inches, and an approach pipe with a 5.0-inch inside diameter. The conical mixing section has a  $15^\circ$  half-cone angle and a 10.0-inch-diameter approach pipe. Changes in the spacing between the exit of the primary-jet nozzle and that of the secondary mixing section were made by inserting straight flanged spacers in the approach pipe ahead of the conical mixing section.

## RESULTS AND DISCUSSION

### Experimental Data

The effect of primary pressure ratio  $P_p/p_0$  and secondary pressure ratio  $P_s/p_0$  on indicated secondary weight flow  $W_s$  for a fixed configuration is of great significance. Figure 3 presents ejector-characteristic curves that are typical of the conical-type mixing-section ejectors investigated. These curves show the variation of secondary weight flow with primary pressure ratio for several secondary pressure ratios. At a primary pressure ratio of 1, (no primary flow), the secondary weight flow is a function of secondary pressure ratio alone. With secondary pressure ratios greater than 1, increasing the primary pressure ratio rapidly blocks the secondary flow, which had been using the total flow area. With secondary pressure ratios less than 1, however, increasing the primary pressure ratio progressively blocks the backward flow through the secondary mixing section (not shown in fig. 3) until a positive secondary flow is obtained.

The secondary weight flow reaches a peak value and then decreases with further increases in primary pressure ratio for the two smaller-diameter-ratio ejectors. This trend is apparently caused by a change in the primary-jet-stream configuration, which progressively fills more of the mixing-section flow area thereby blocking, to varying degrees, the secondary flow.

This phenomenon occurred quite consistently in the experiments but with varying effectiveness, being less effective at larger diameter ratios. For example, the 1.21 diameter-ratio ejector (fig. 3(a)) shows only a slight over-all blocking effect between primary pressure ratios of 1.8 and 2.0; whereas the secondary weight flow for the 1.00-diameter-ratio ejector (fig. 3(c)) rapidly decreases to zero slightly beyond a primary pressure ratio of 1.8. Figure 4 shows a plot of secondary weight flow  $W_s$  against primary weight flow  $W_p$  for secondary pressure ratio of 1.000 for the configurations of figure 3.

#### Generalization of Experimental Data

The data for each configuration are plotted nondimensionally in figures 5 to 7. Because the model was comparatively large, the model data can probably be applied to ejectors of various sizes with negligible scale effect. These curves present secondary-to-primary-weight-flow ratio  $W_s/W_p$  hereinafter designated weight-flow ratio plotted against primary pressure ratio for a series of secondary pressure ratios. Theoretically, the curves of weight-flow ratio at secondary pressure ratios greater or less than 1 extend to positive and negative infinity, respectively, as the primary pressure ratio decreases to 1.0. These phenomena are indicated in figures 5 to 7 by the rapid rise in weight-flow ratio that accompanies decrease in primary pressure ratio at secondary pressure ratios greater than 1.0 and by the decrease in weight-flow ratio that occurs when the secondary pressure ratio is less than 1. For a secondary pressure ratio of 1.0, however, as the primary pressure ratio approaches 1.0, the weight-flow ratio approaches a value of the slope of the curve at zero as shown in figure 4.

#### Spacing for Maximum Weight-Flow Ratio

Figure 8 consists of cross plots of figures 5 to 7 showing weight-flow ratio plotted against spacing  $S/D_p$  at various secondary pressure ratios and various primary pressure ratios. With a diameter ratio of 1.21 or 1.10, as shown in figures 8(a) and 8(b), the spacing that produces maximum weight-flow ratio is unchanged by change in secondary pressure ratio or in primary pressure ratio.

At a diameter ratio of 1.00, however, the spacing appears to be much more critical, as shown in figure 8(c). There is a slight decrease in spacing for maximum weight-flow ratio with decreasing secondary pressure ratio and a definite decrease in this spacing with increasing primary pressure ratio. For the secondary pressure ratios of 1.000 and 0.985 at a diameter ratio of 1.00, the secondary weight-flow under most conditions was so small that a high degree of accuracy was unobtainable with the apparatus used. Therefore, the weight-flow ratios indicated in figure 8(b) for secondary pressure ratios less than 1.050 are questionable. The curves show, however, the approximate weight-flow ratios to be expected and give an indication of the critical operation of ejectors at the diameter ratio of 1.00. The range of spacings for positive ejector pumping action decreases and shifts to smaller spacings with decreasing diameter ratio. At a diameter ratio of 1.00 (fig. 8(c)), the range also decreases with increasing primary pressure ratio and decreasing secondary pressure ratio; therefore, the spacing for an ejector design of this diameter ratio must be carefully selected to insure positive pumping action at all operating points over a range of pressure conditions. This relation further emphasizes the fact that ejector operation at a diameter ratio of 1.00 is comparatively critical and should be avoided on turbojet-engine installations.

### Ejector Thrust

The effect of the use of an ejector located within the spacing range for maximum weight-flow ratio on total thrust is shown in figure 9. The solid line is the curve of thrust developed by the primary-jet nozzle alone and is plotted against primary pressure ratio. The data points represent values of thrust obtained with ejector configurations of diameter ratios of 1.21, 1.10, and 1.00 at several secondary pressure ratios. The plot indicates a slight decrease in thrust from use of the ejectors. The effect on thrust of varying the spacing of ejectors having diameter ratios of 1.21, 1.10, and 1.00 are shown in figures 10(a), 10(b), and 10(c), respectively. These curves indicate a decrease in thrust with an increase in spacing. At small spacings and some pressure conditions, total thrust is slightly greater than primary thrust. In general, however, the conical nozzle ejector has little effect on jet thrust.

### Ejector Configurations for Constant

#### Weight-Flow Ratio

Charts were constructed from figure 8 to show the variation of spacing  $S/D_p$  with diameter ratio  $D_s/D_p$  for constant weight-flow

ratio  $W_s/W_p$  (fig. 11). Each chart has been plotted for one particular primary pressure ratio  $P_p/p_0$  and one secondary pressure ratio  $P_s/p_0$ .

The lines of constant weight-flow ratio  $W_s/W_p$  define a series of ejector configurations that will pump a particular weight-flow ratio under the stated primary and secondary pressure conditions. There is a minimum value of diameter ratio and of spacing that will pump each value of weight-flow ratio. In figure 11(a), lines of minimum diameter ratio and minimum spacing have been drawn through the respective minimum points.

The ejector configurations bounded by the lines of minimum diameter ratio and minimum spacing are the configurations that will, in general, be of interest to ejector designers. Within this region the designer has a certain amount of latitude in the selection of spacing and diameter ratio for a particular value of weight-flow ratio. Reduction in the required spacing can be obtained by increasing the diameter ratio the proper amount; the inverse is also true. Outside of this range of configurations, however, both diameter ratio and spacing must be increased to obtain a particular value of weight-flow ratio.

At some pressure conditions, particularly those of higher secondary pressure ratios, the configurations at minimum spacing were not reached within the range of diameter ratios and positive spacings investigated. The charts, however, indicate that the designer can make considerable reduction in spacing from that used at the minimum diameter ratio.

### Selection of Ejector Design

Considerable reduction in spacing from spacing at minimum diameter ratio can be realized by increasing the diameter ratio (fig. 11). In airplane installations, use of ejectors with the minimum spacing is desirable because of space limitations and also because the smaller spacings provide the least loss in thrust. Design limitations determine the amount of increase in diameter ratio that can be allowed in order to obtain reduction in spacing.

In addition, consideration must be given to the performance of the ejector at several operating conditions, particularly if several critical conditions exist around which the ejector must be designed. The pumping characteristics over a range of pressure conditions can be varied to a limited extent by selection of spacing and diameter ratio. An example of variation in pumping characteristics that can be obtained

with two ejectors that pump the same weight flow at a particular design operating condition is given in figure 12. One configuration is the minimum-diameter-ratio configuration and the other is at the minimum-spacing configuration. Figure 12(a) shows the variation of the weight-flow ratio with secondary pressure ratio  $P_s/p_0$  for the two configurations, and 12(b) shows the weight-flow ratio plotted against primary pressure ratio  $P_p/p_0$ . Both plots indicate that the ejector at minimum spacing gives the least deviation in weight-flow ratio from that at the design pressure condition.

### SUMMARY OF RESULTS

Performance investigations were conducted ON model conical-mixing-section ejectors with ratios of mixing-section minimum diameter to primary-jet-nozzle diameter of 1.21, 1.10, and 1.00, and several axial spacings, using unheated air. Results were cross-plotted in order to show the performance of ejectors with configurations within the range of those investigated. The ejectors investigated conducted secondary air flows of about 15 percent of the primary flow when the secondary pressure ratio was less than or equal to 1.0. In general, the net thrust of the ejector was negligibly different from the thrust of the primary jet alone.

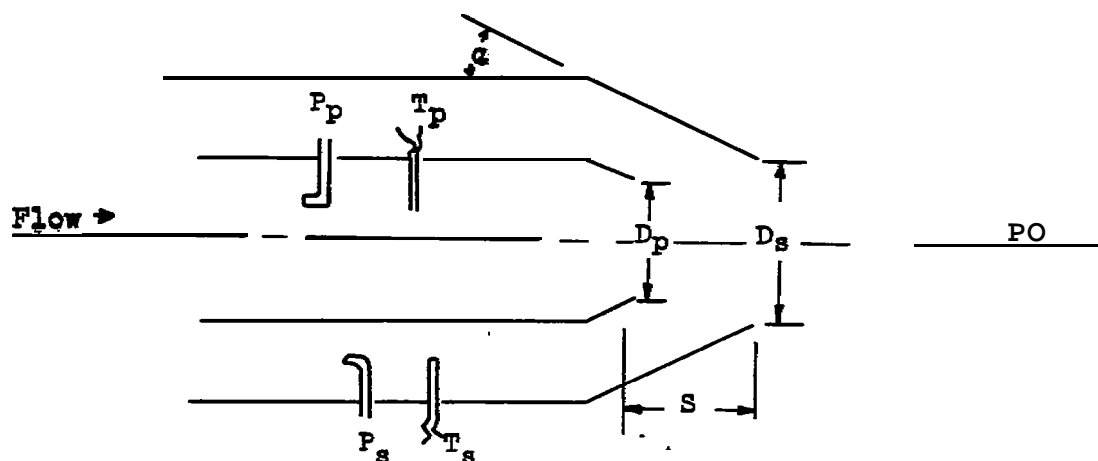
The ejector spacing required to pump maximum weight flow was independent of primary and secondary pressure ratios for diameter ratios of 1.21 and 1.10. The spacing for the 1.00-diameter-ratio ejector varied considerably with primary pressure ratio and to a lesser extent with secondary pressure ratio. The range of spacings giving measurable secondary weight flows decreased rapidly with decrease in diameter ratio to an extremely narrow useful spacing range at a diameter ratio of 1.00. The narrow range of usable spacings and the variation of ejector effectiveness with change in primary and secondary pressure ratio indicated that operation of the 1.00-diameter-ratio ejector was very critical. The use of ejectors with diameter ratios near 1.00 should therefore be avoided. The larger the diameter ratio the less sensitive the ejector was to operational and constructional variables.

Flight Propulsion Research Laboratory,  
National Advisory Committee for Aeronautics,  
Cleveland, Ohio.



## REFERENCES

1. Morrison, Reeves: Jet Ejectors and Augmentation. NACA ACR, Sept. 1942.
2. Keenan, J. H., and Neuman, E. P.: A Simple Air Ejector. Jour. Appl. Mech., vol. 9, no. 2, June 1942, pp. A75-A81.



$D_p$  exit diameter of primary nozzle

$D_s$  exit diameter of mixing section

$P_p$  total primary pressure

$P_s$  total secondary pressure

$P_0$  ambient pressure

$S$  distance from primary exit to mixing-section exit

$T_p$  primary air temperature,  $^{\circ}\text{F}$

$T_s$  secondary air temperature,  $^{\circ}\text{F}$

$W_p$  primary weight flow, lb/sec

$W_s$  secondary weight flow, lb/sec

$\alpha$  half-cone angle, deg

$P_p/P_0$  primary pressure ratio

$P_s/P_0$  secondary pressure ratio



Figure 1. - Nomenclature for jet injector with conical mixing sections.

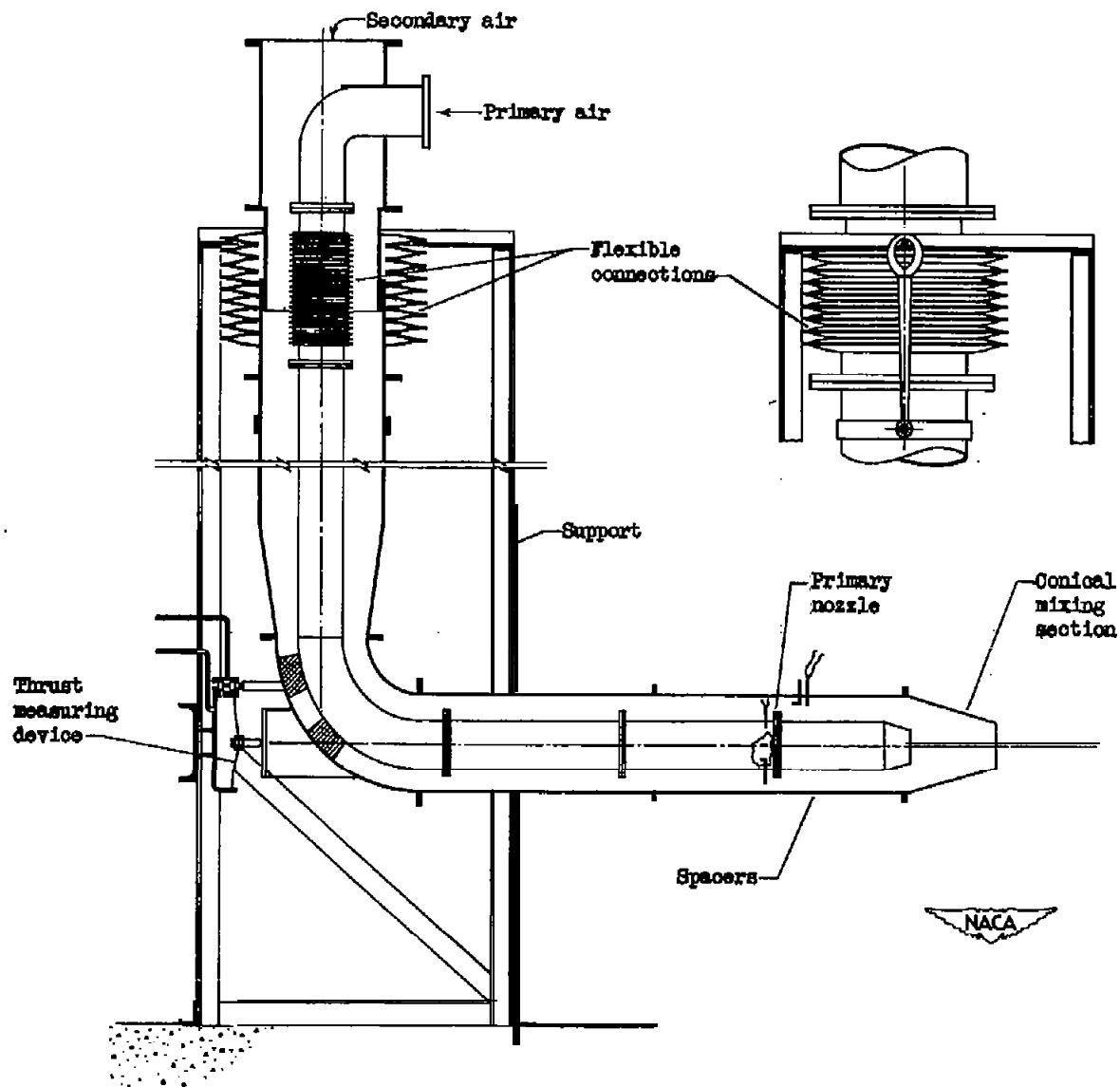
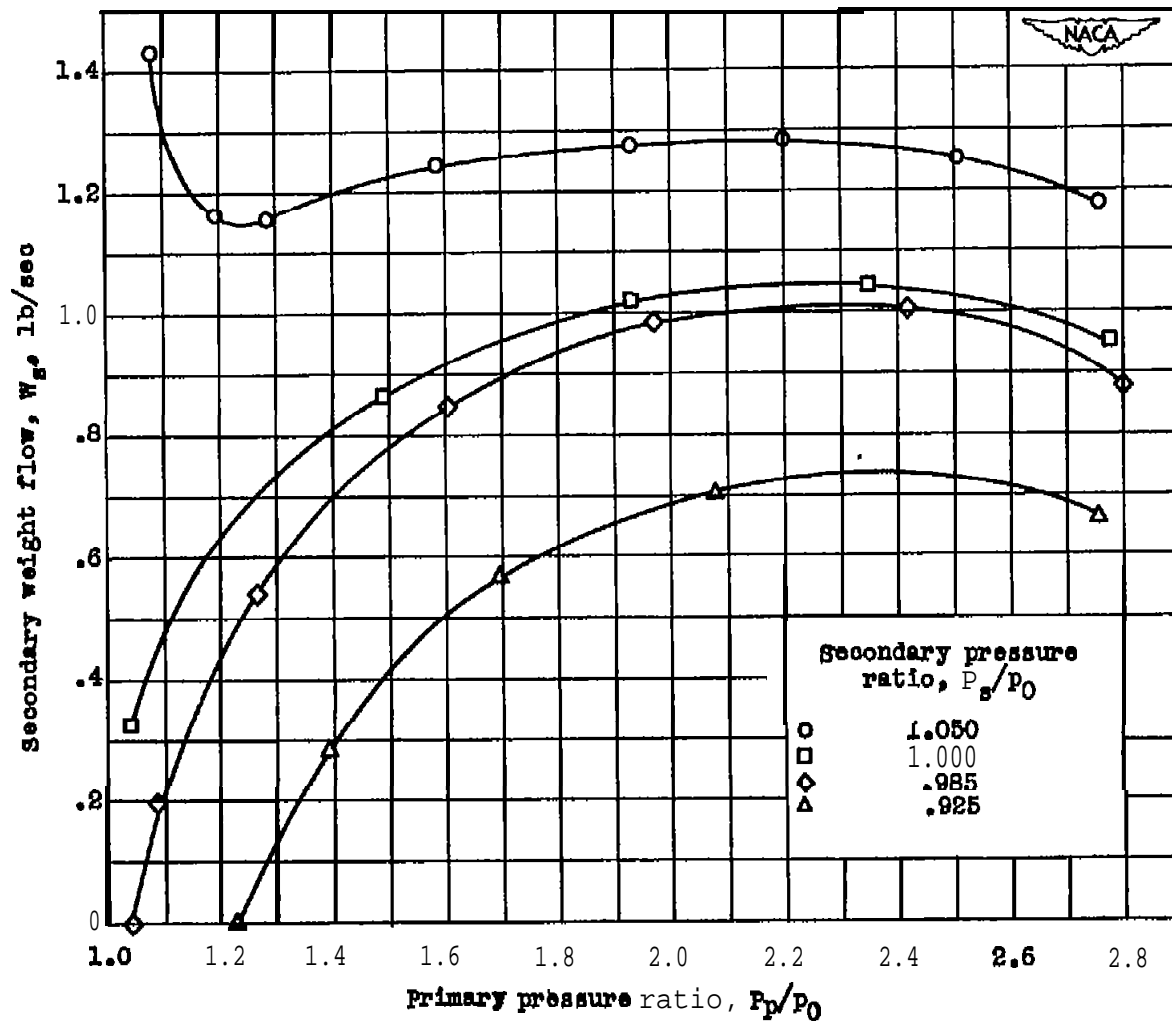
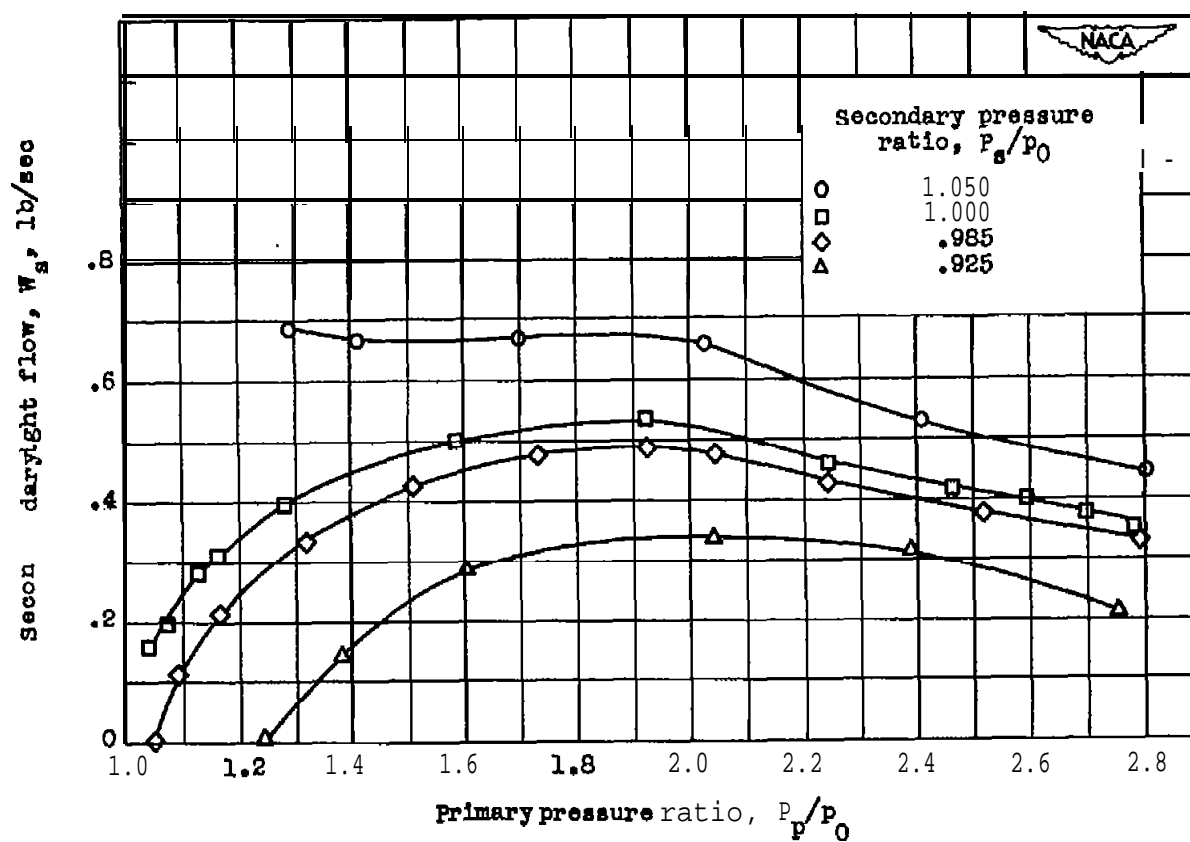


Figure 2. - Schematic diagram of model setup for ejector investigation.



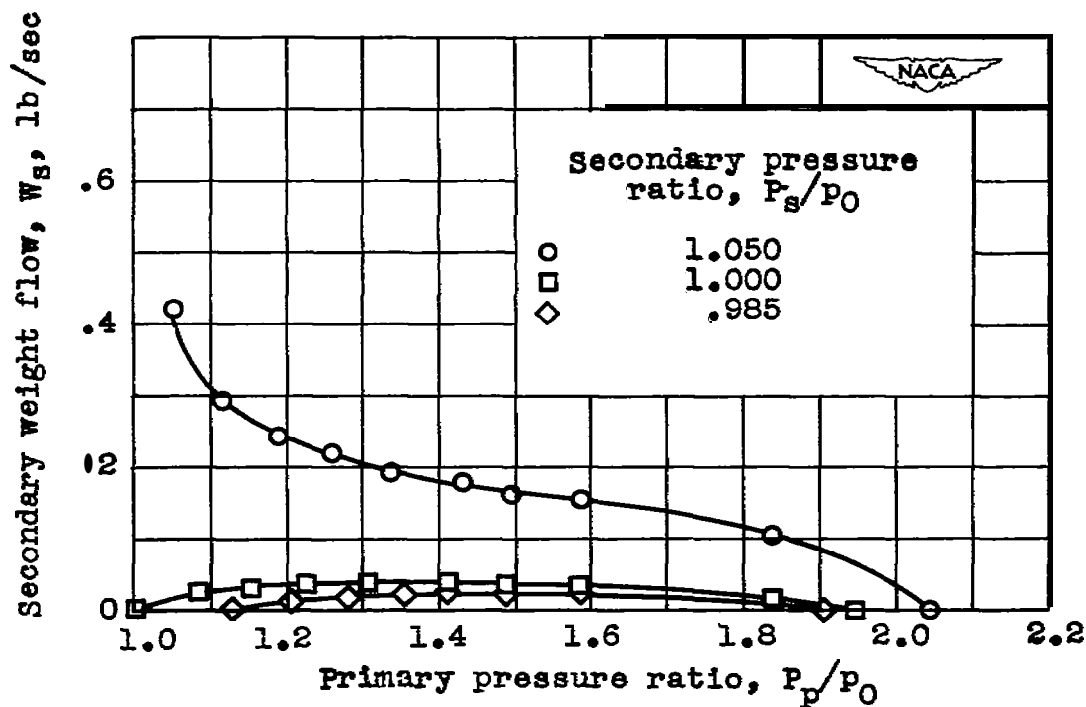
(a) Spacing  $S/D_p$ , 1.790; diameter ratio  $D_s/D_p$ , 1.21.

Figure 3. - Effect of primary and secondary pressure ratios on induced secondary weight flow for conical-mixing-section ejector. Secondary-to-primary-air temperature ratio  $T_s/T_p$ , 1.0.



(b) Spacing  $S/D_p$ , 1.100; diameter ratio  $D_s/D_p$ , 1.10.

Figure 3. - continued. Effect of primary and secondary pressure ratios on induced secondary weight flow for conical-mixing-section ejector. Secondary-to-primary-air temperature ratio  $T_s/T_p$ , 1.0.



(c) Spacing  $S/D_p$ , 0.440; diameter ratio  $D_s/D_p$ , 1.00.

Figure 3. - Concluded. Effect of primary and secondary pressure ratios on induced secondary weight flow for conical-mixing-section ejector. Secondary-to-primary-air temperature ratio  $T_s/T_p$ , 1.0.

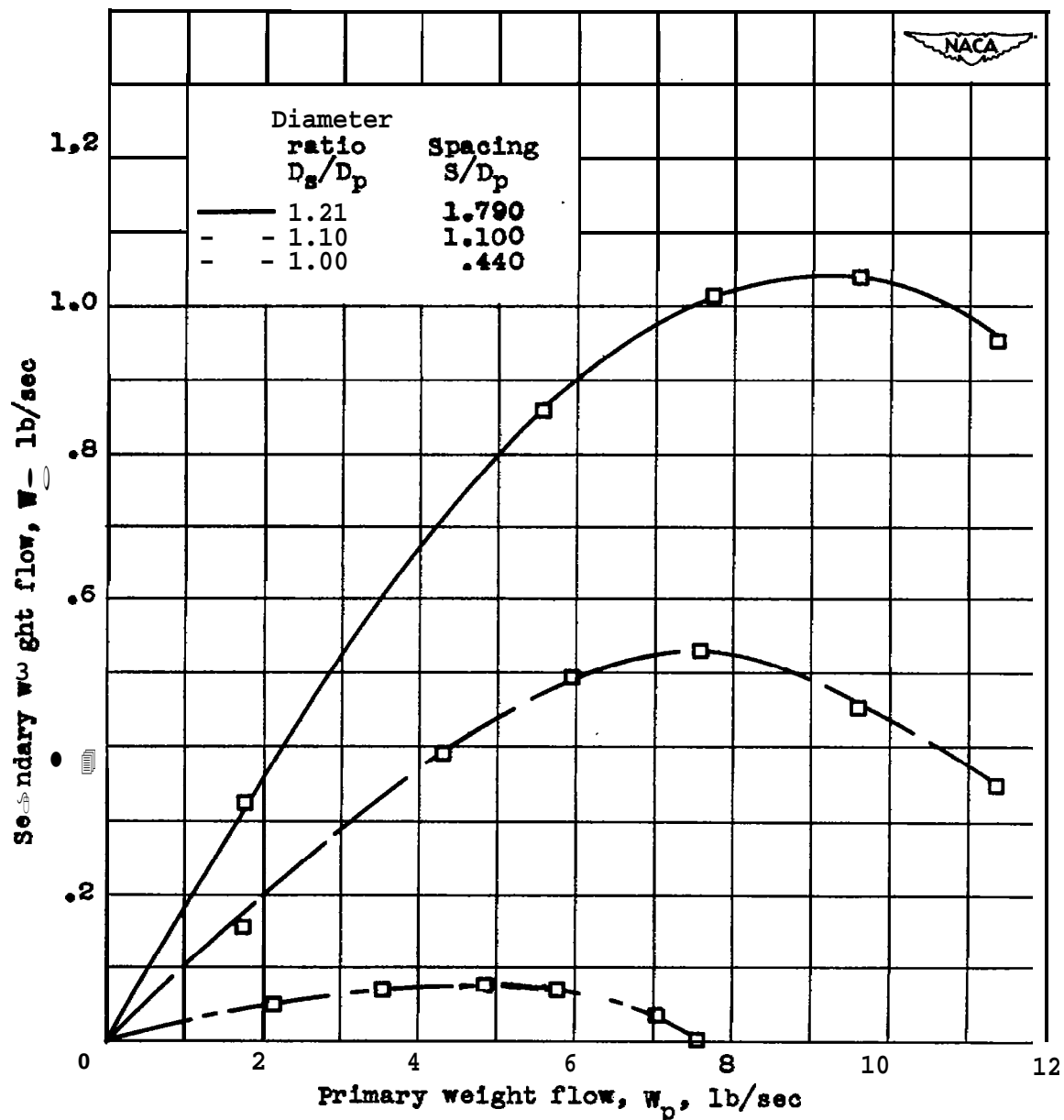
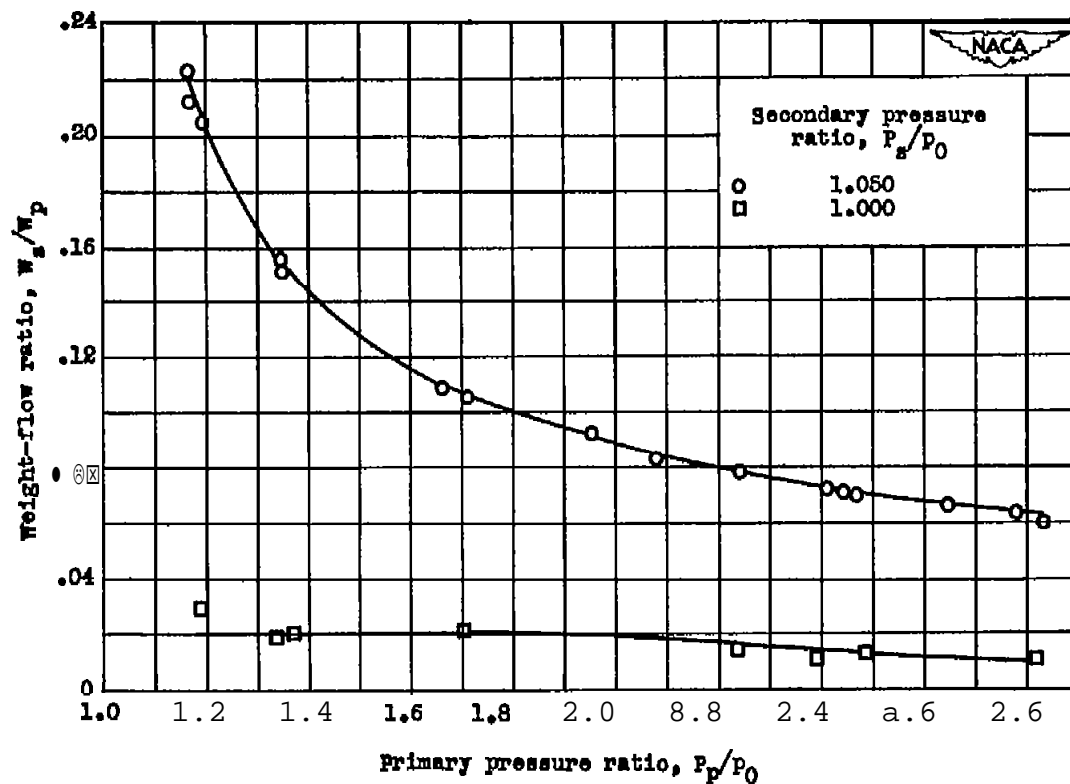


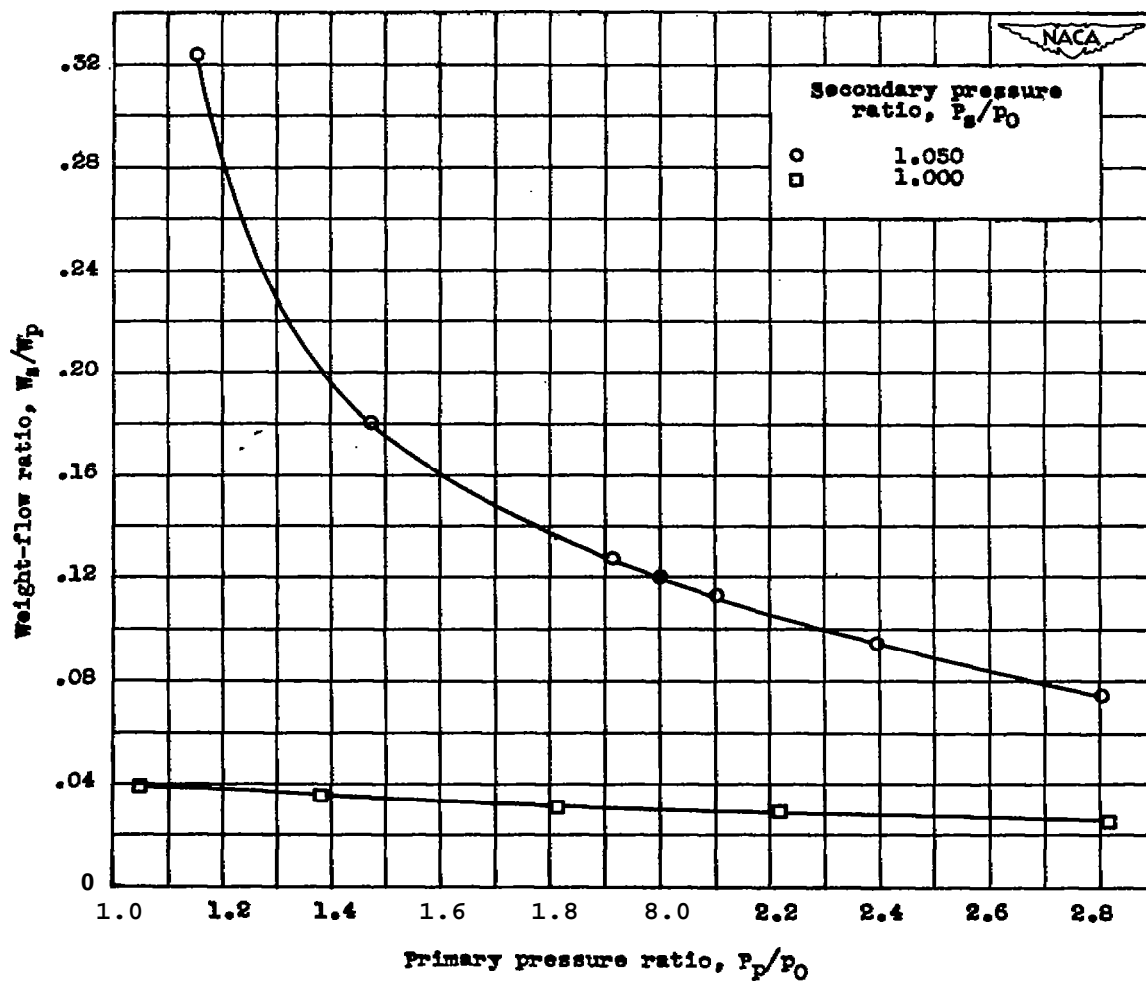
Figure 4. - Variation of secondary weight flow with primary weight flow for three ejectors. Secondary pressure ratio  $P_s/P_0$ , 1.000.



(a) Spacing  $S/D_p$ , 0.016.

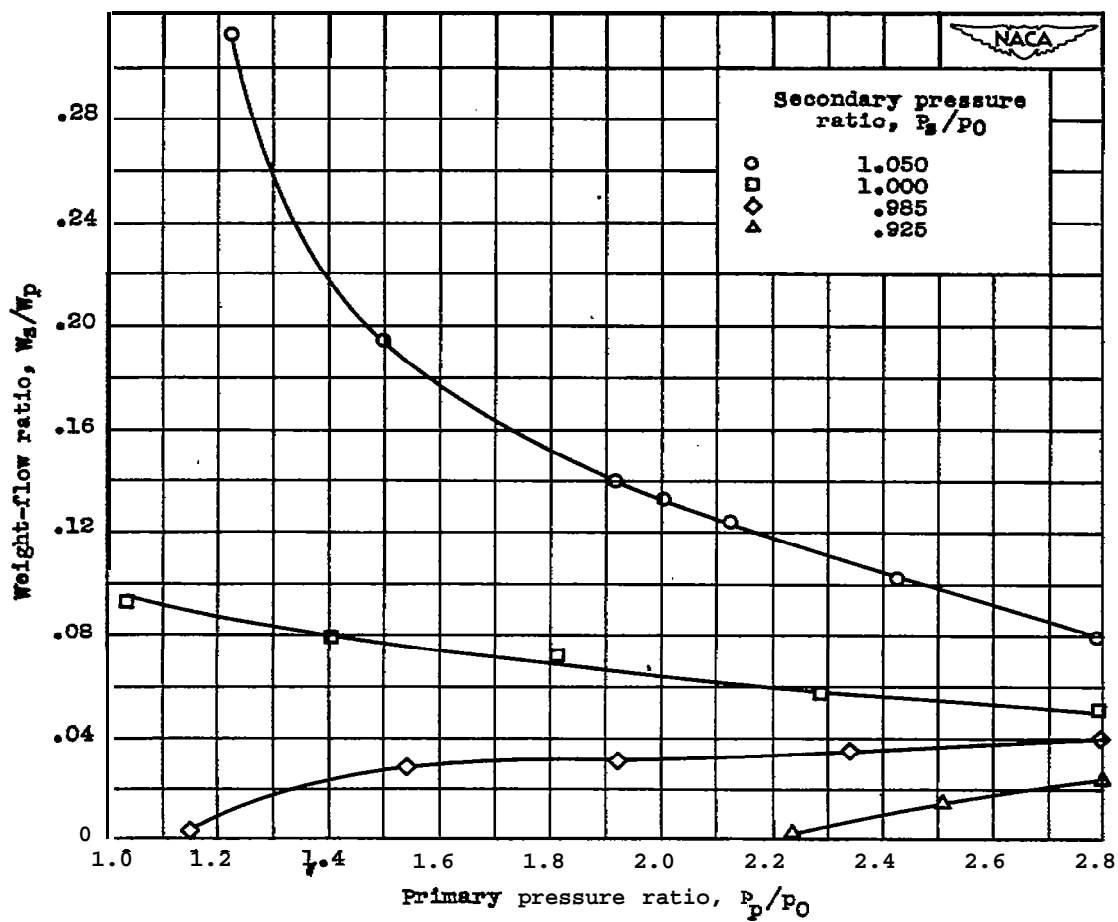
Figure 5. - Effect of primary and secondary pressure ratios and spacing on ejector weight-flow ratio for a conical-mixing-section ejector having diameter ratio of 1.21. Secondary-to-primary-air temperature ratio  $T_s/T_p$ , 1.0,





(b) Spacing  $S/D_p$ , 0.266.

Figure 5. - Continued. Effect of primary and secondary pressure ratios and spacing on ejector weight-flow ratio for a conical-mixing-section ejector having diameter ratio of 1.21. Secondary-to-primary-air temperature ratio  $T_s/T_p$ , 1.0.



(c) spacing  $S/D_p$ , 0.520.

Figure 5. - Continued. Effect of primary and secondary pressure ratios and spacing on ejector weight-flow ratio for a conical-mixing-section ejector having diameter ratio of 1.21. secondary-to-primary-air temperature ratio  $T_s/T_p$ , 1.0.

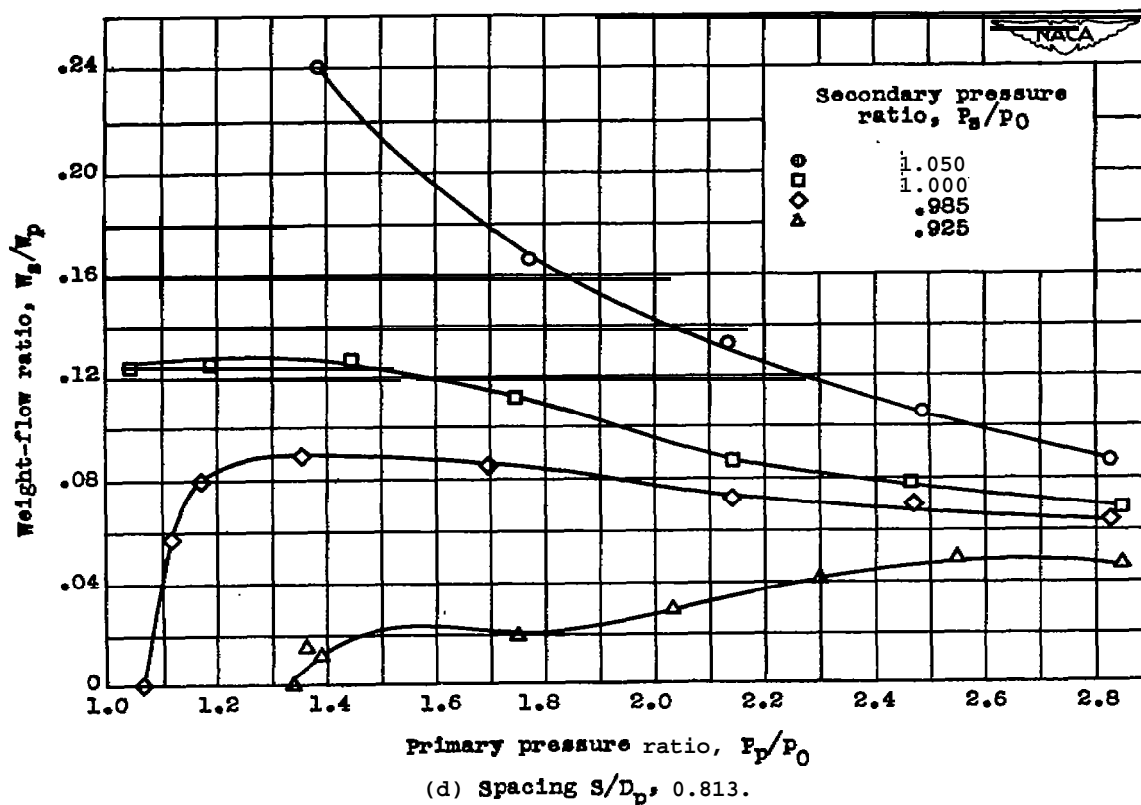
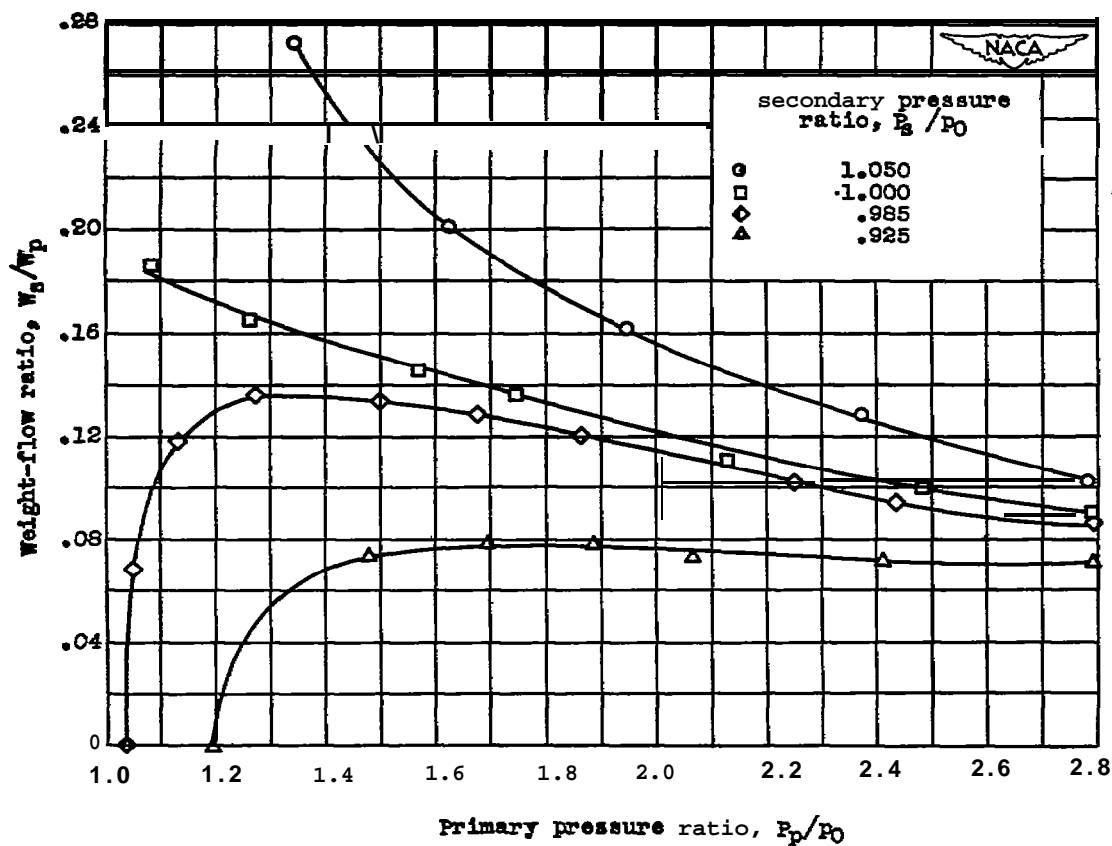


Figure 5. - Continued. Effect of primary and secondary pressure ratios and spacing on ejector weight-flow ratio for a conical-mixing-section ejector having diameter ratio of 1.21. Secondary-to-primary-air temperature ratio  $T_s/T_p$ , 1.0.



(e) Spacing  $S/D_p$ , 1.349.

Figure 5. - continued. Effect of primary and secondary pressure ratios and spacing on ejector weight-flow ratio for a conical-mixing-section ejector having diameter ratio of 1.21. Secondary-to-primary-air temperature ratio  $T_s/T_p$ , 1.0.

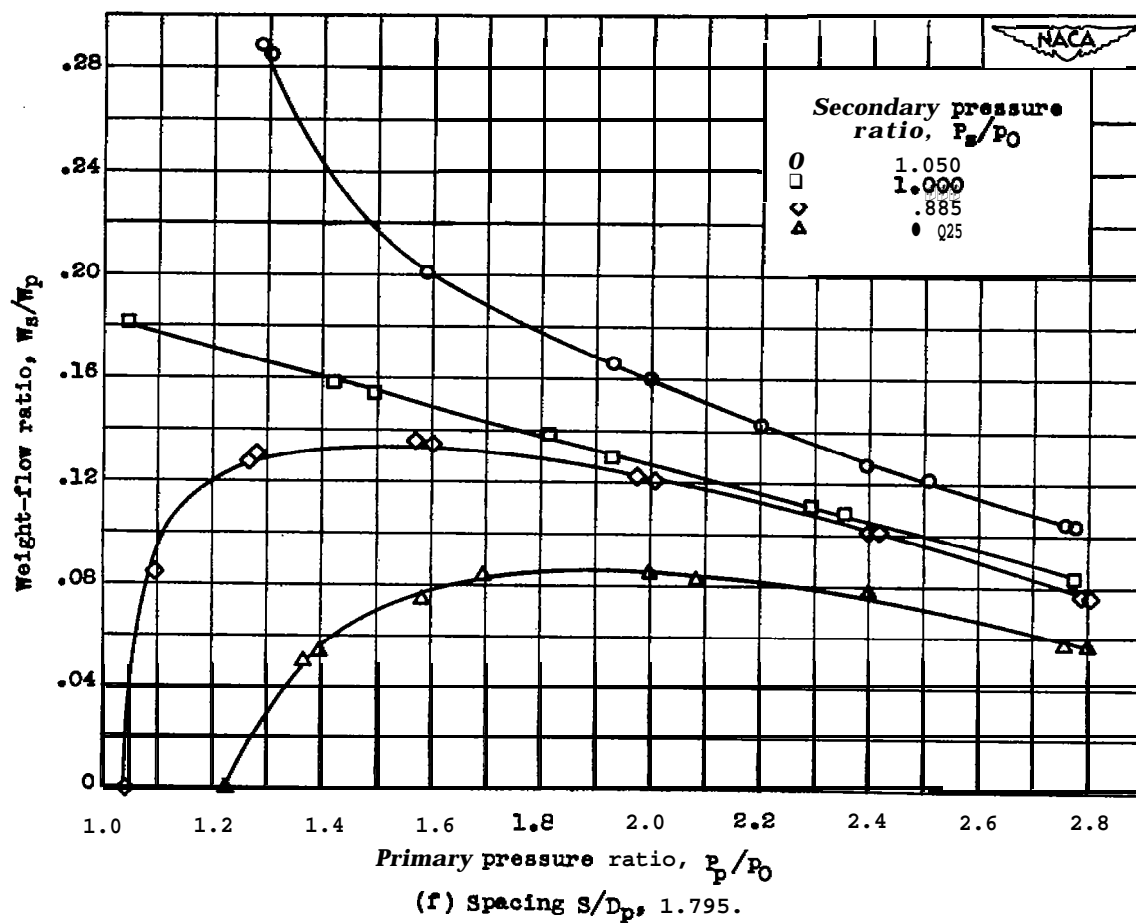


Figure 5. - Continued. Effect of primary and secondary pressure ratios and spacing on ejector weight-flow ratio for a conical-mixing-section ejector having diameter ratio of 1.21. secondary-to-primary-air temperature ratio  $T_s/T_p$ , 1.0.

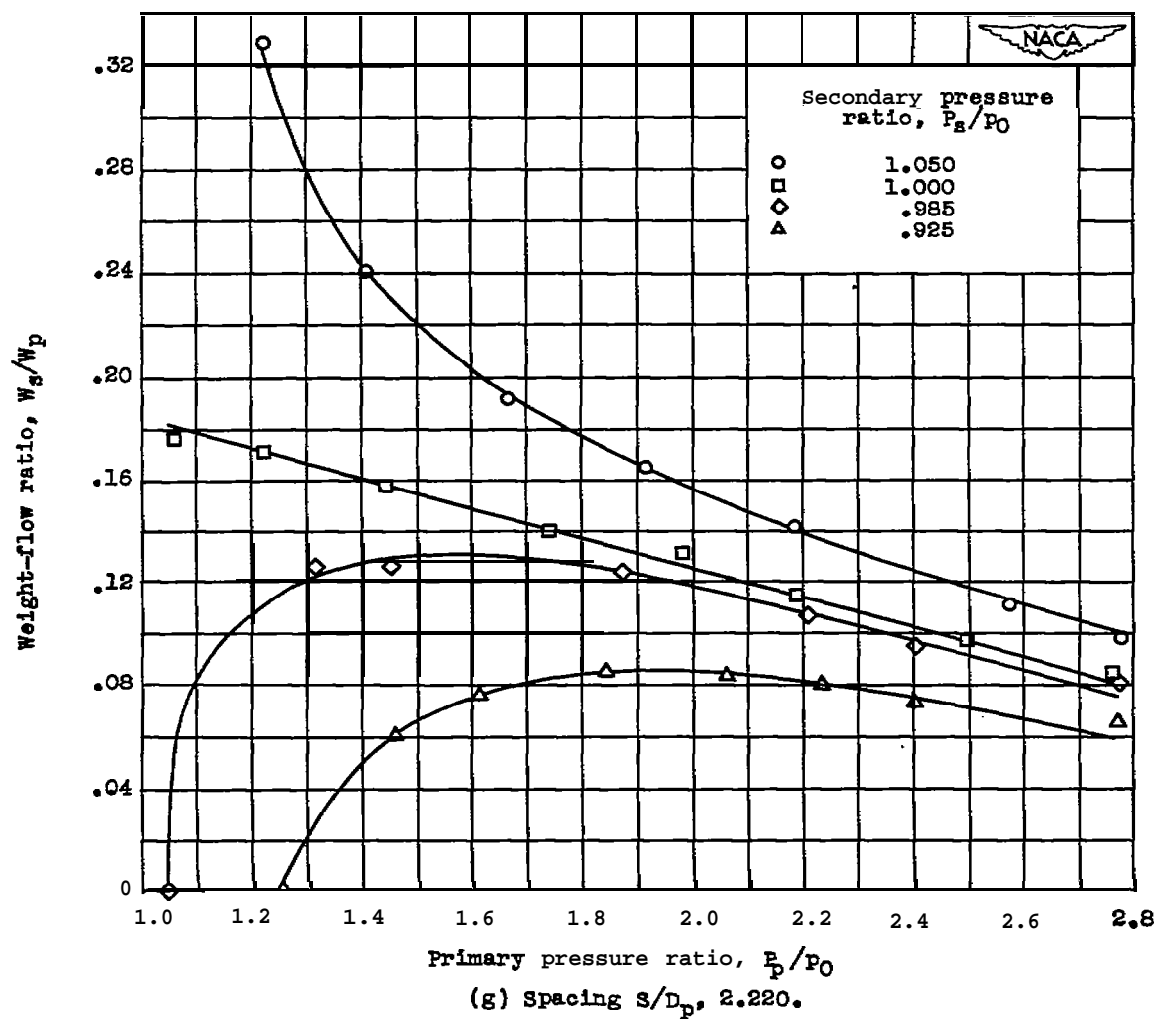


Figure 5. - Continued. Effect of primary and secondary pressure ratios and spacing on ejector weight-flow ratio for a conical-mixing-section ejector having diameter ratio of 1.21. secondary-to-primary-air temperature ratio  $T_s/T_p$ , 1.0.

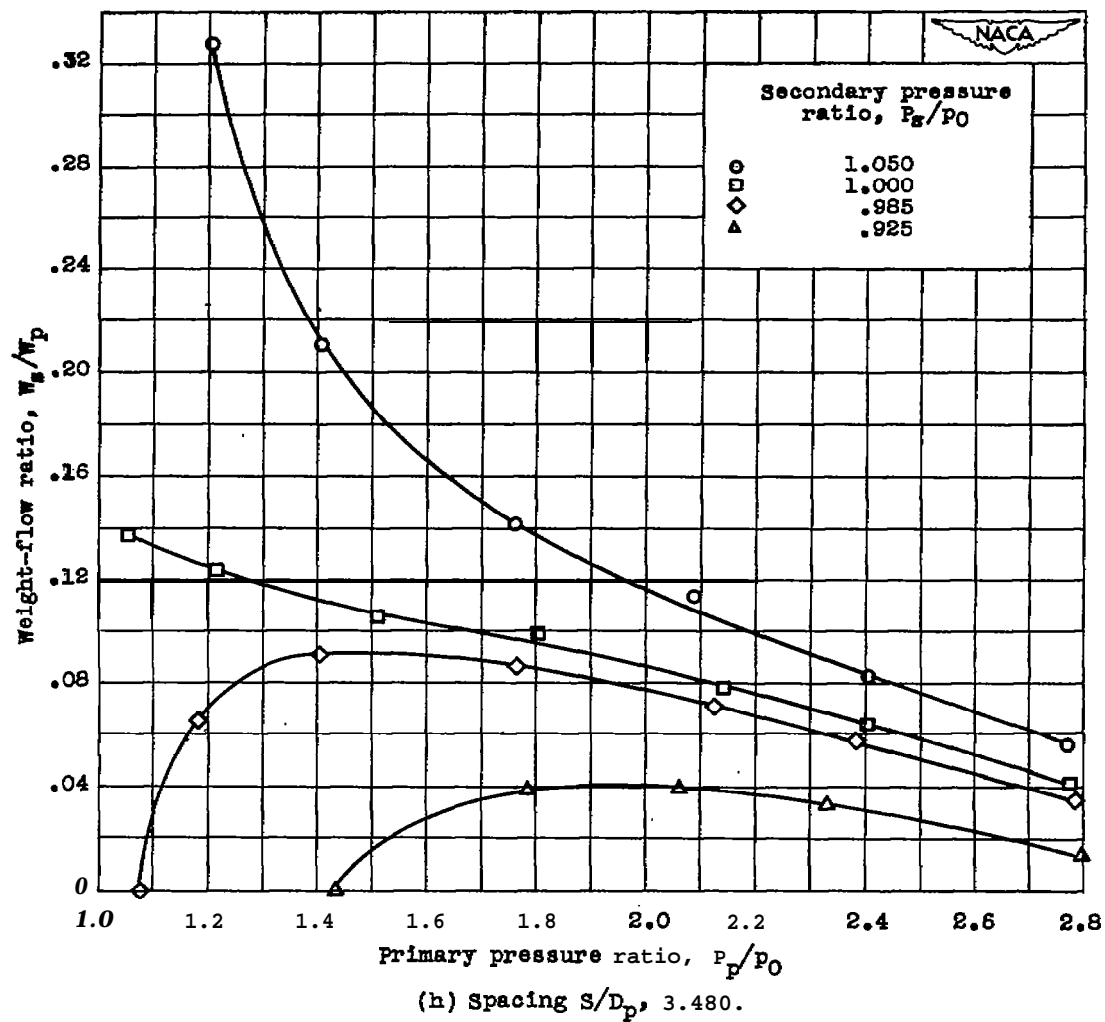


Figure 5. - Concluded. Effect of primary and secondary pressure ratios and spacing on ejector weight-flow ratio for a conical-mixing-section ejector having diameter ratio of 1.21. Secondary-to-primary-air temperature ratio  $T_s/T_p$ , 1.0.

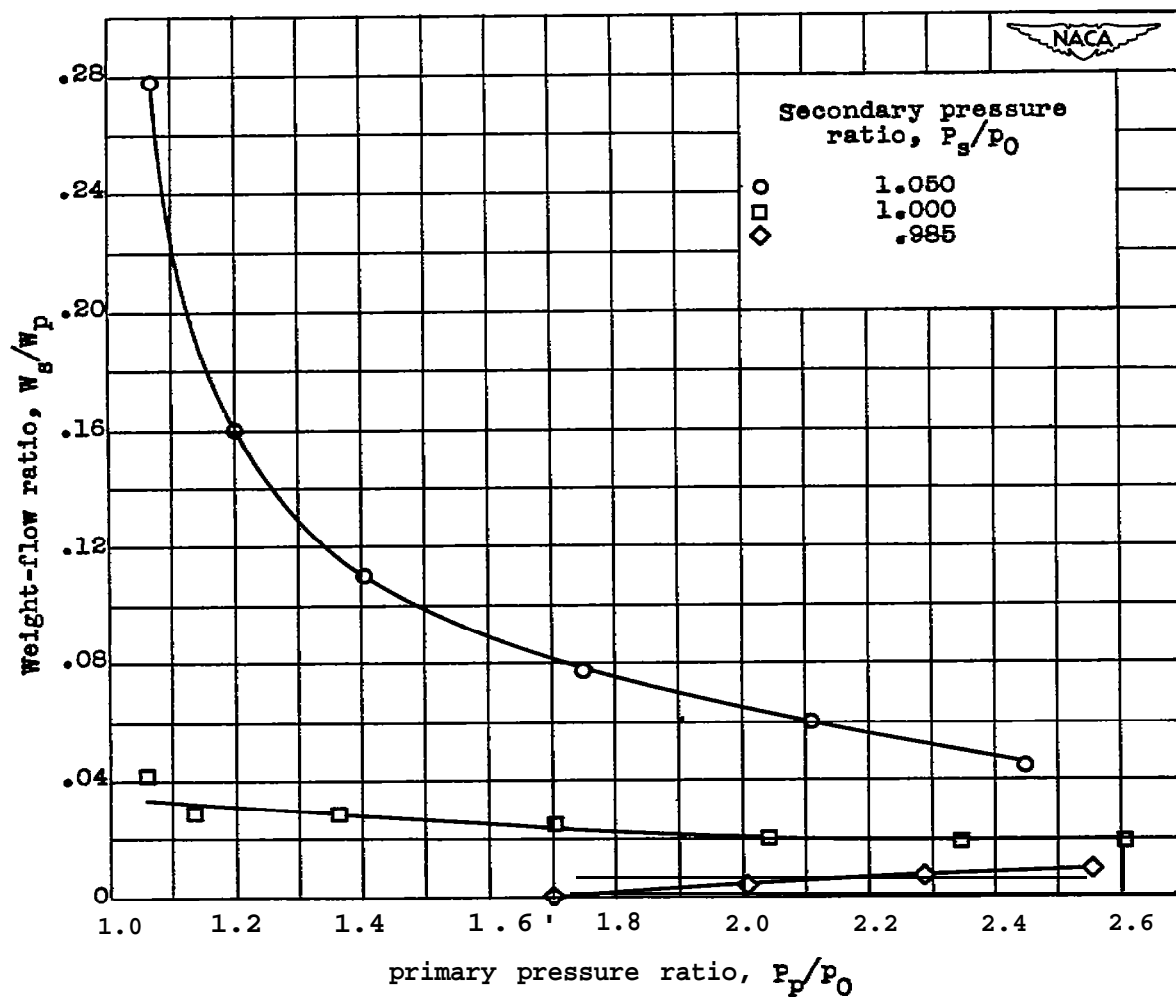
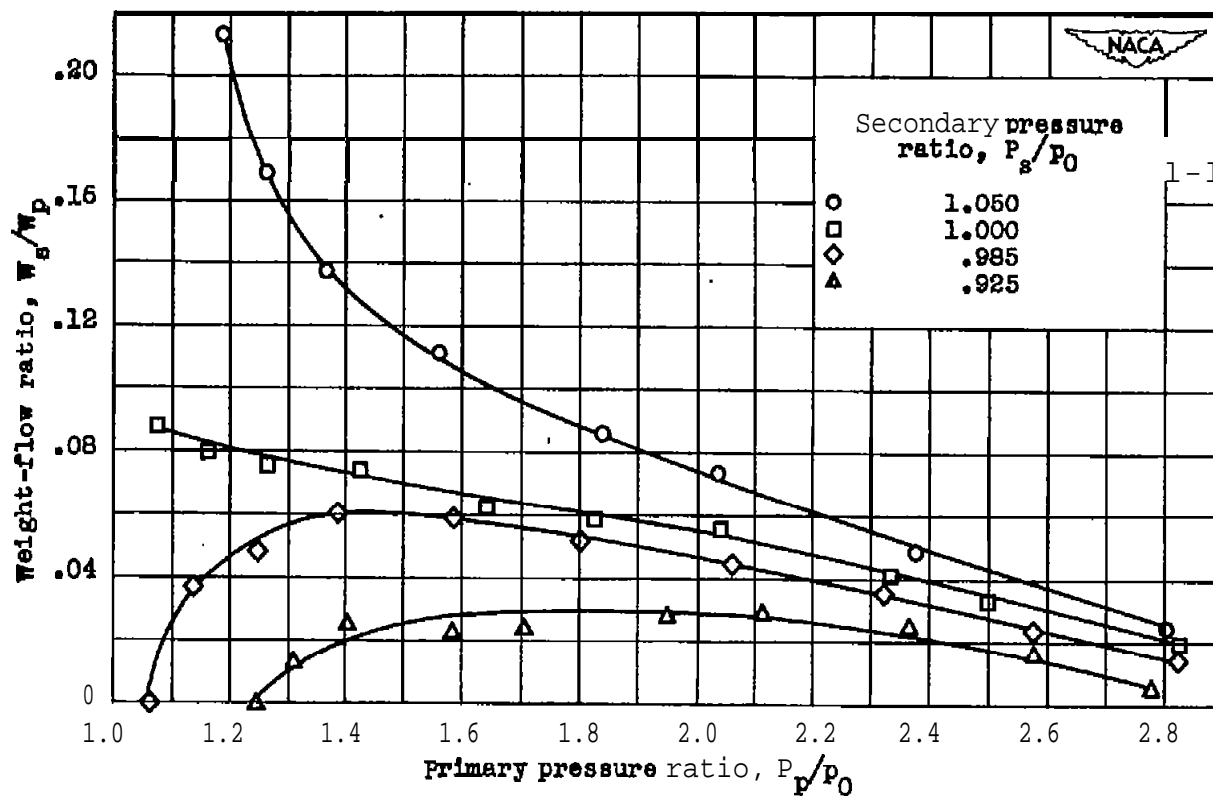
(a) Spacing  $S/D_p$ , 0.234.

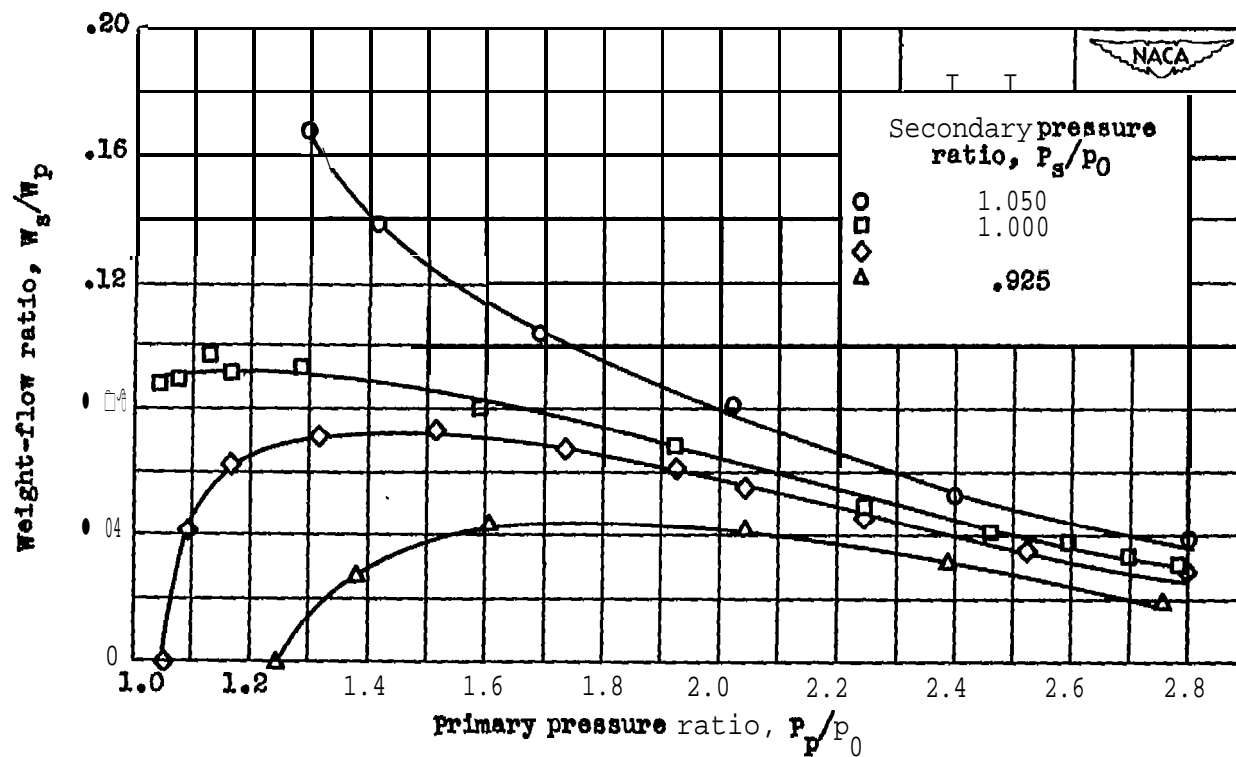
Figure 6. - Effect of primary and secondary pressure ratios and spacing on ejector weight-flow ratio for a conical-mixing-section ejector having diameter ratio of 1.10. Secondary-to-primary-air temperature ratio  $T_s/T_p$  1.0.





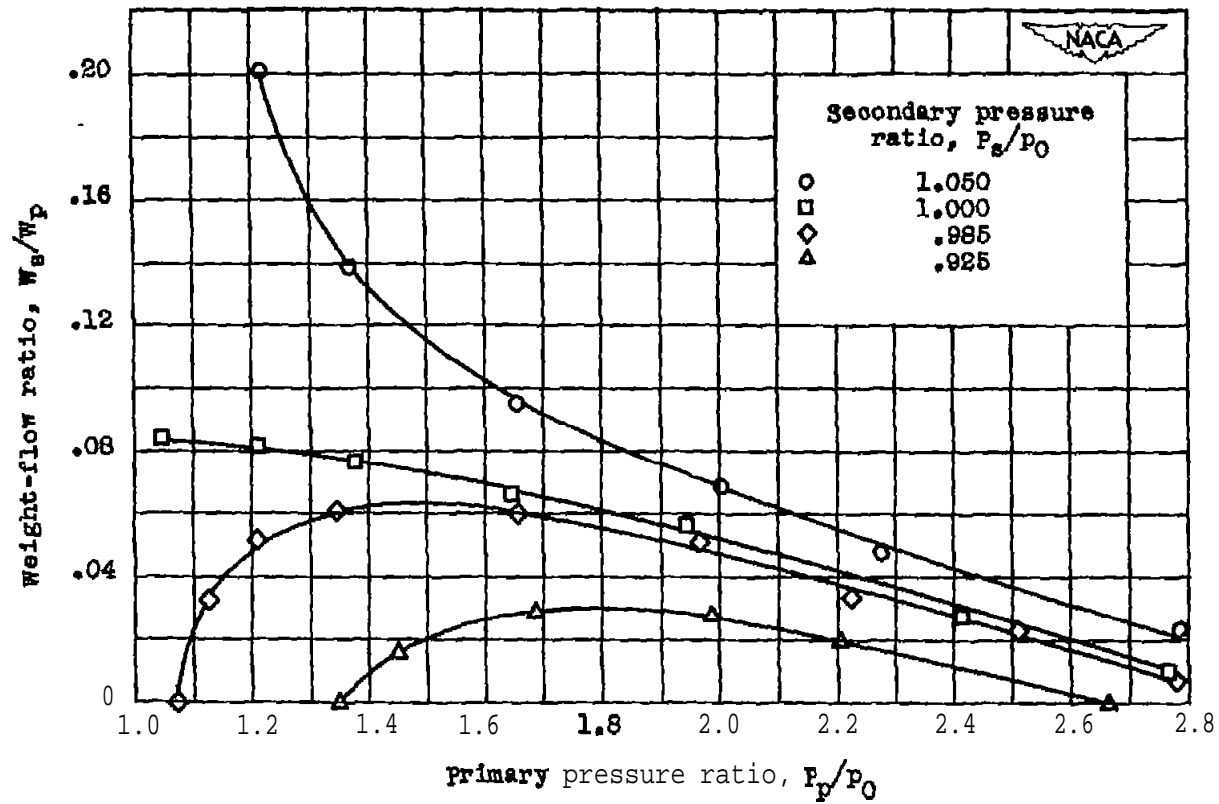
(b) Spacing  $s/D_p$ , 0.660.

Figure 6. - continued. Effect of primary and secondary pressure ratios and spacing on ejector weight-flow ratio for a conical-mixing-section ejector having diameter ratio of 1.10. Secondary-to-primary-air temperature ratio  $T_s/T_p$ , 1.0.



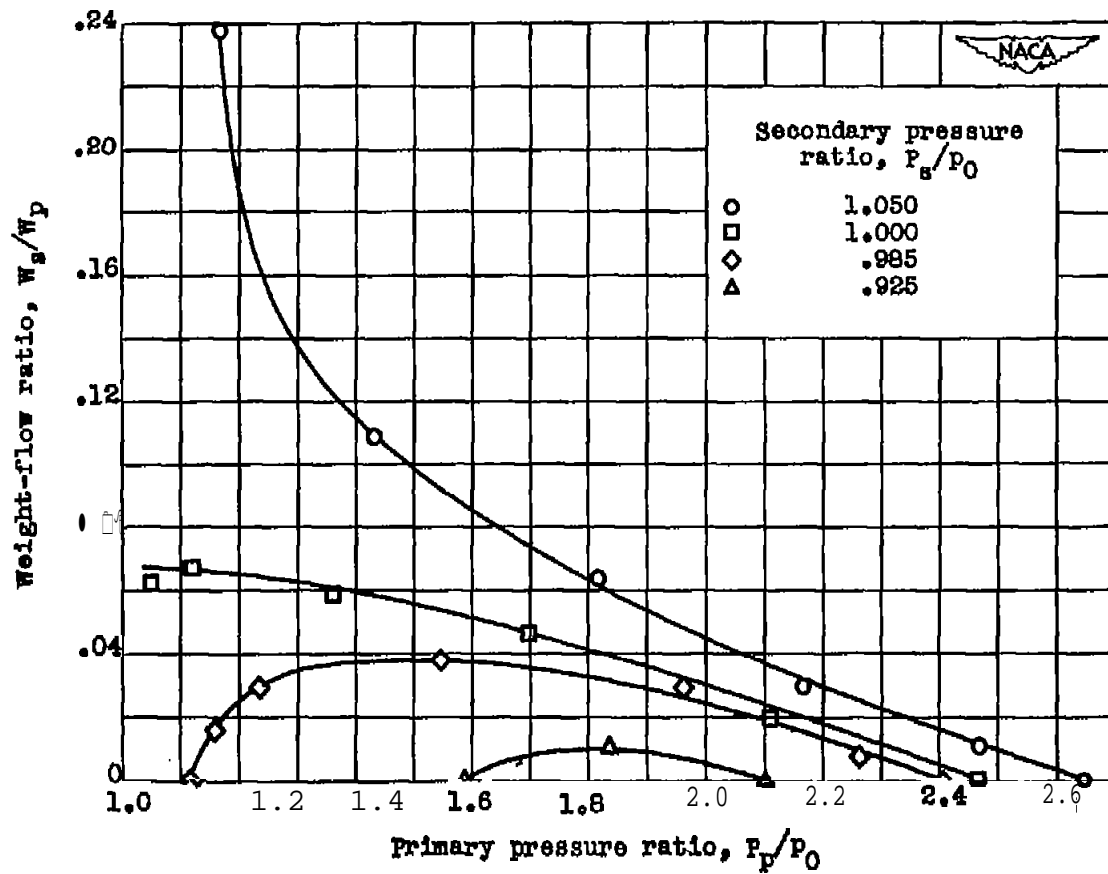
(c) Spacing  $S/D_p$ , 1.095.

Figure 6. - Continued. Effect of primary and secondary pressure ratios and spacing on ejector weight-flow ratio for a conical-mixing-section ejector having diameter ratio of 1.10. Secondary-to-primary-air temperature ratio  $T_s/T_p$ , 1.0.



(d) Spacing  $S/D_p$ , 1.670.

Figure 6. - Continued. Effect of primary and secondary pressure ratios and spacing on ejector weight-flow ratio for a conical-mixing-section ejector having diameter ratio of 1.10. Secondary-to-primary-air temperature ratio  $T_s/T_p$ , 1.0.



(c) Spacing  $S/D_p$ , 2.230.

Figure 6. - Concluded. Effect of primary and secondary pressure ratios and spacing on ejector weight-flow ratio for a conical-mixing-section ejector having diameter ratio of 1.10. Secondary-to-primary-air temperature ratio  $T_s/T_p$ , 1.0.

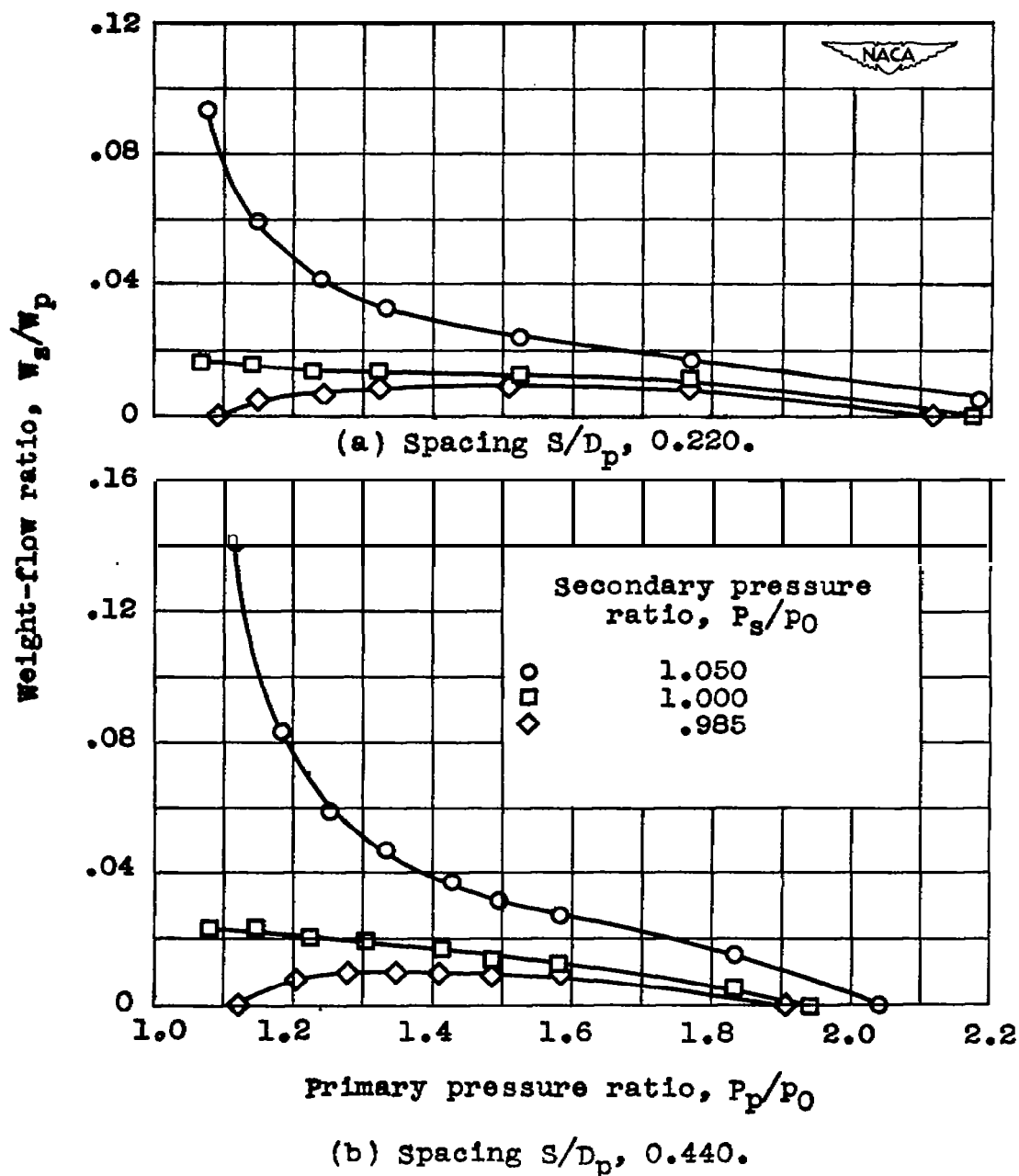


Figure 7. - Effect of primary and secondary pressure ratios and spacing on ejector weight-flow ratio for conical-mixing-section ejector having diameter ratio of 1.00. Secondary-to-primary-air temperature ratio  $T_s/T_p$ , 1.0.

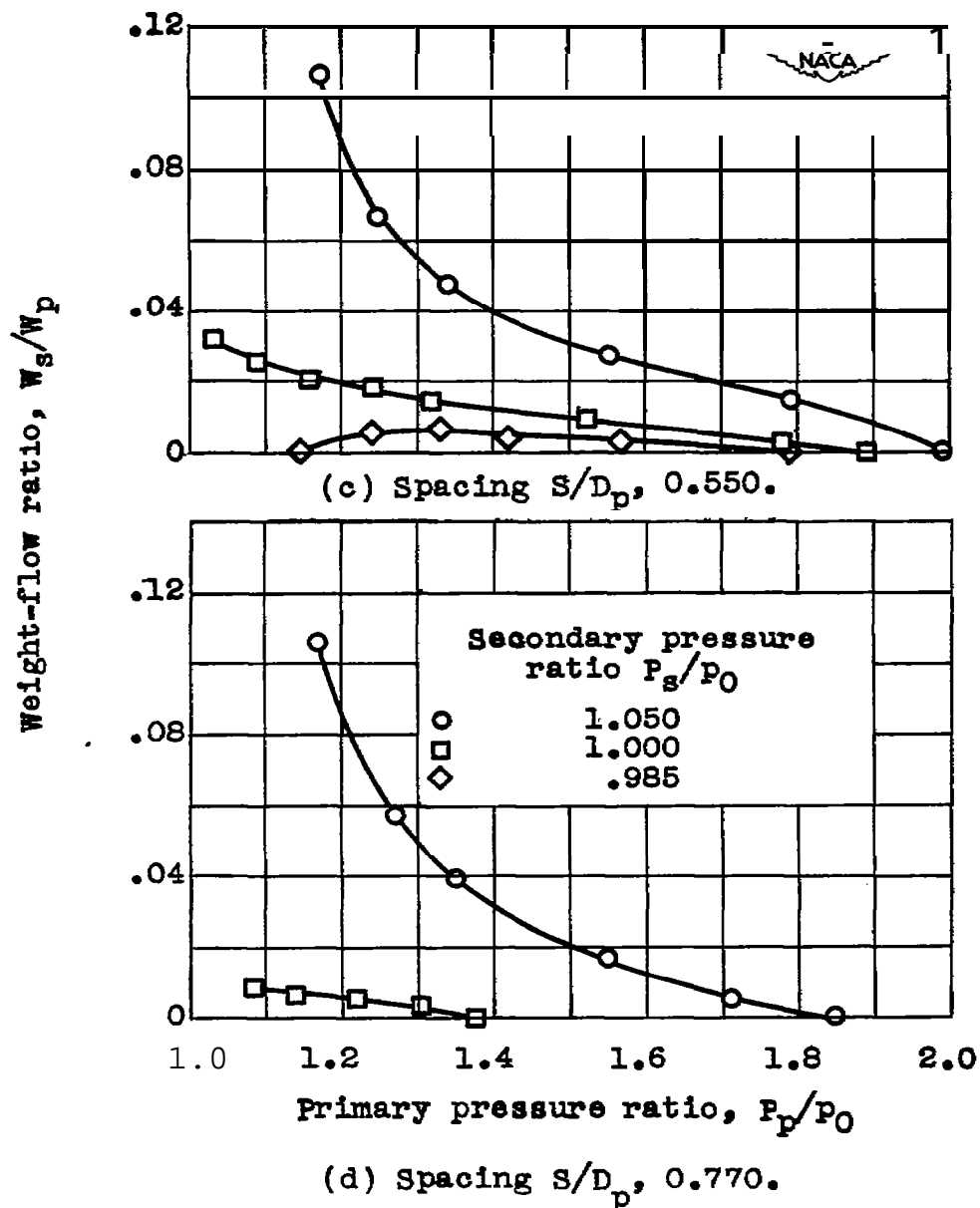
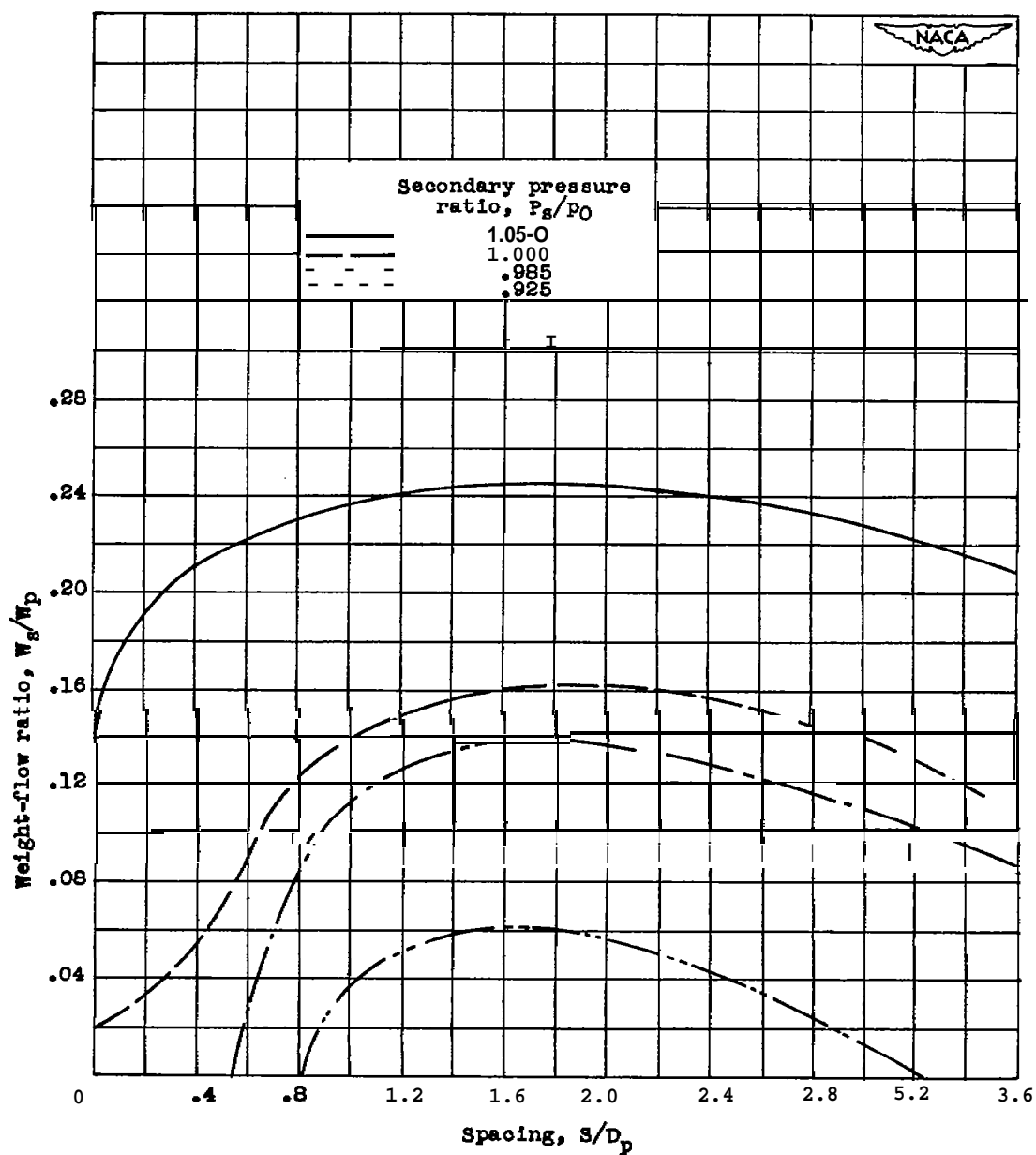
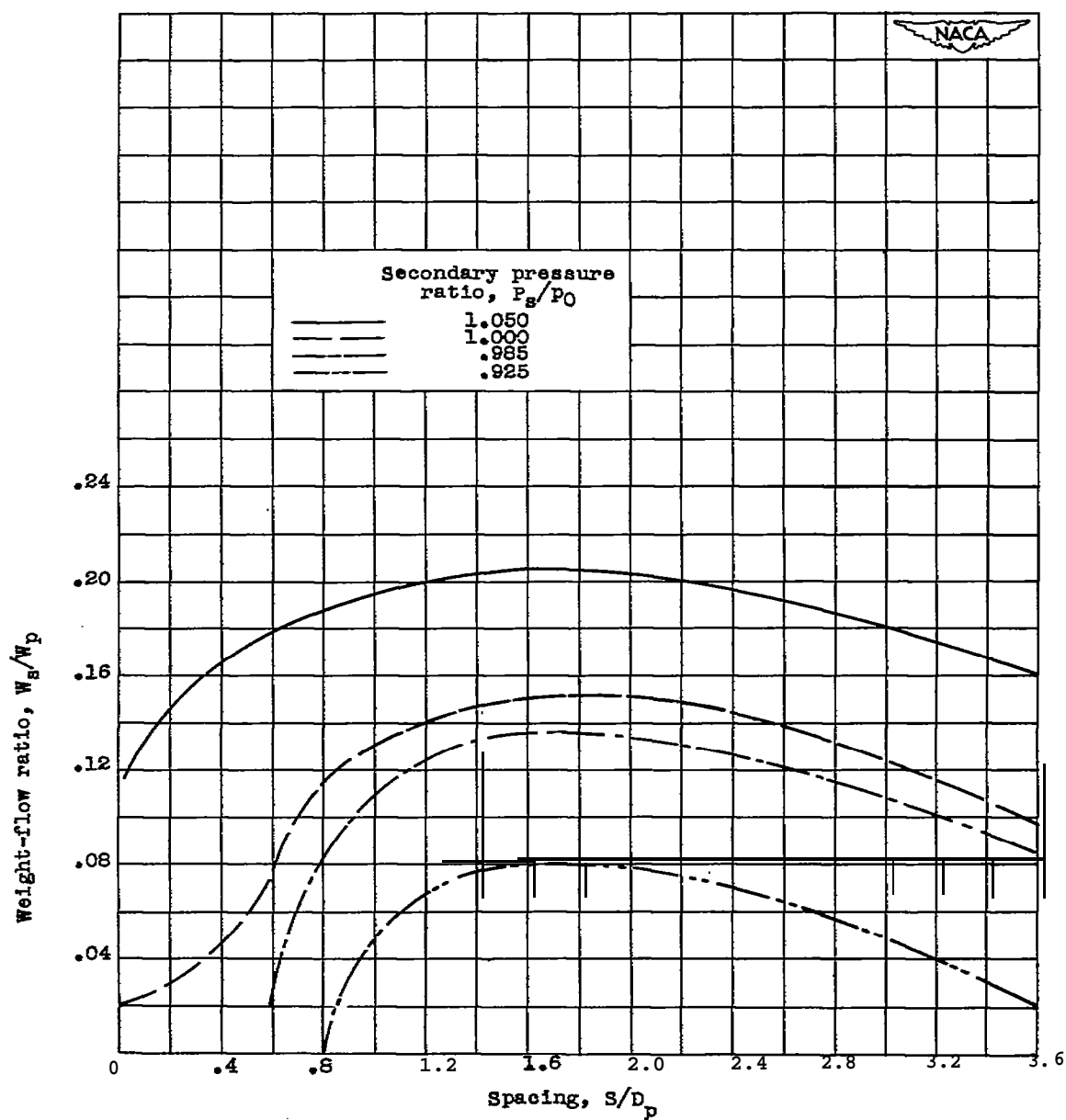


Figure 7. - Concluded. Effect of primary and secondary pressure ratios and spacing on ejector weight-flow ratio for conical-mixing-section ejector having diameter ratio of 1.00. Secondary-to-primary-air temperature ratio  $T_s/T_p$ , 1.0.



(a) Diameter ratio  $D_s/D_p$ , 1.21; primary pressure ratio  $P_p/p_0$ , 1.4.

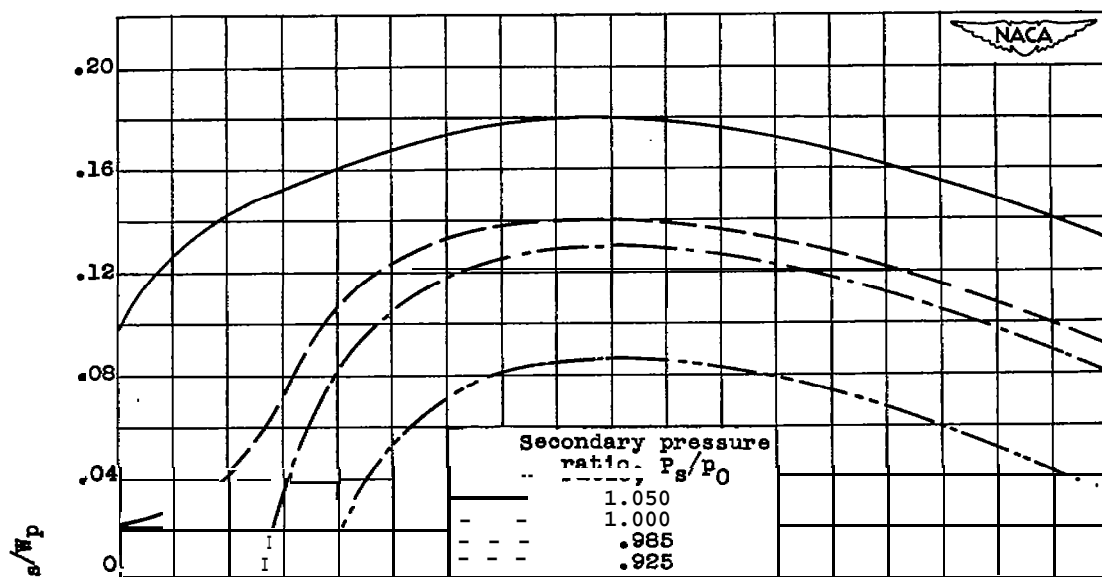
Figure 8. - Effect of spacing on ejector weight-flow ratio for selected primary and secondary pressure ratios. Secondary-to-primary-air temperature ratio  $T_s/T_p$ , 1.0.



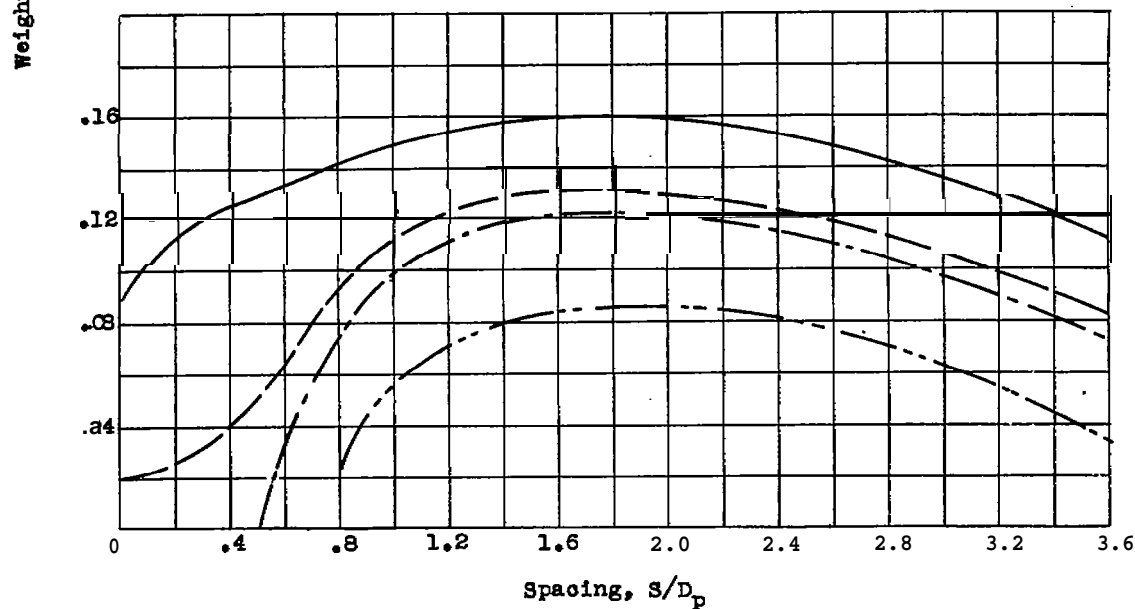
(a) Continued.. Diameter ratio  $D_g/D_p$ , 1.21; primary pressure ratio  $P_p/P_0$ , 1.6.

Figure 8. - continued. Effect of spacing on ejector weight-flow ratio for selected primary and secondary pressure ratios. Secondary-to-primary-air temperature ratio  $T_g/T_p$ , 1.0.



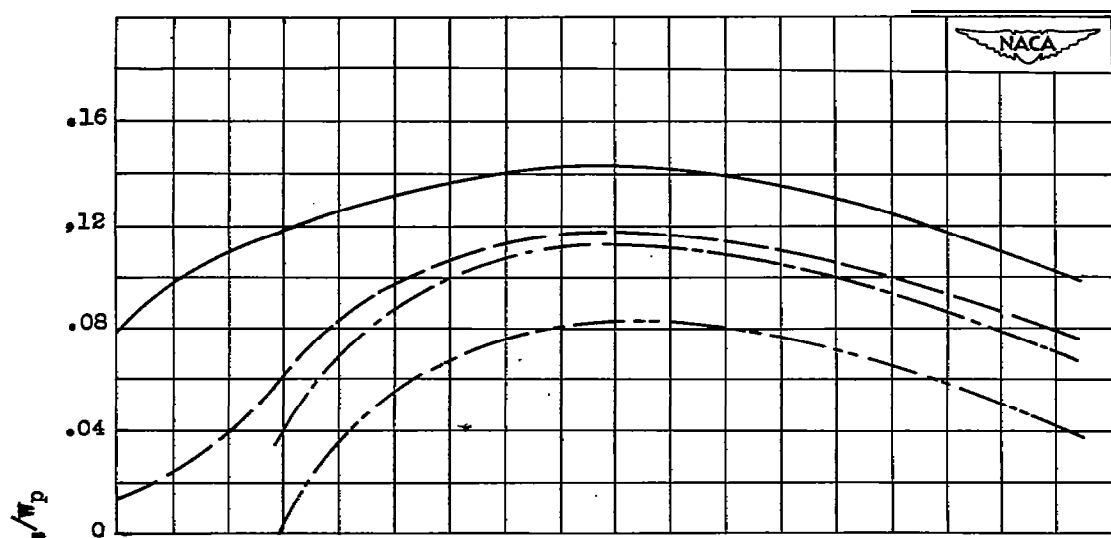


(a) Continued. Diameter ratio  $D_g/D_p$ , 1.21; primary pressure ratio  $P_p/P_0$ , 1.8.

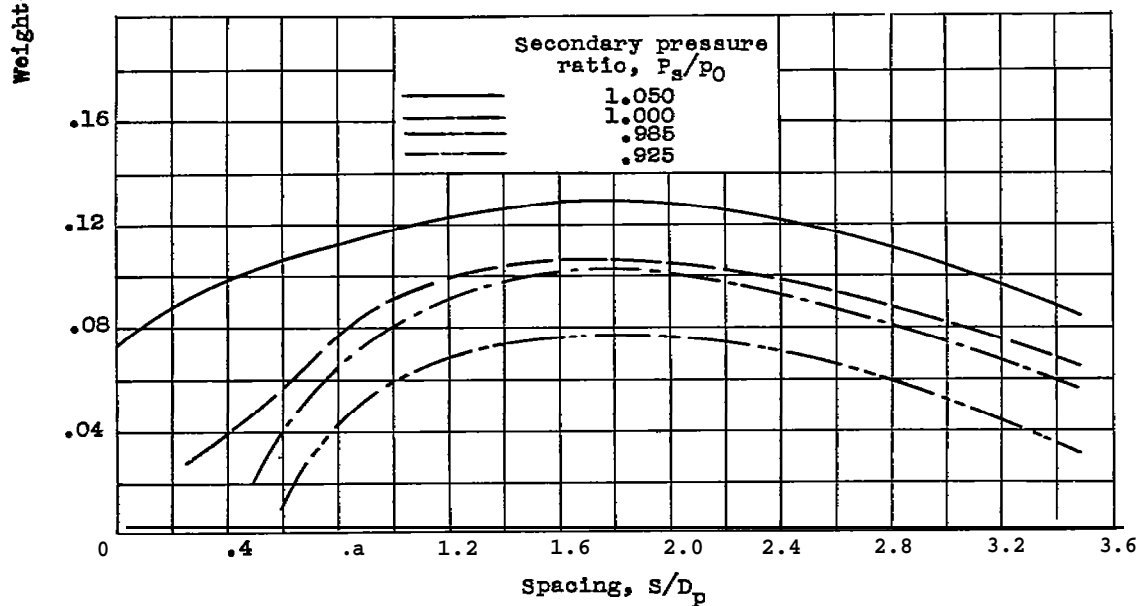


(a) Continued. Diameter ratio  $D_g/D_p$ , 1.21; primary pressure ratio  $P_p/P_0$ , 2.0.

Figure 8. - Continued. Effect of spacing on ejector weight-flow ratio for selected primary and secondary pressure ratios. Secondary-to-primary-air temperature ratio  $T_g/T_p$ , 1.0.

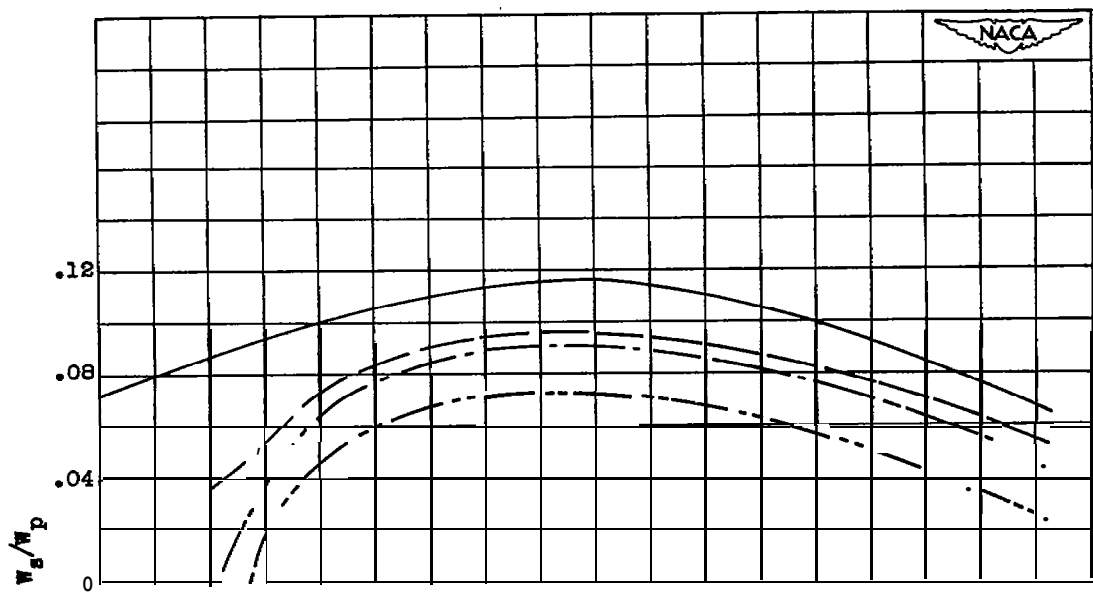


(a) Continued. Diameter ratio  $D_s/D_p$ , 1.21; primary pressure ratio  $P_p/P_0$ , 2.2.

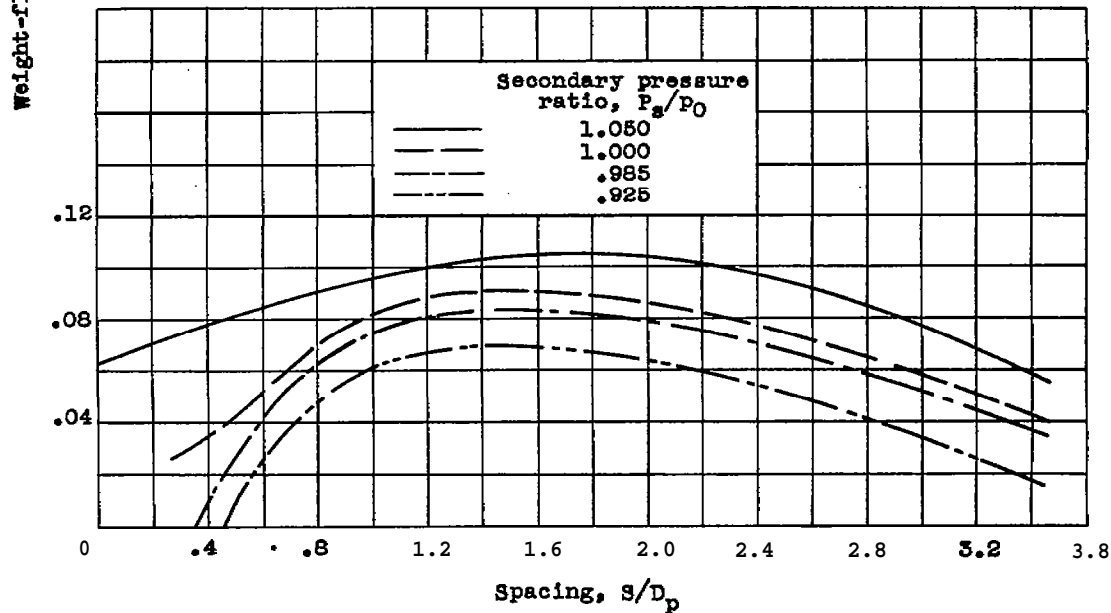


(a) continued. Diameter ratio  $D_s/D_p$ , 1.21; primary pressure ratio  $P_p/P_0$ , 2.4.

Figure 8. - continued. Effect of spacing on ejector weight-flow ratio for selected primary and secondary pressure ratios. Secondary-to-primary-air temperature ratio  $T_s/T_p$ , 1.0.



(a) Continued. Diameter ratio  $D_g/D_p$ , 1.21; primary pressure ratio  $P_p/P_0$ , 2-6.



(a) Concluded. Diameter ratio  $D_g/D_p$ , 1.21; primary pressure ratio  $P_p/P_0$ , 2.8.

Figure 8. - Continued, Effect of spacing on ejector weight-flow ratio for selected primary and secondary preasure ratios. Secondary-to-primary-air temperature ratio  $T_g/T_p$ , 1.0.

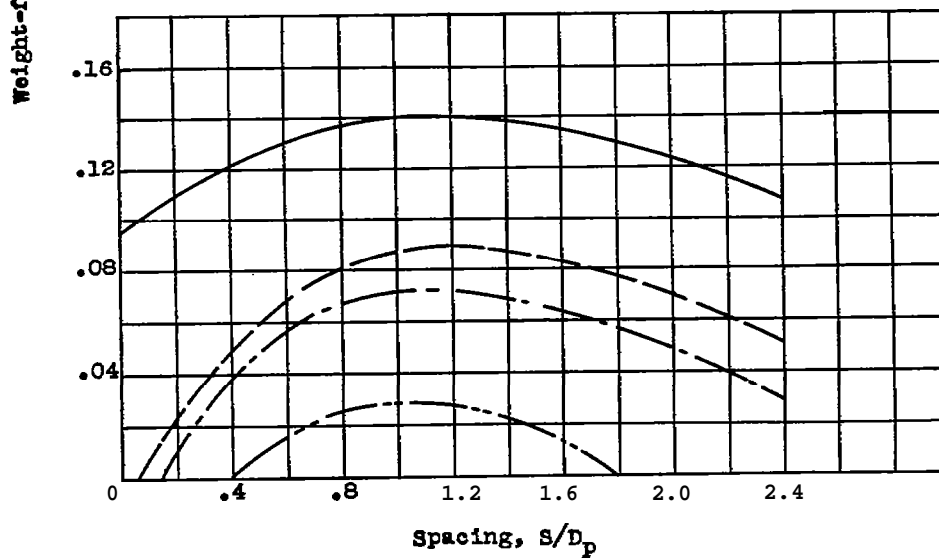
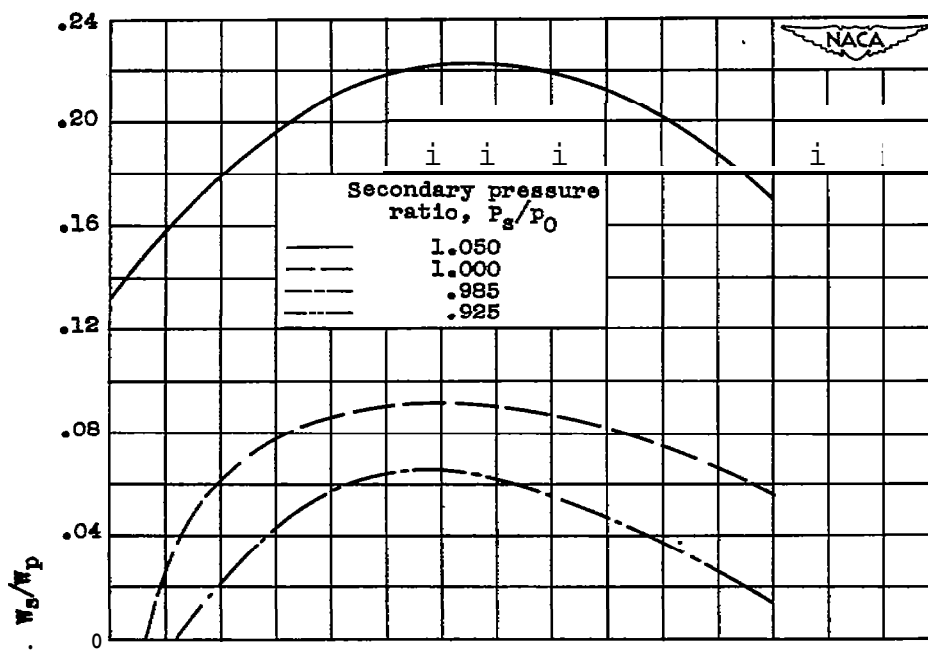
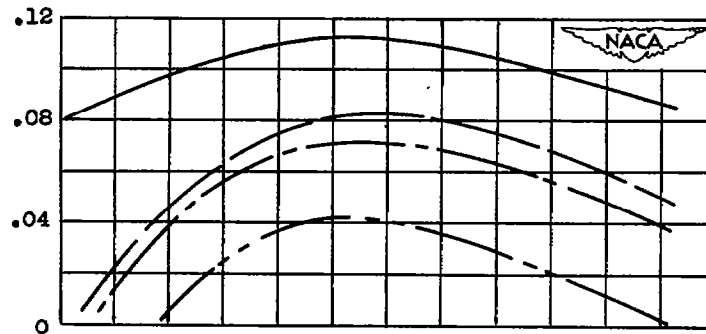
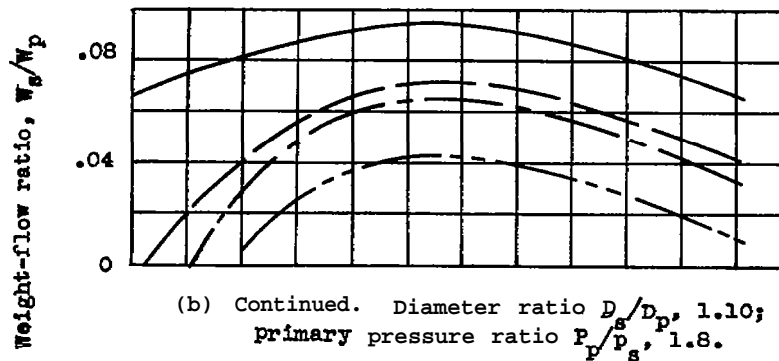


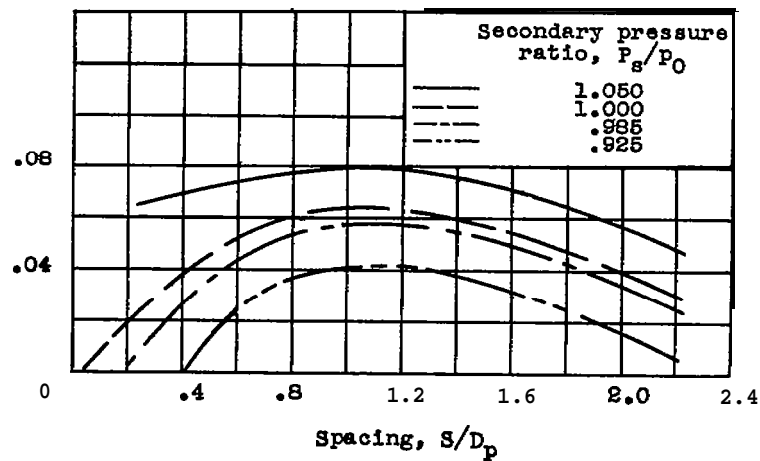
Figure 8. - Continued. Effect of spacing on ejector weight-flow ratio for selected primary and secondary pressure ratios. Secondary-to-primary-air temperature ratio  $T_s/T_p$ , 1.0.



(b) continued. Diameter ratio  $D_s/D_p$ , 1.10;  
primary pressure ratio  $P_p/P_0$ , 1.6.

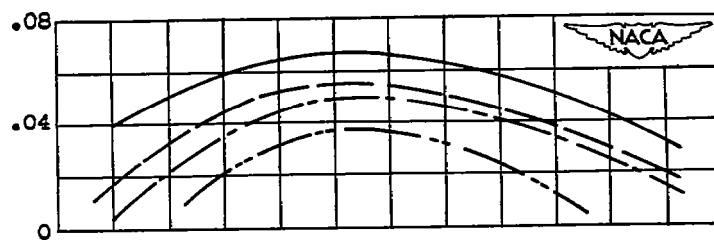


(b) Continued. Diameter ratio  $D_s/D_p$ , 1.10;  
primary pressure ratio  $P_p/P_0$ , 1.8.

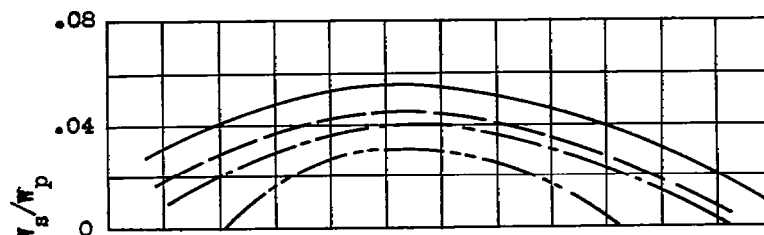


(b) Continued. Diameter ratio  $D_s/D_p$ , 1.10;  
primary pressure ratio  $P_p/P_0$ , 2.0.

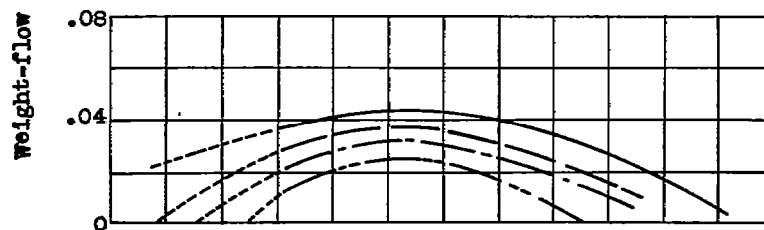
Figure 8. - Continued. Effect of spacing on ejector weight-flow ratio for selected primary and secondary pressure ratios. Secondary-to-primary-air temperature ratio  $T_s/T_p$ , 1.0.



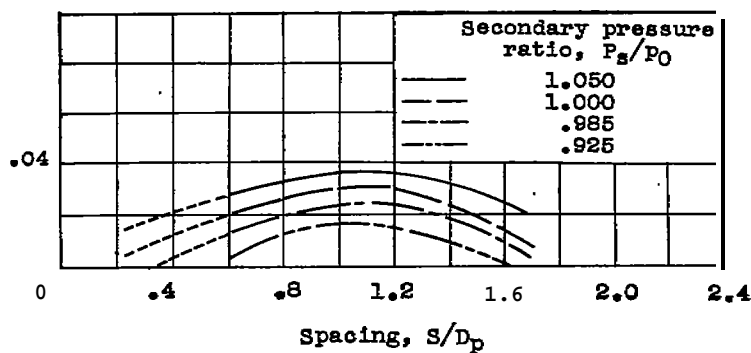
(b) continued. Diameter ratio  $D_s/D_p$ , 1.10;  
primary pressure ratio  $P_p/P_0$ , 2.2.



(b) Continued. Diameter ratio  $D_s/D_p$ , 1.10;  
primary pressure ratio  $P_p/P_0$ , 2.4.



(b) Continued. Diameter ratio  $D_s/D_p$ , 1.10;  
primary pressure ratio  $P_p/P_0$ , 2.6.



(b) Concluded. Diameter ratio  $D_s/D_p$ , 1.10;  
primary pressure ratio  $P_p/P_0$ , 2.8.

Figure 8. - Continued. Effect of spacing on ejector weight-flow ratio for selected primary and secondary pressure ratios. Secondary-to-primary-air temperature ratio  $T_s/T_p$ , 1.0.

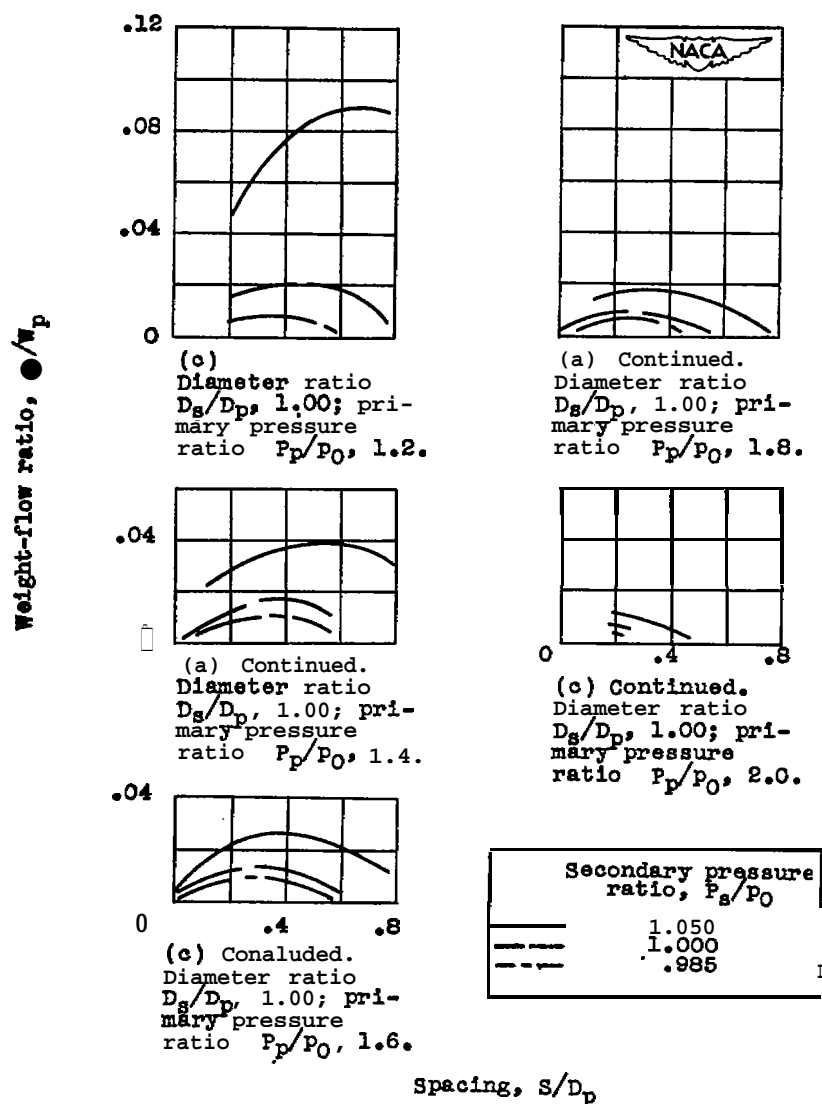


Figure 8. - Concluded. Effect of spacing on ejector weight-flow ratio for selected primary and secondary pressure ratios. Secondary-to-primary air temperature ratio  $T_s/T_p$ , 1.0.

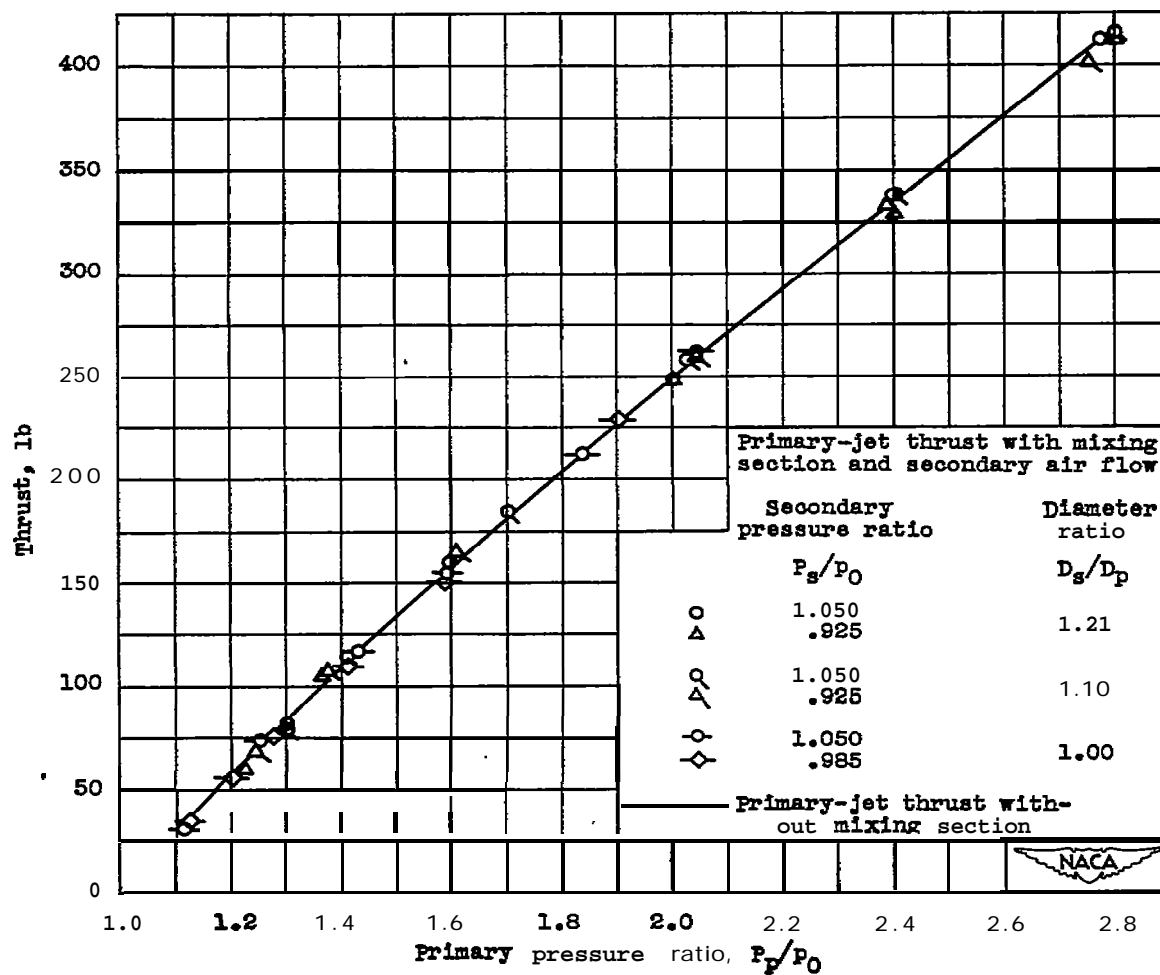
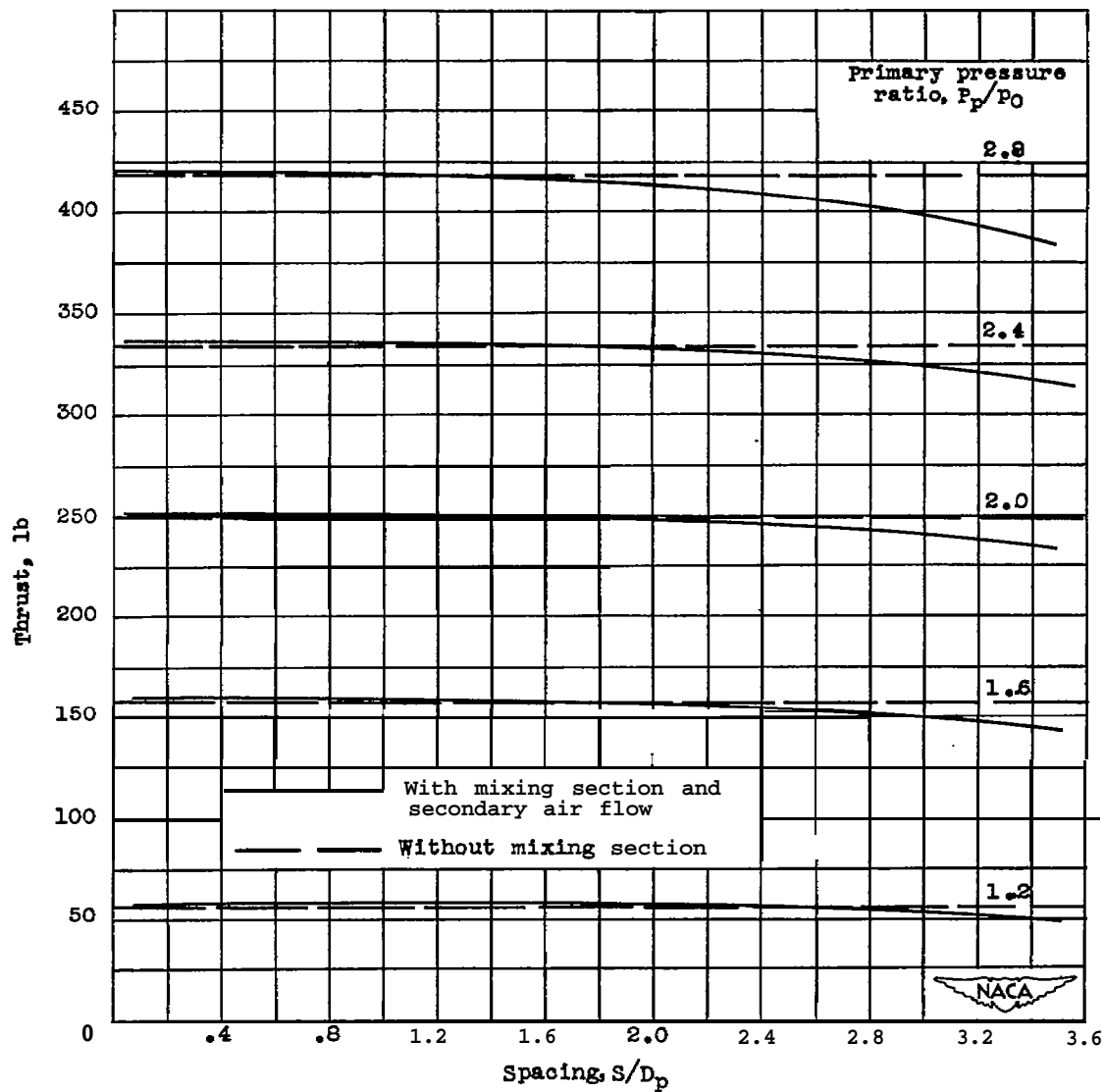


Figure 9. - Comparison of ejector thrust (at spacing for maximum weight-flow ratio) with primary-jet thrust.





(a) Diameter ratio  $D_s/D_p$ , 1.21.

Figure 10. - Effect of spacing on ejector thrust for a conical-mixing-section ejector at a secondary pressure ratio of 1.000.

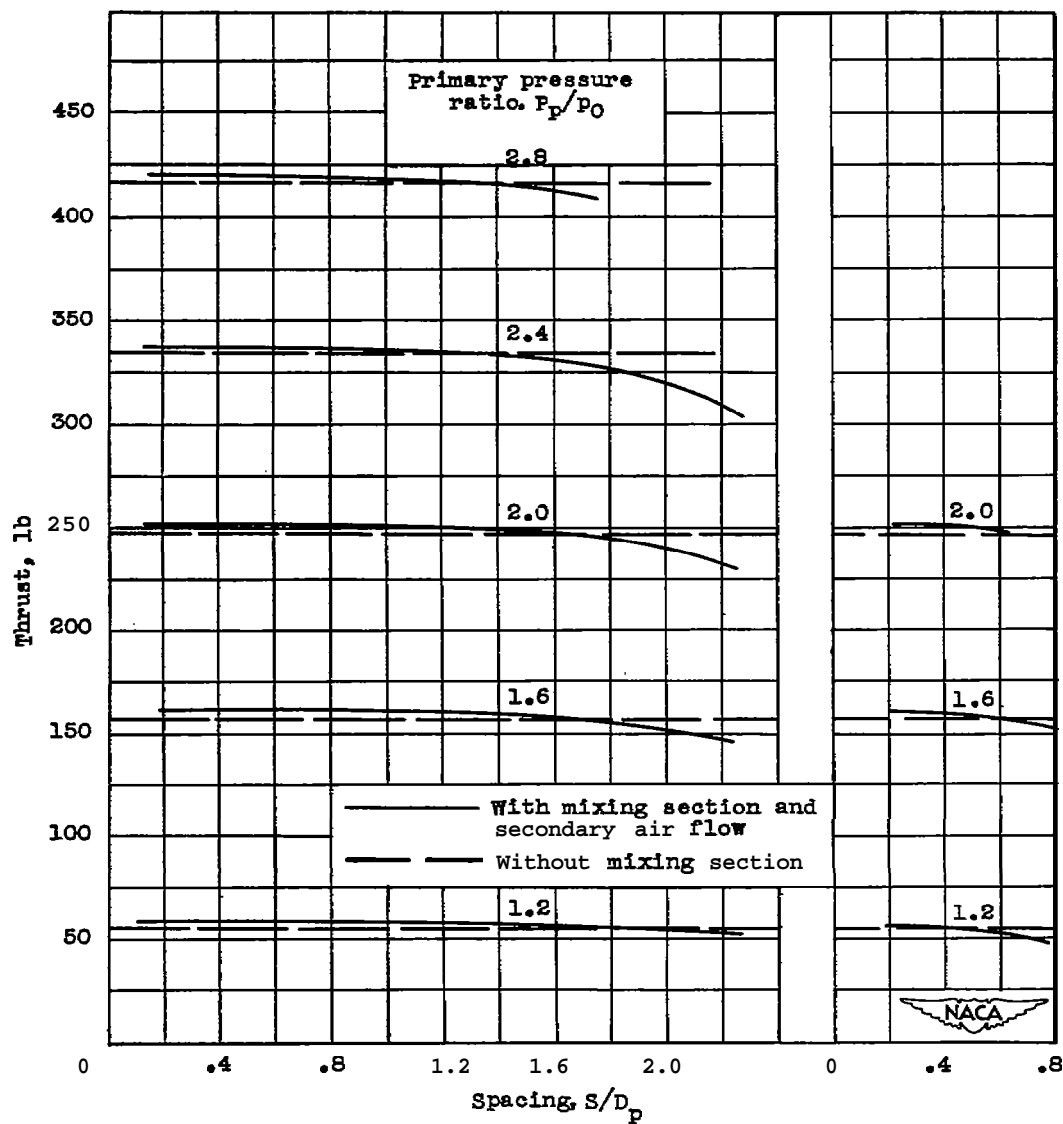
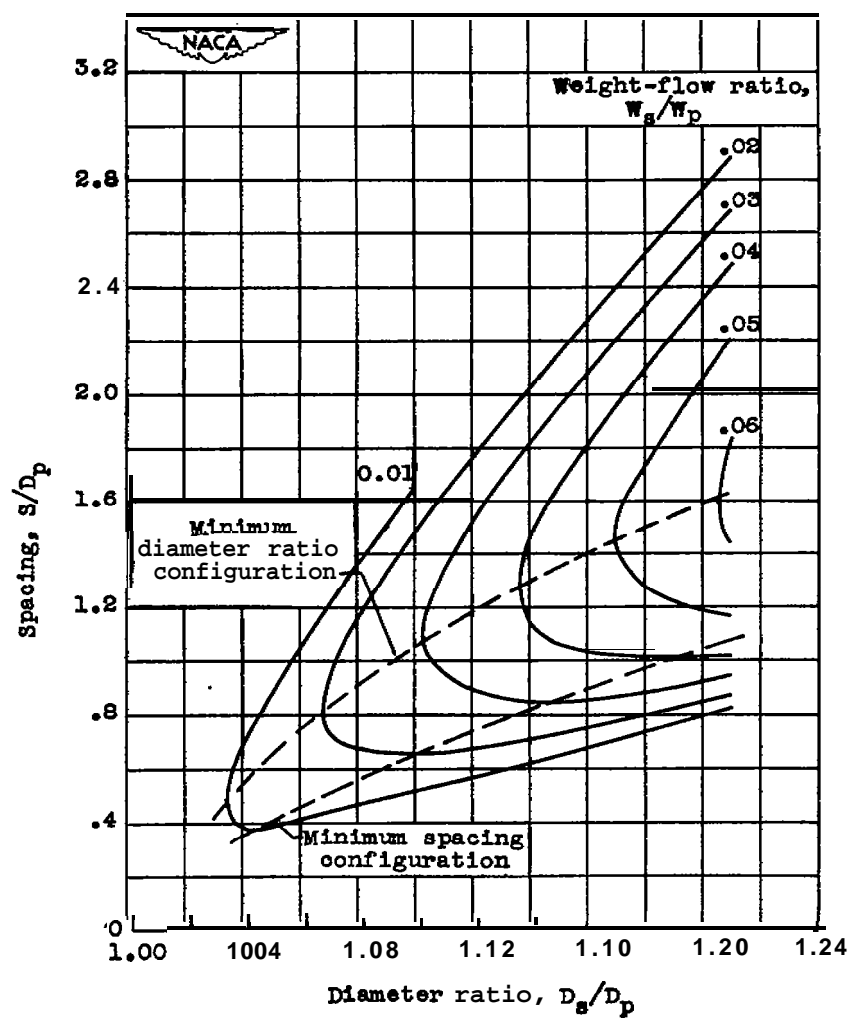
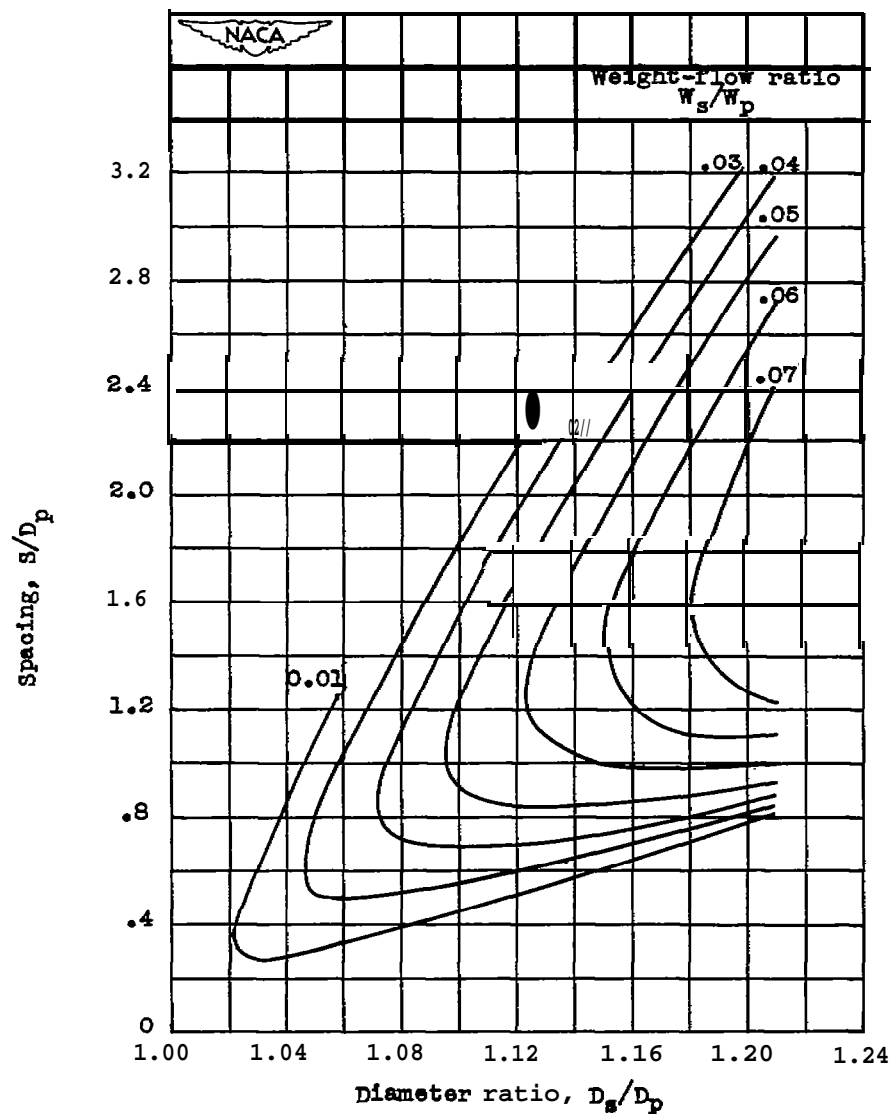


Figure 10. - Concluded. Effect of spacing on ejector thrust for a conical-mixing-section ejector at a secondary pressure ratio of 1.000.



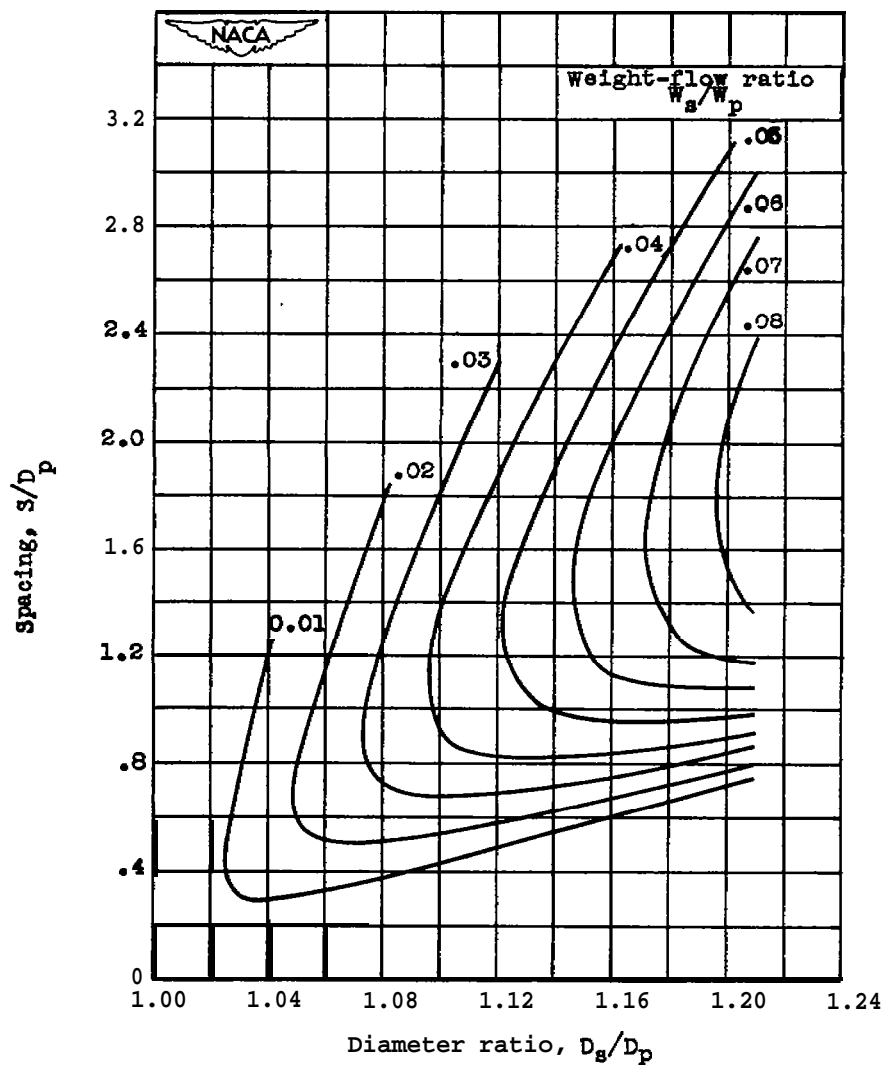
(a) Secondary pressure ratio  $P_s/P_0$ , 0.925; primary pressure ratio  $P_p/P_0$ , 1.4.

Figure 11. - Variation of spacing with diameter ratio for constant weight-flow ratios and constant pressure ratios.



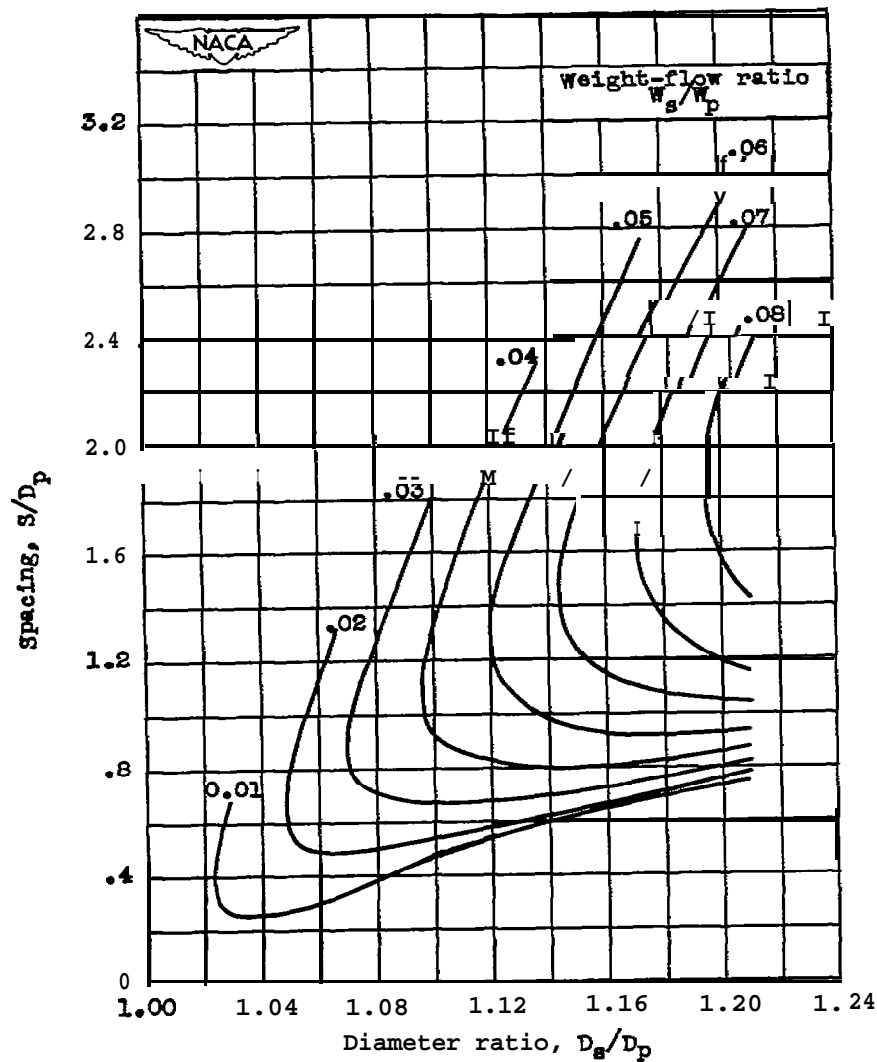
(a) Continued. Secondary pressure ratio  $P_s/P_0$ , 0.926; primary pressure ratio  $P_p/P_0$ , 1.6.

Figure 11. - Continued. Variation of spacing with diameter ratio for constant weight-flow ratios and constant pressure ratios.



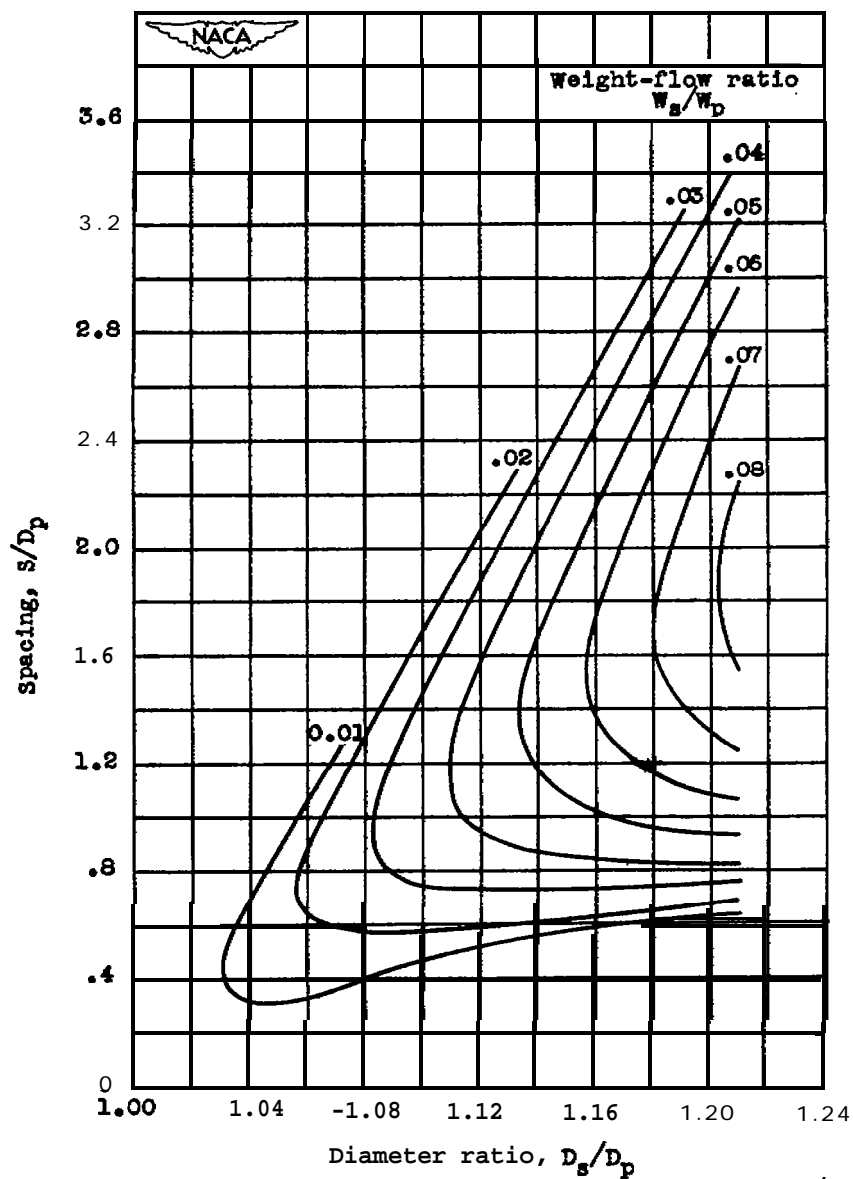
(a) Continued. Secondary pressure ratio  $P_s/P_0$ , 0.925; primary pressure ratio  $P_p/P_0$ , 1.8.

Figure 11. - Continued. Variation of spacing with diameter ratio for constant weight-flow ratios and constant pressure ratios.



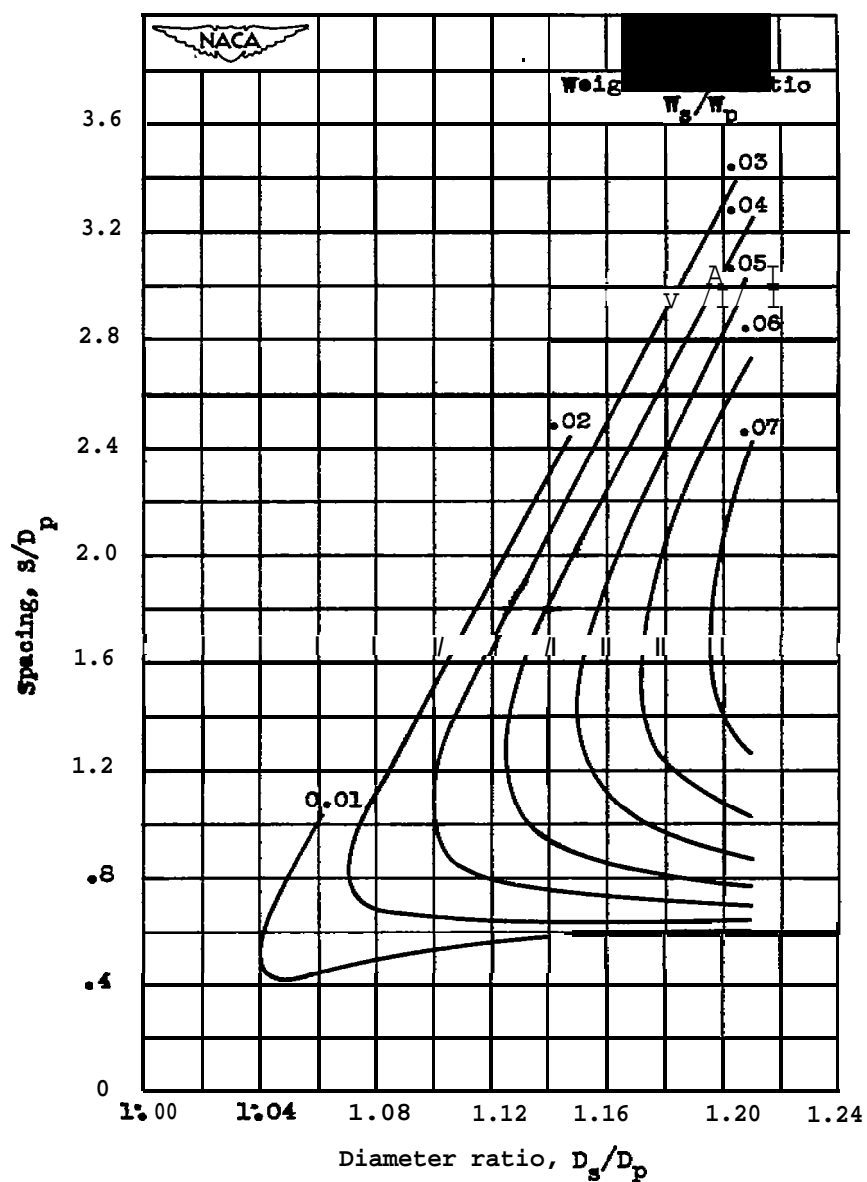
(a) Continued. Secondary pressure ratio  $P_s/P_0$ , 0.925; primary pressure ratio  $P_p/P_0$ , 2.0.

Figure 11. - continued. variation of spacing with diameter ratio for constant weight-flow ratios and constant pressure ratios.



(a) Continued. Secondary pressure ratio  $P_s/P_0$ , 0.225; primary pressure ratio  $P_p/P_0$ , 2.2.

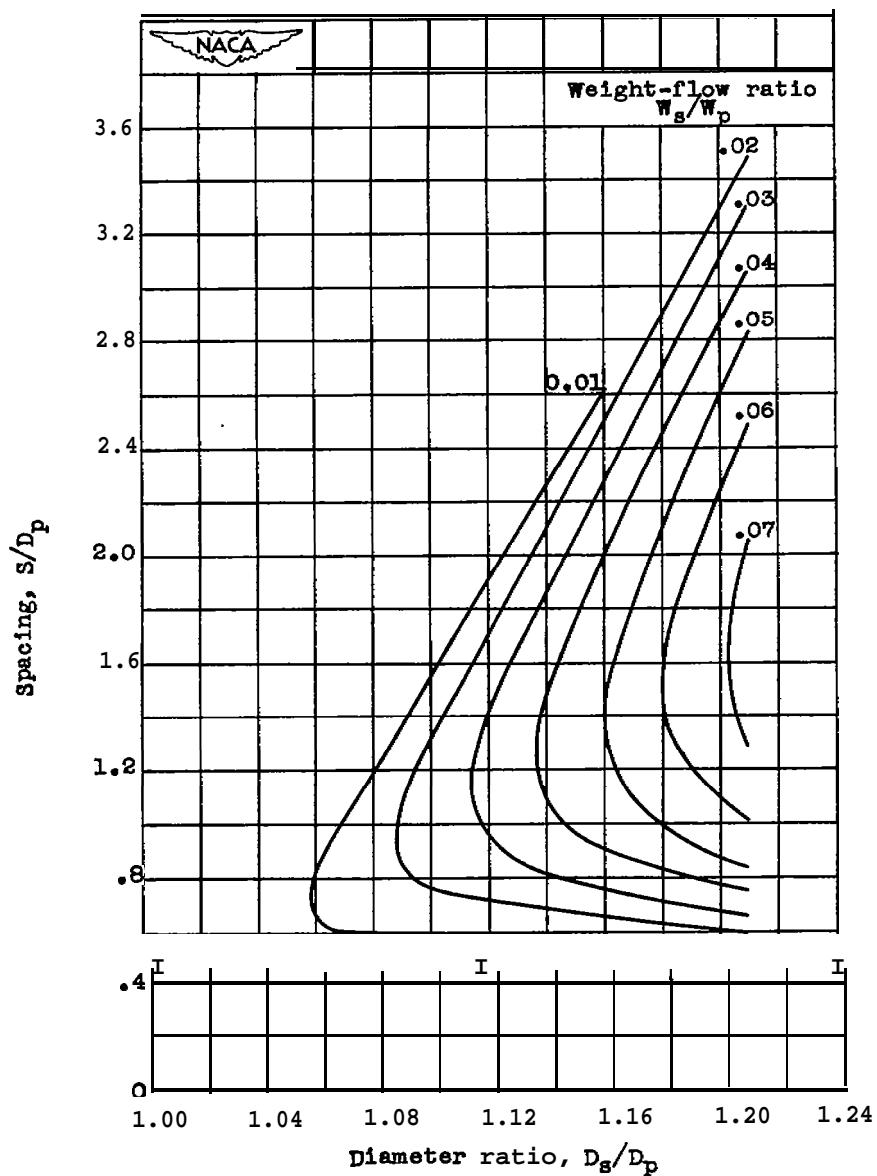
Figure 11. - continued. Variation of spacing with diameter ratio for constant weight-flow ratios and constant pressure ratios.



(a) Continued. secondary pressure ratio  $P_s/P_0$ ,  
0.925; primary pressure ratio  $P_p/P_0$ , 2.4.

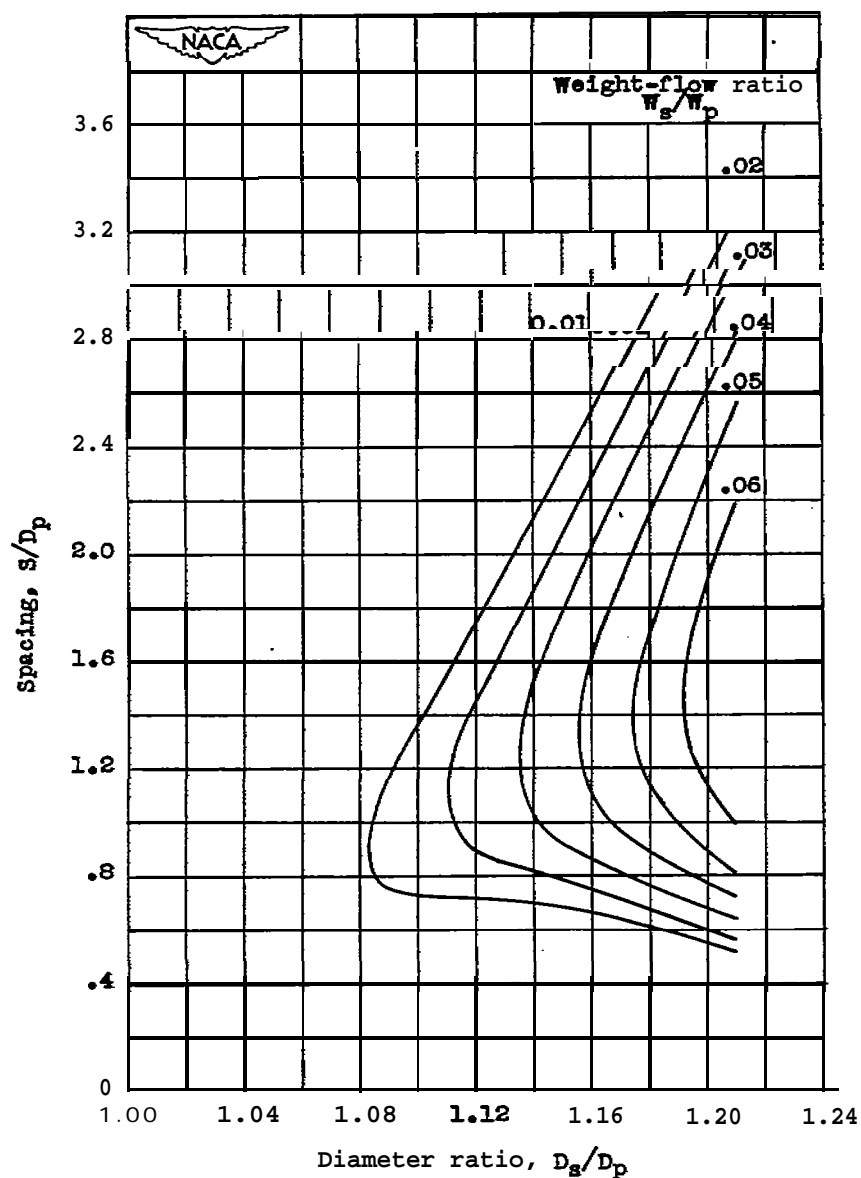
Figure 11. - Continued. Variation of spacing with diameter ratio for constant weight-flow ratios and constant pressure ratios.





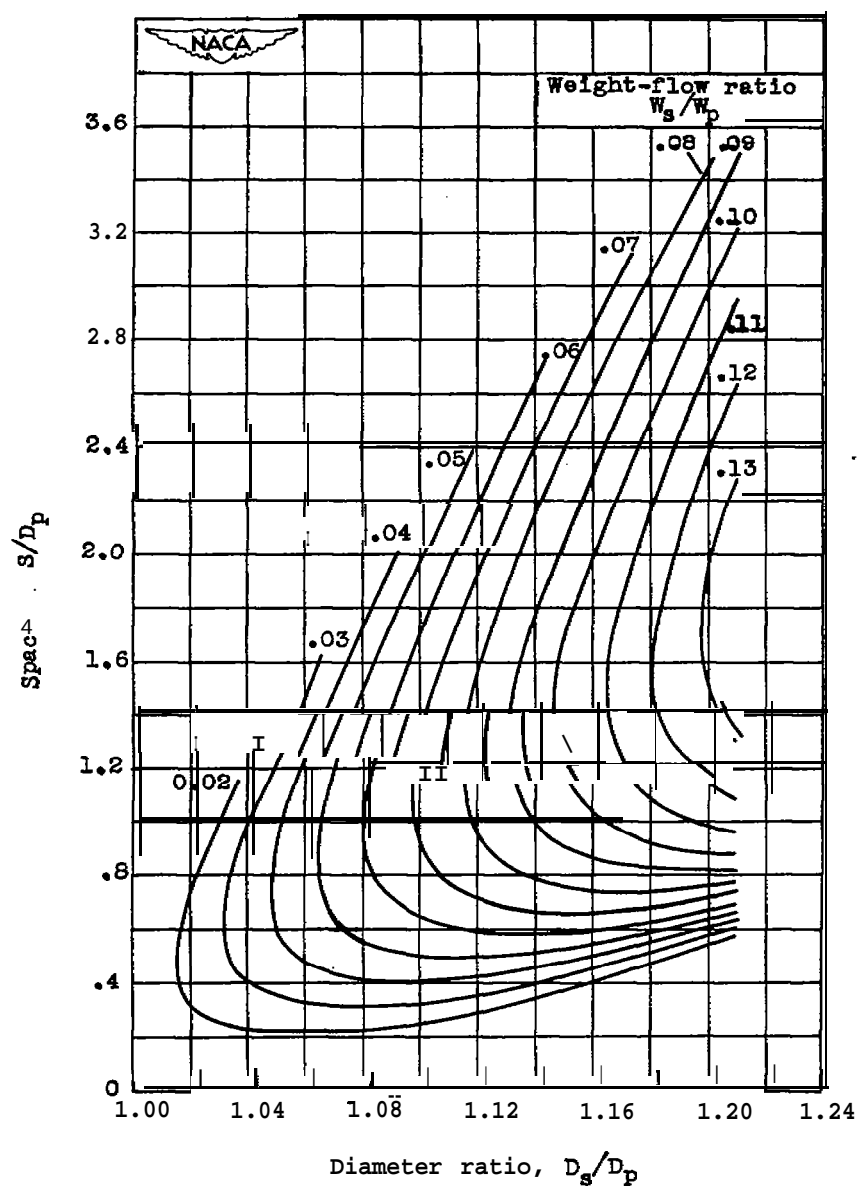
(a) Continued. Secondary pressure ratio  $P_s/P_0$ , 0.925; primary pressure  $P_p/P_0$ , 2.6.

Figure 11. - Continued. Variation of spacing with diameter ratio for constant weight-flow ratios and constant pressure ratios.



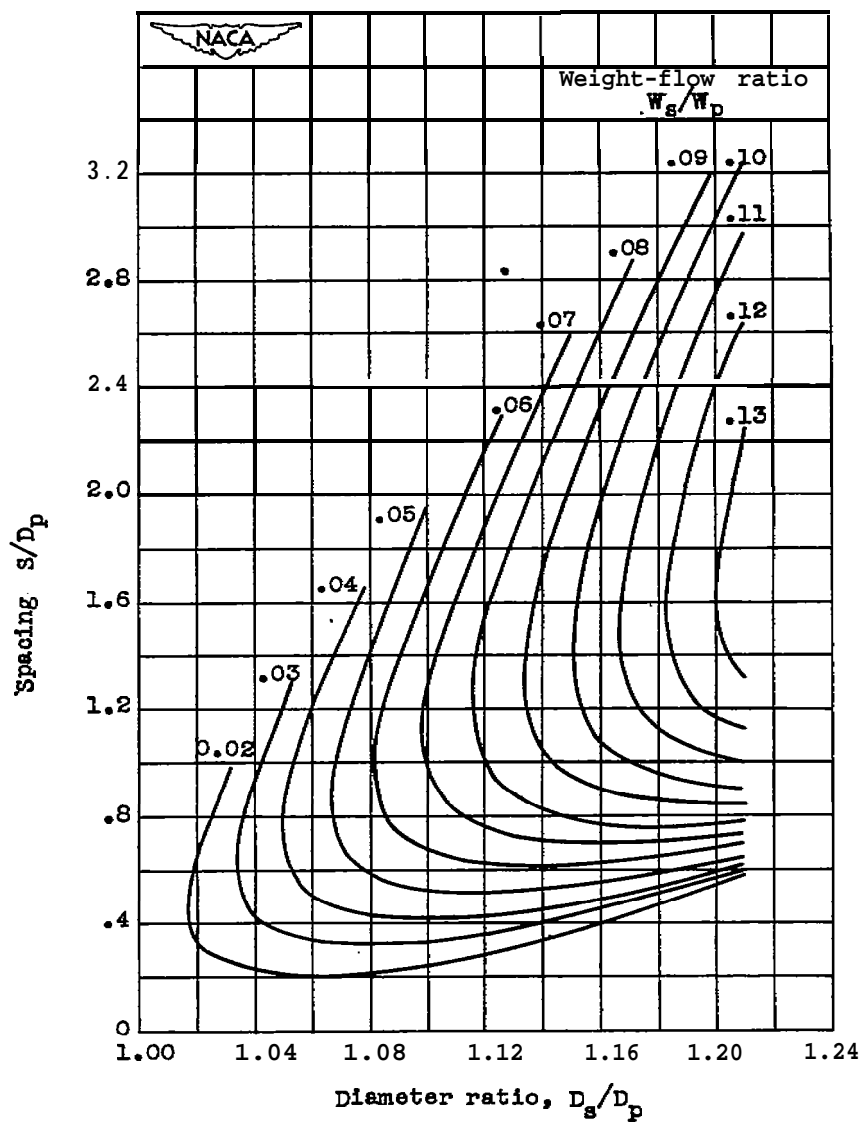
(a) Concluded. secondary pressure ratio  $P_s/P_0$ , 0.925; primary pressure  $P_p/P_0$ , 2.8.

Figure 11. - Continued. Variation of spacing with diameter ratio for constant weight-flow ratios and constant pressure ratios.



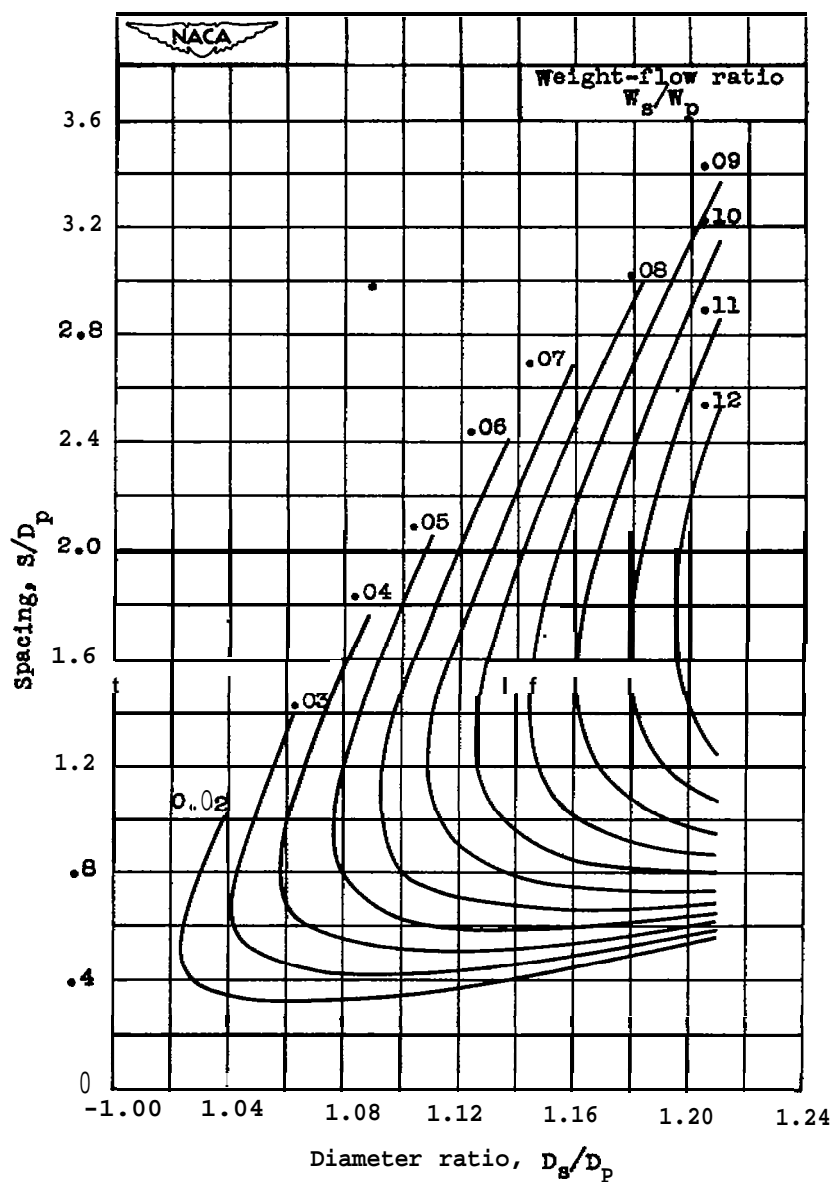
(b) Secondary pressure ratio  $P_s/P_0$ , 0.985;  
primary pressure ratio  $P_p/P_0$ , 1.4.

Figure 11. - continued. Variation of spacing with diameter ratio for constant weight-flow ratios and constant pressure ratios.



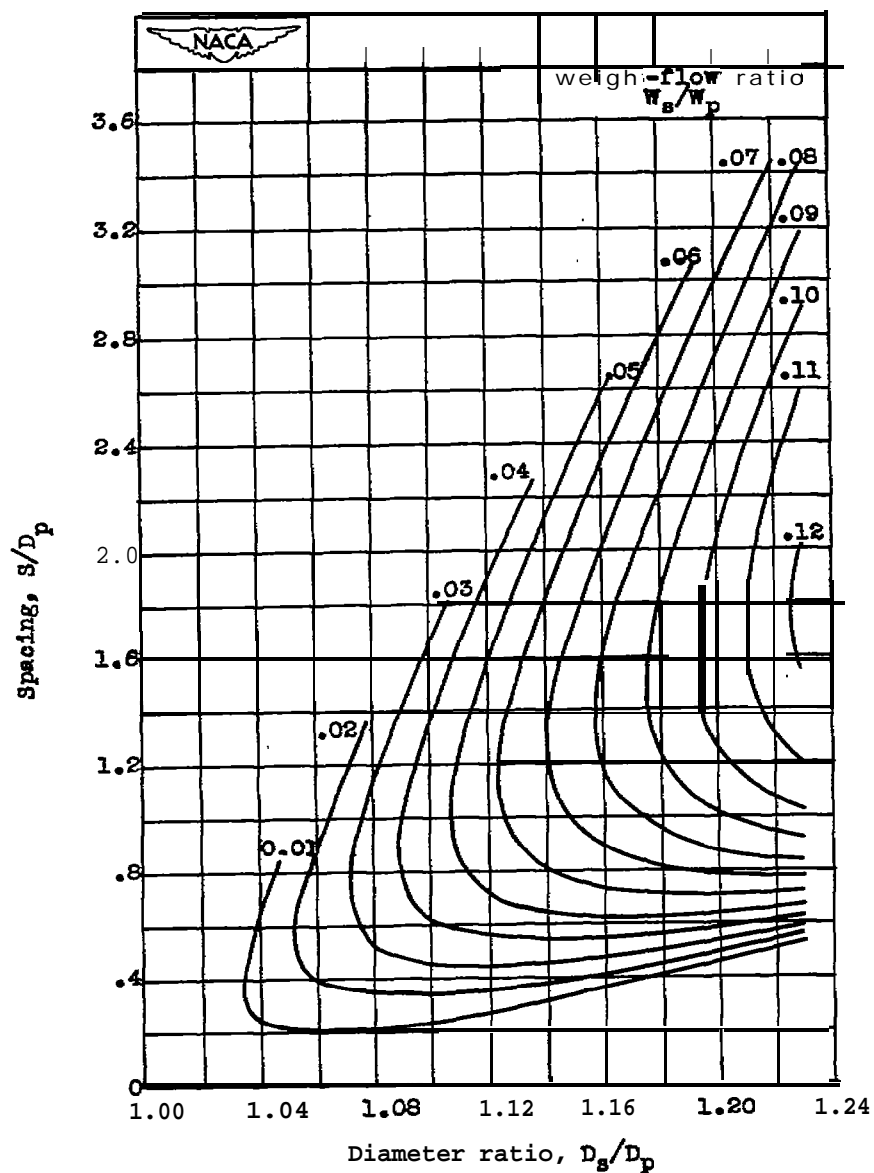
(b) Continued. Secondary pressure ratio  $P_s/P_0$ , 0.085; primary pressure ratio  $P_p/P_0$ , 1.6.

Figure 11. - Continued. Variation of spacing with diameter ratio for constant weight-flow ratios and constant pressure ratios.



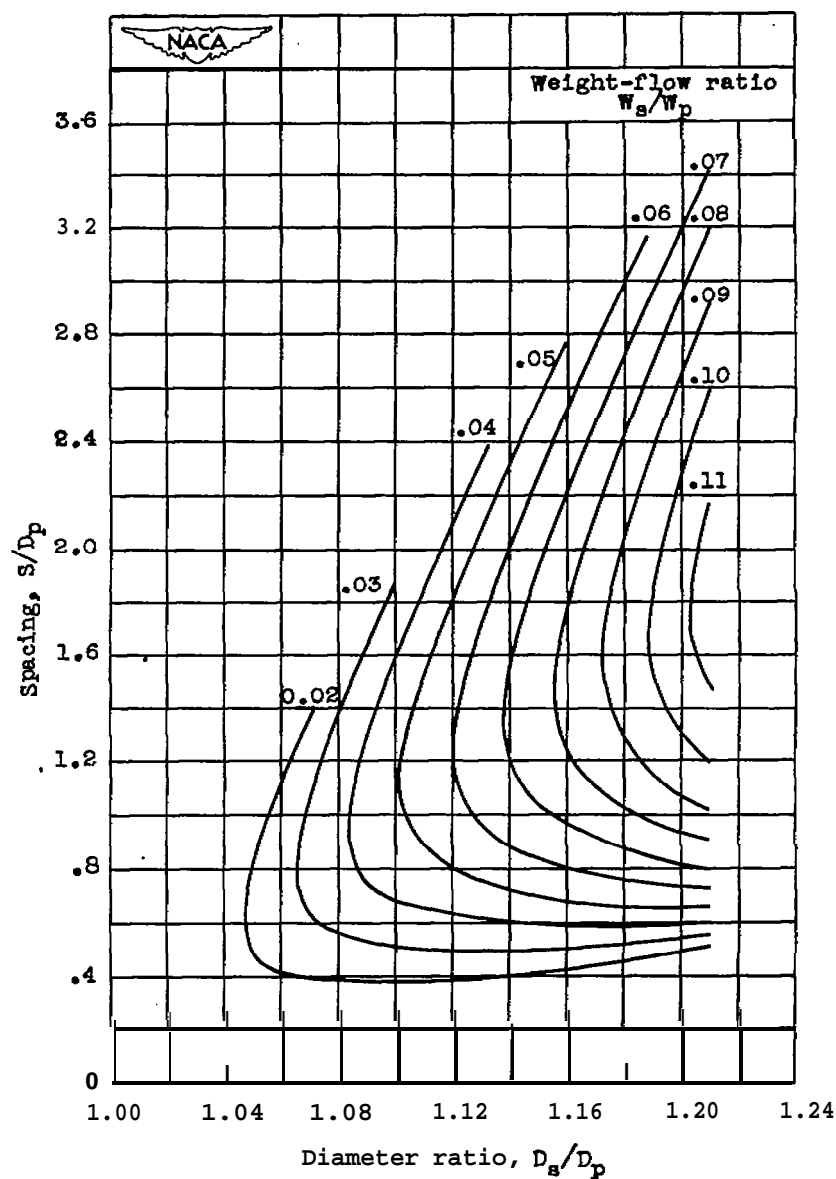
(b) Continued. secondary pressure ratio  $P_s/P_0$ , 0.985; primary pressure ratio  $P_p/P_0$ , 1.8.

Figure 11. - Continued. Variation of spacing with diameter ratio for constant weight-flow ratios and constant pressure ratios.



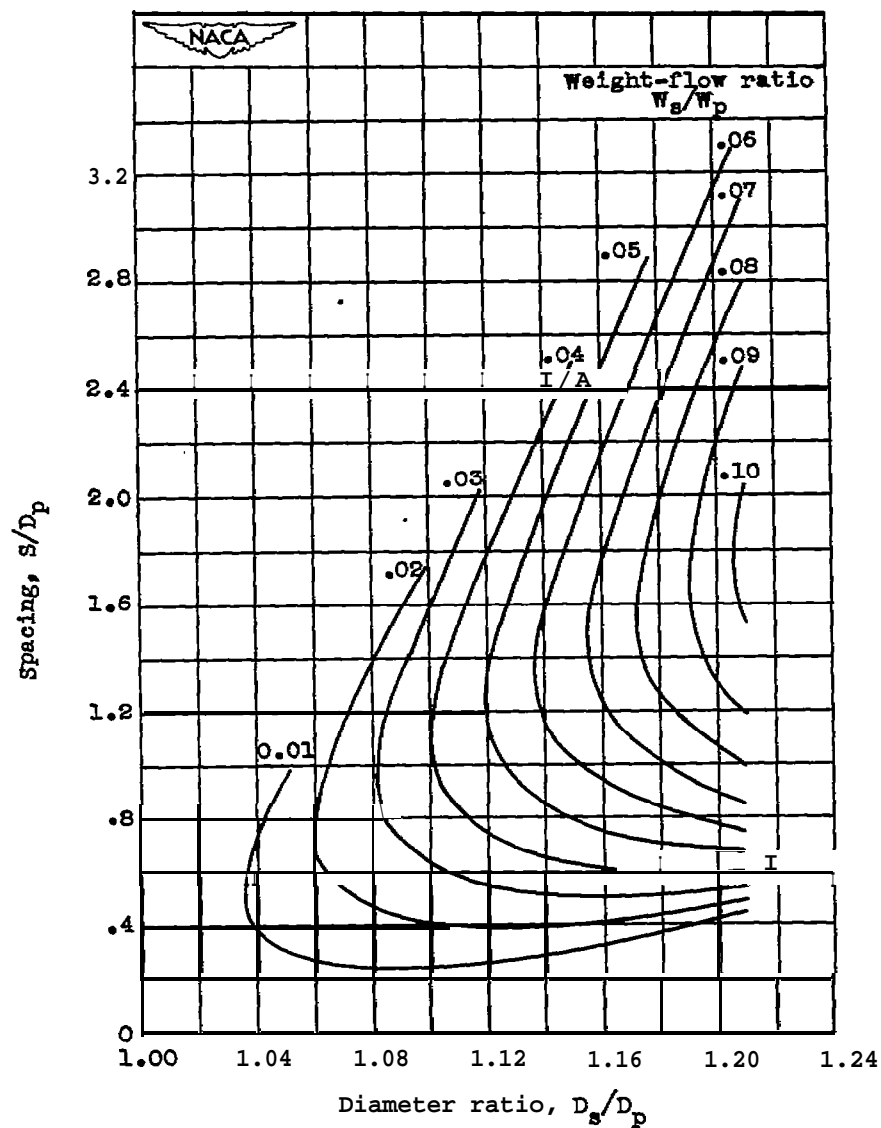
(b) Continued. Secondary pressure ratio  $P_s/P_0$ , 0.986; primary pressure ratio  $P_p/P_0$ , 2.0.

Figure 11. - Continued. variation of spacing with diameter ratio for constant weight-flow ratios and constant pressure ratios.



(b) continued. Secondary pressure ratio  $P_s/P_0$ , 0.985; primary pressure ratio  $P_p/P_0$ , 2.2.

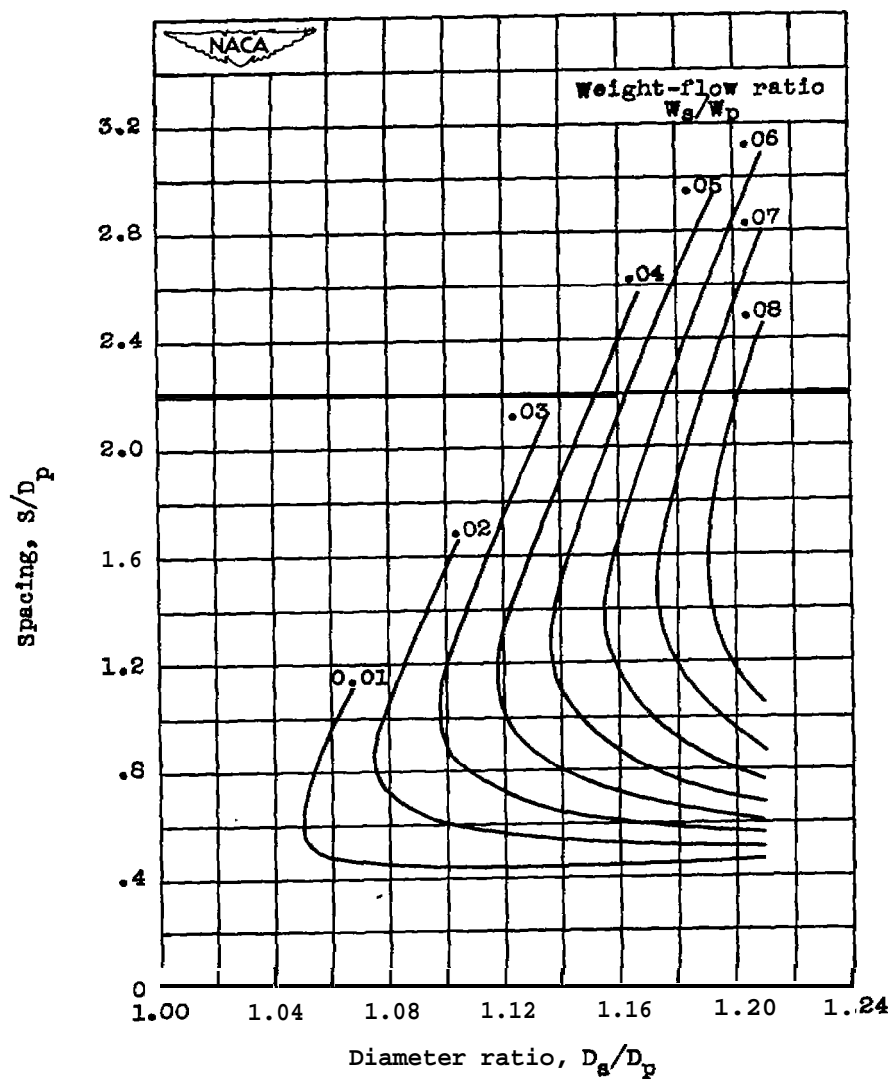
Figure 11. - Continued. Variation of spacing with diameter ratio for constant weight-flow ratios and constant pressure ratios.



(b) Continued. secondary pressure ratio  $P_s/P_0$ , 0.985; primary pressure ratio  $P_p/P_0$ , 2.4.

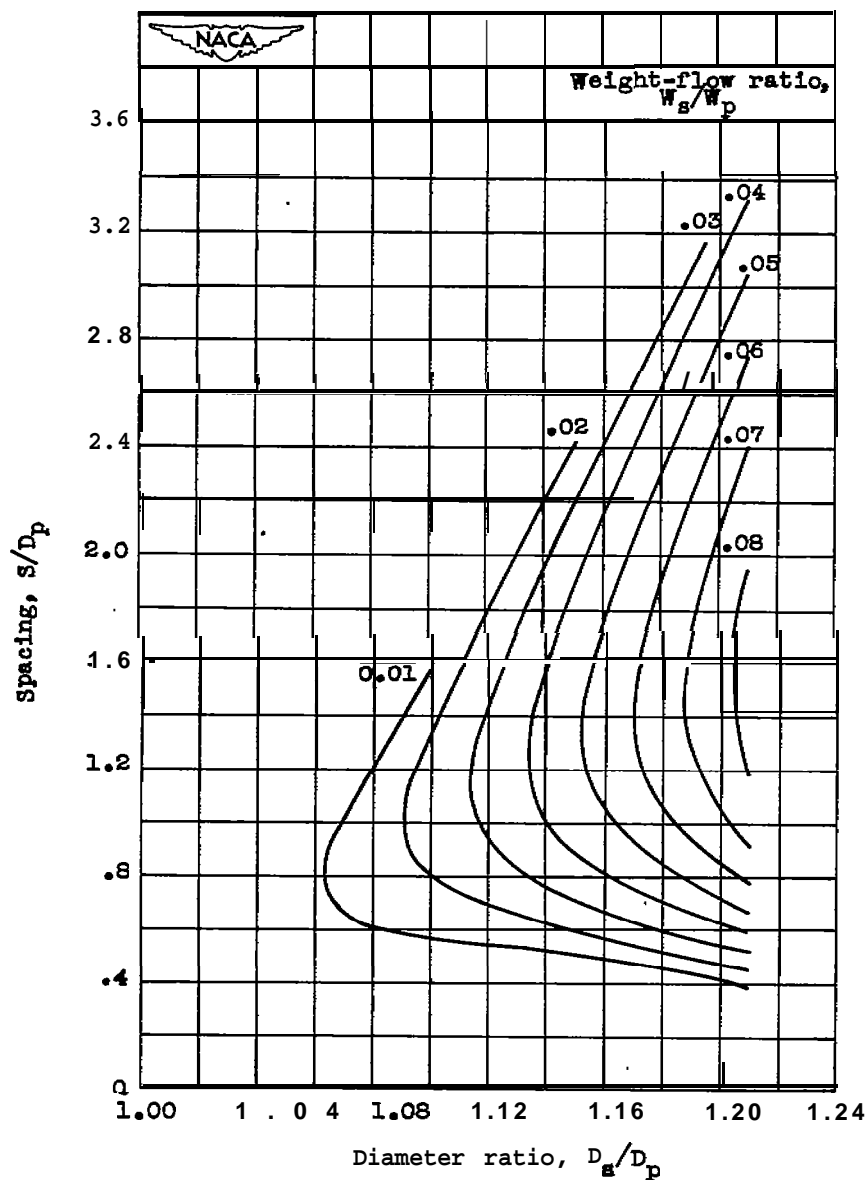
Figure 11. - Continued. Variation of spacing with diameter ratio for constant weight-flow ratios and constant pressure ratios.





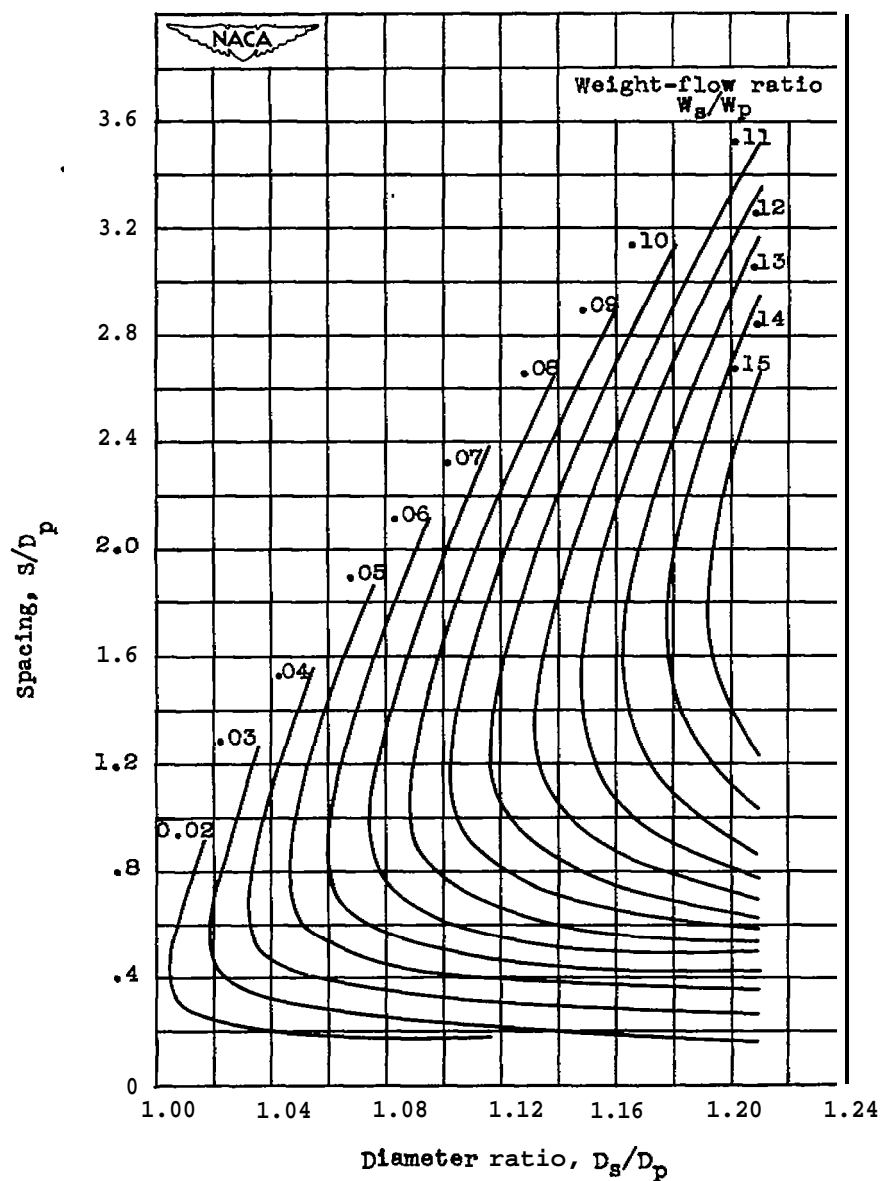
(b) Continued. Secondary pressure ratio  $P_s/P_0$ , 0.985; primary pressure ratio  $P_p/P_0$ , 2.6.

Figure 11. - Continued. Variation of spacing with diameter ratio for constant weight-flow ratios and constant pressure ratios.



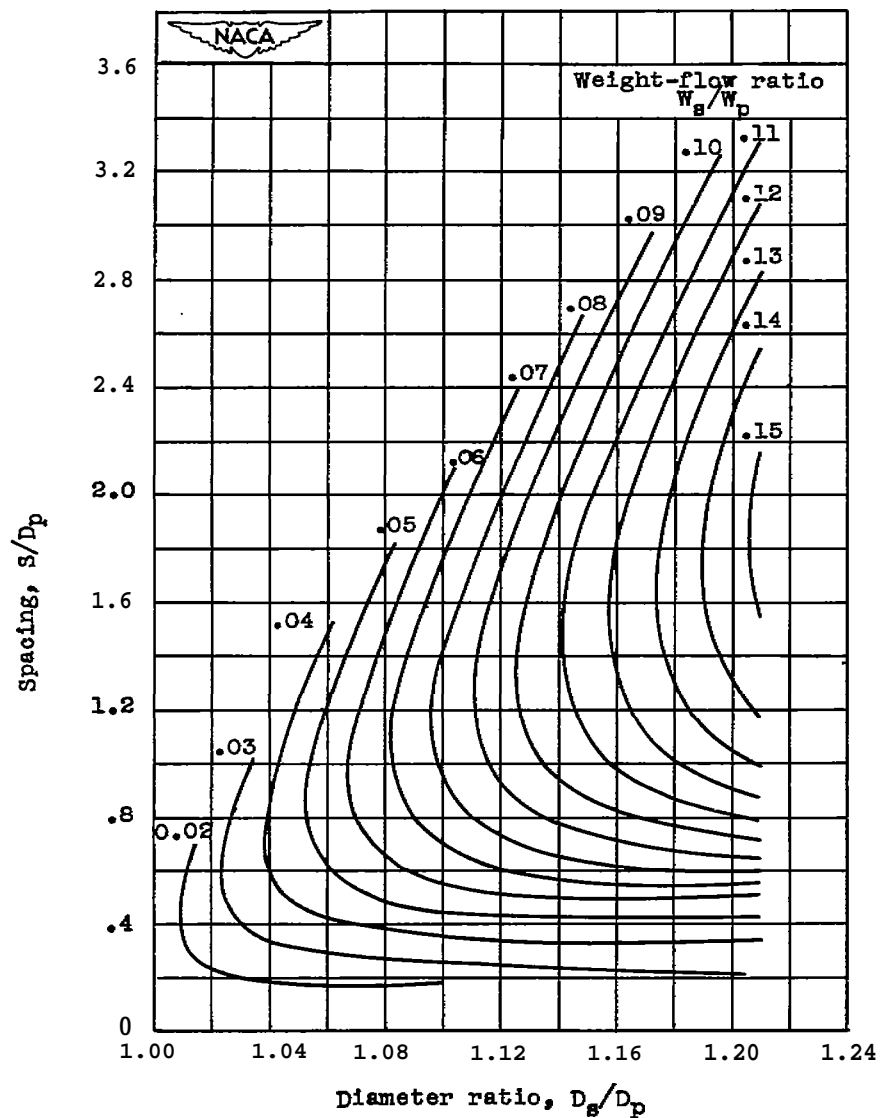
(b) Concluded. Secondary pressure ratio  $P_s/P_0$ , 0.986; primary pressure ratio  $P_p/P_0$ , 2.8.

Figure 11. - Continued. Variation of spacing with diameter ratio for constant weight-flow ratios and constant pressure ratios.



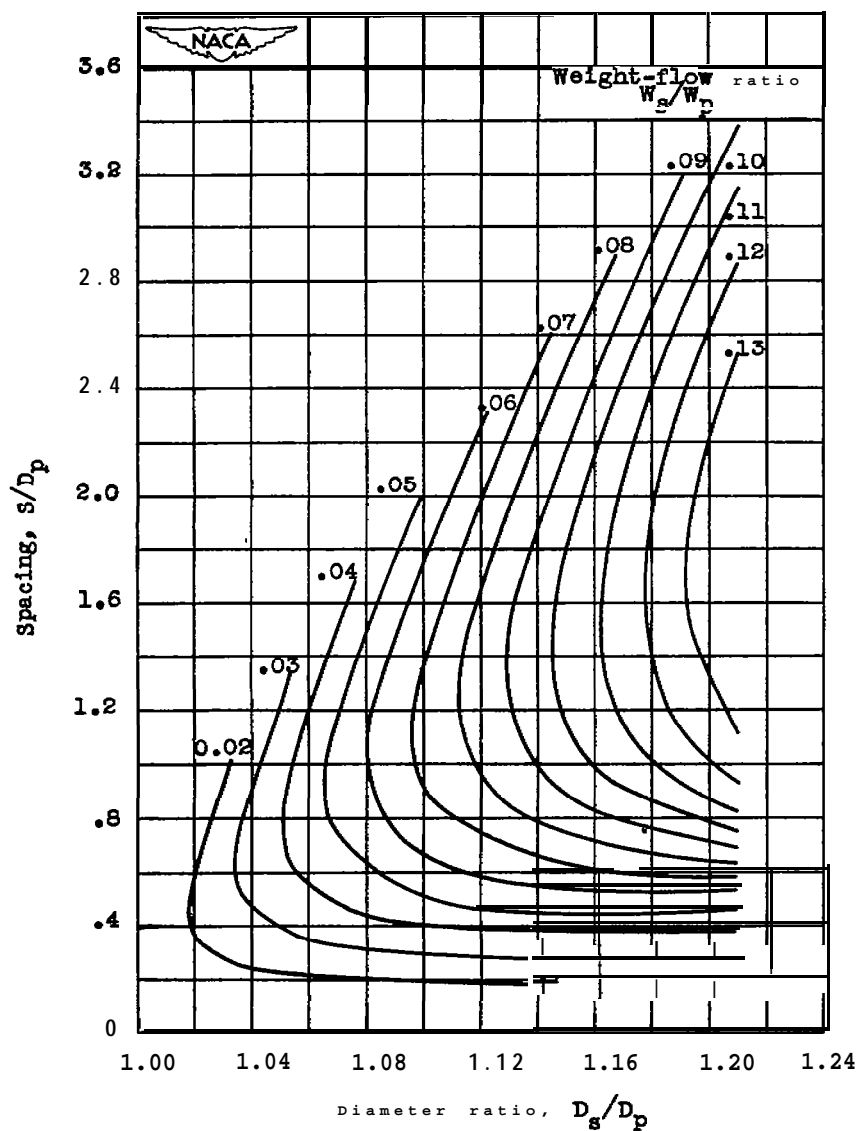
(c) Secondary pressure ratio  $P_s/P_0$ , 1.000; primary pressure ratio  $P_p/P_0$ , 1.4.

Figure 11. - Continued. Variation of spacing with diameter ratio for constant weight-flow ratios and constant pressure ratios.



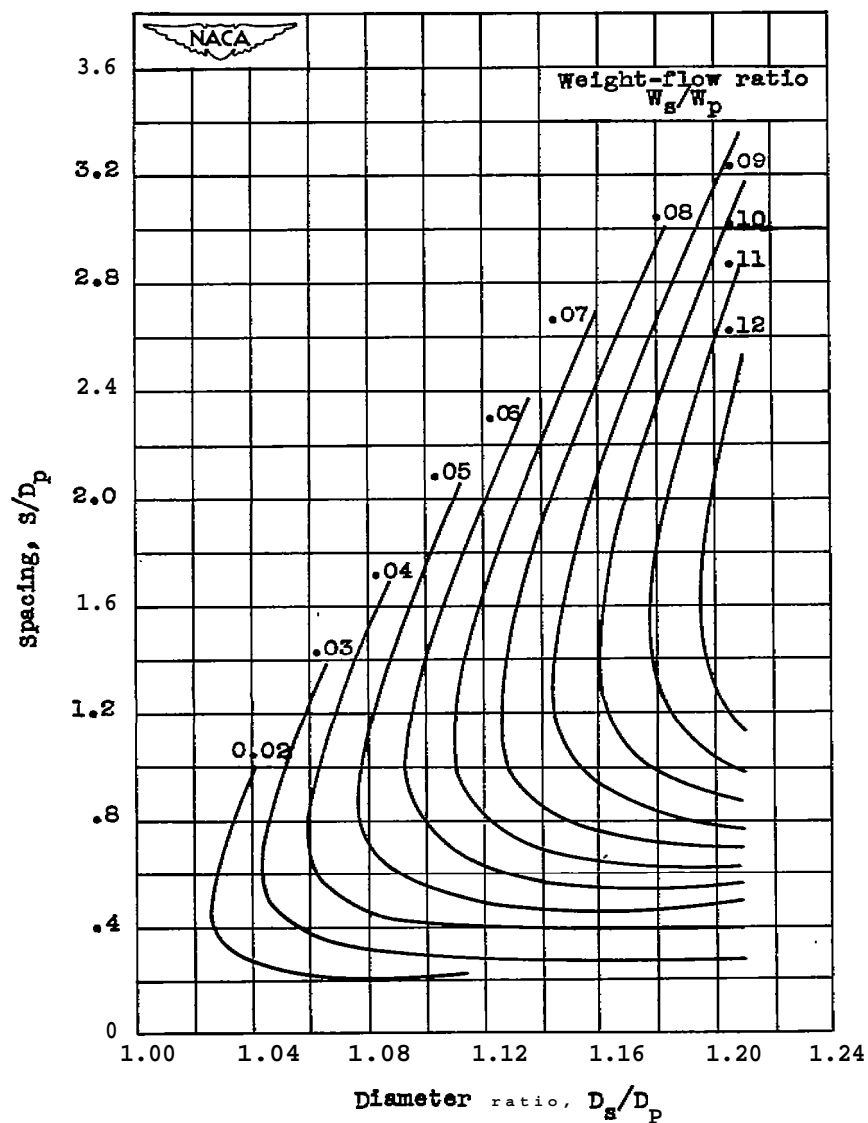
(c) continued. Secondary pressure ratio  $P_s/P_0$ , 1.000; primary pressure ratio  $P_p/P_0$ , 1.6.

Figure 11. - continued. Variation of spacing with diameter ratio for constant weight-flow ratios and constant pressure ratios.



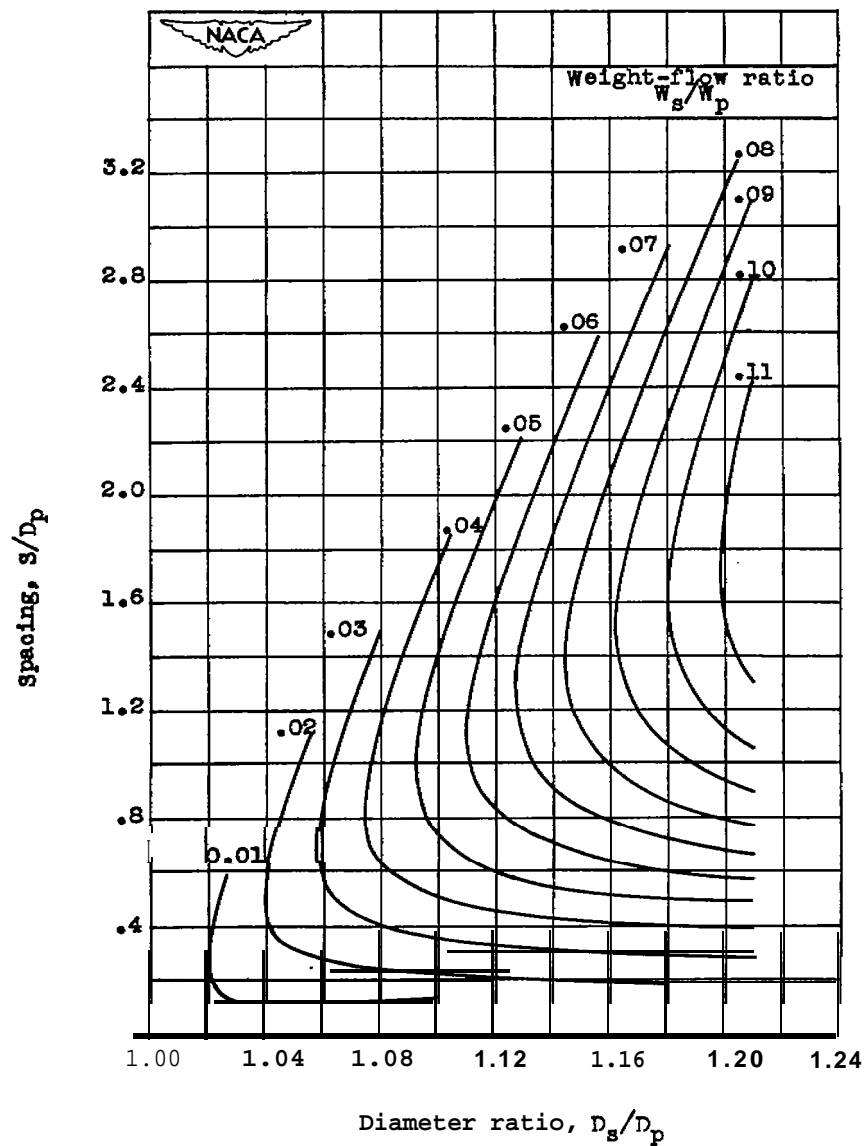
(c) Continued. Secondary pressure ratio  $P_s/P_0$ , 1.000; primary pressure ratio  $P_p/P_0$ , 1.8.

Figure 11. - Continued. Variation of spacing with diameter ratio for constant weight-flow ratios and constant pressure ratios.



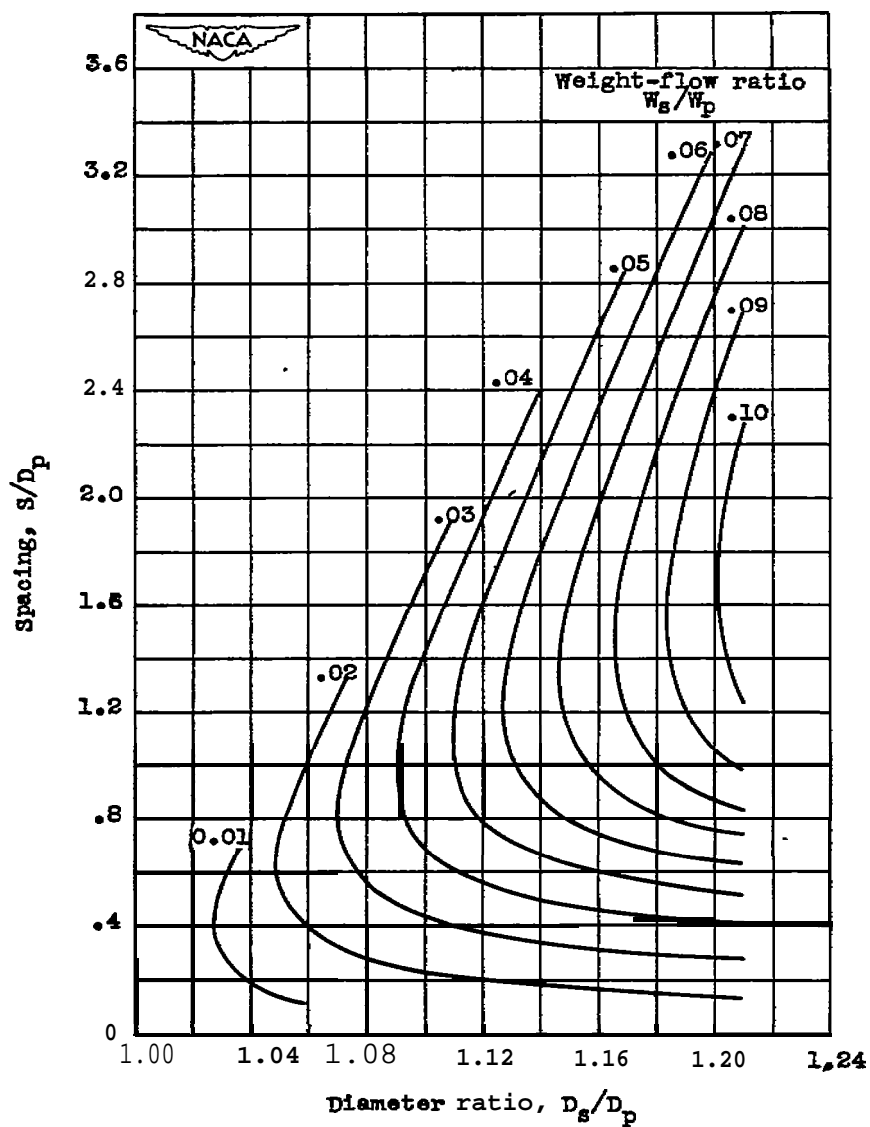
(c) Continued. Secondary pressure ratio  $P_s/P_0$ , . . .  
1.000; primary pressure ratio  $P_p/P_0$ , 2.0.

Figure 11. - continued. variation of spacing with diameter ratio for constant weight-flow ratios and constant pressure ratios.



[c] Continued. Secondary pressure ratio  $P_s/P_0$ , 1.000; primary pressure ratio  $P/P_0$ , 2.2.

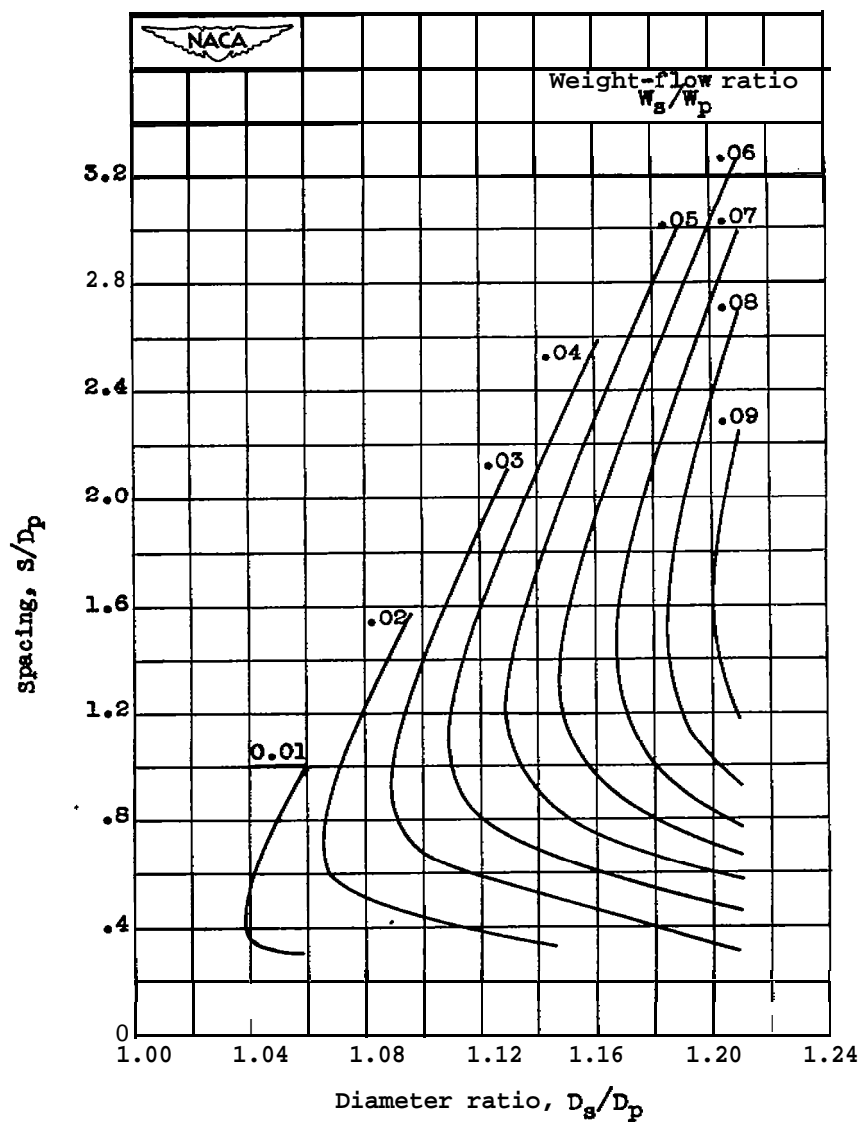
Figure 11. - Continued. Variation of spacing with diameter ratio for constant weight-flow ratios and constant pressure ratios.



(c) continued. Secondary-pressure ratio  $P_s/P_0$ , 1.000; primary pressure ratio  $P/P_0$ , 2.4,

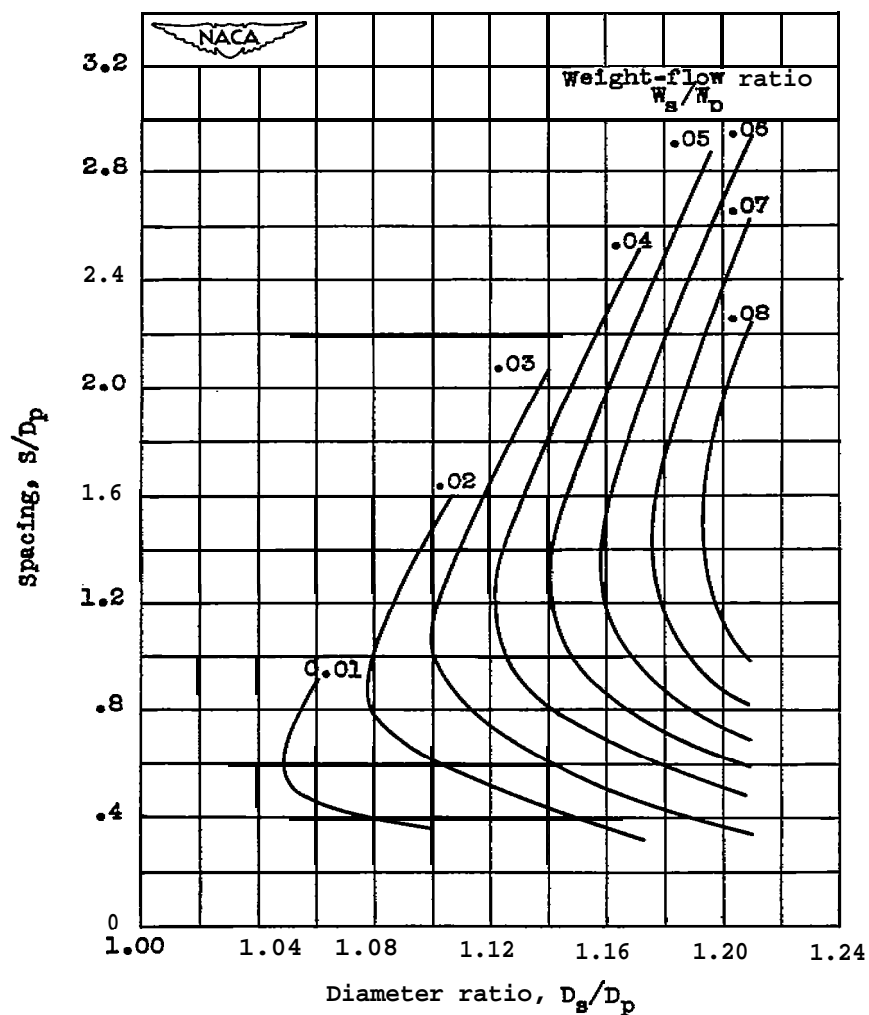
Figure 11. - continued. Variation of spacing with diameter ratio for constant weight-flow ratios and constant pressure ratios.





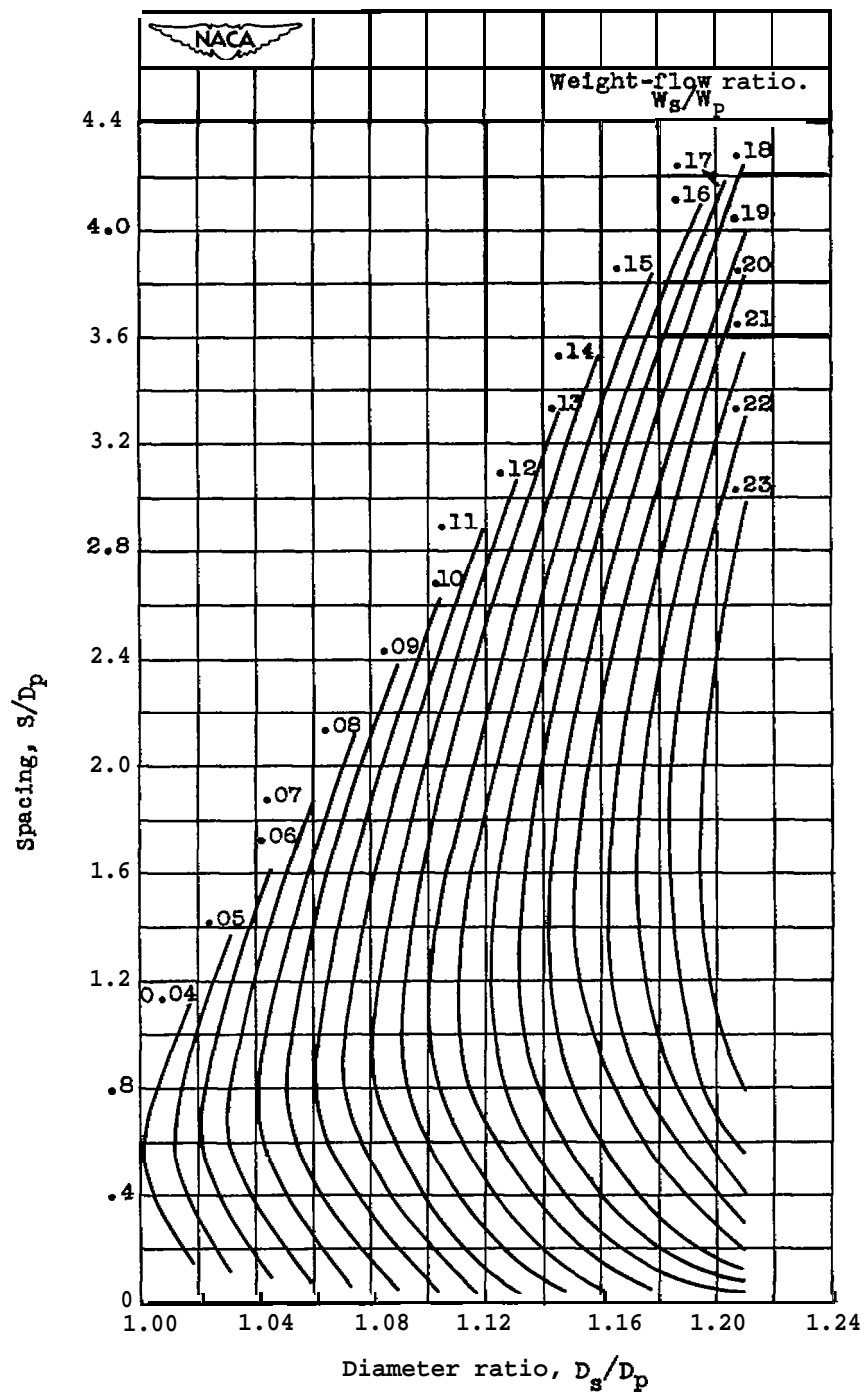
(c) Continued. Secondary pressure ratio  $P_s/P_0$ , 1.000; primary pressure ratio  $P_p/P_0$ , 2.6.

Figure 11. - continued. Variation of spacing with diameter ratio for constant weight-flow ratios and constant pressure ratios.



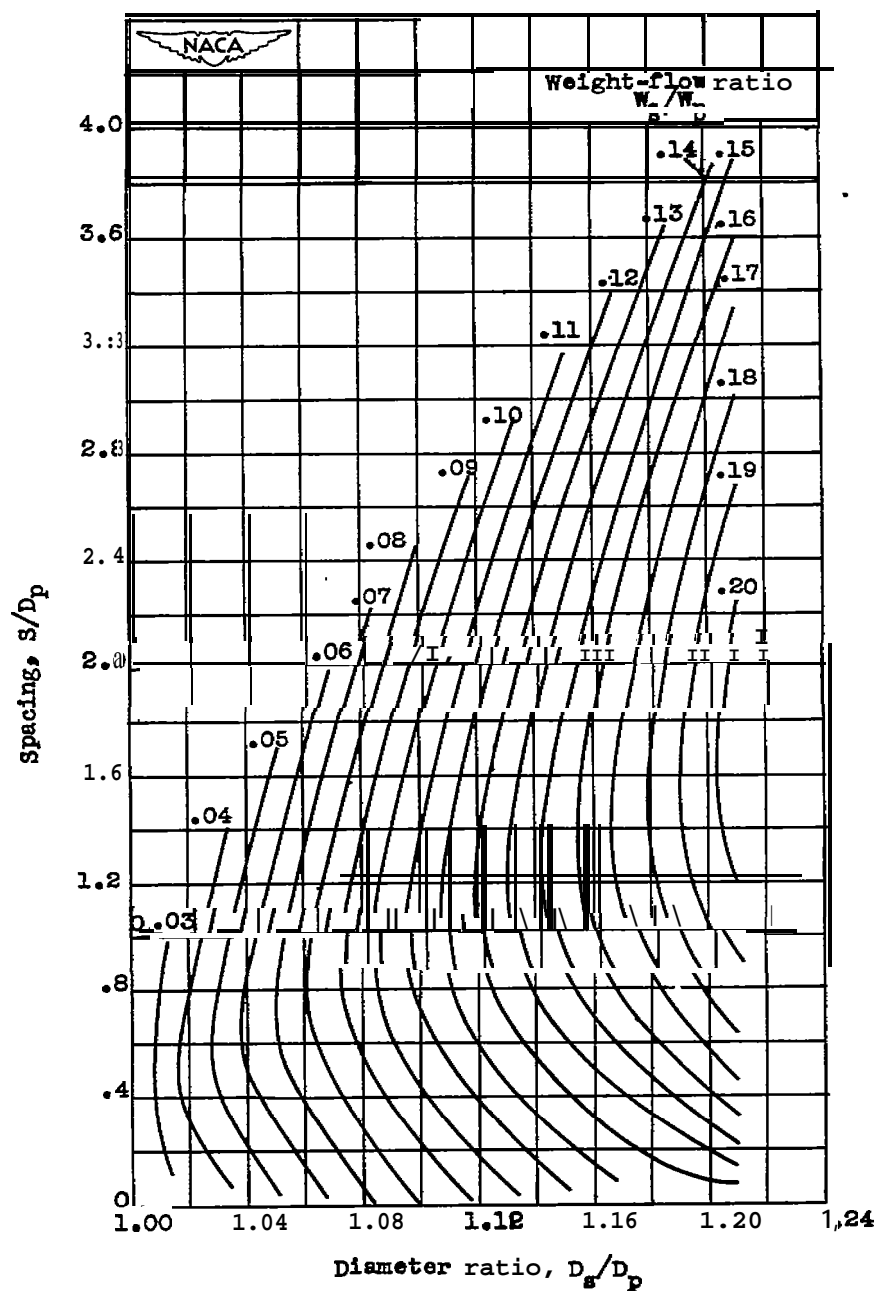
(c) concluded. secondary pressure ratio  $P/P_0$ , 1.000; primary pressure ratio  $P_p/P_0$ , 8.8.

Figure 11. - Continued. Variation of spacing with diameter ratio for constant weight-flow ratios and constant pressure ratios.



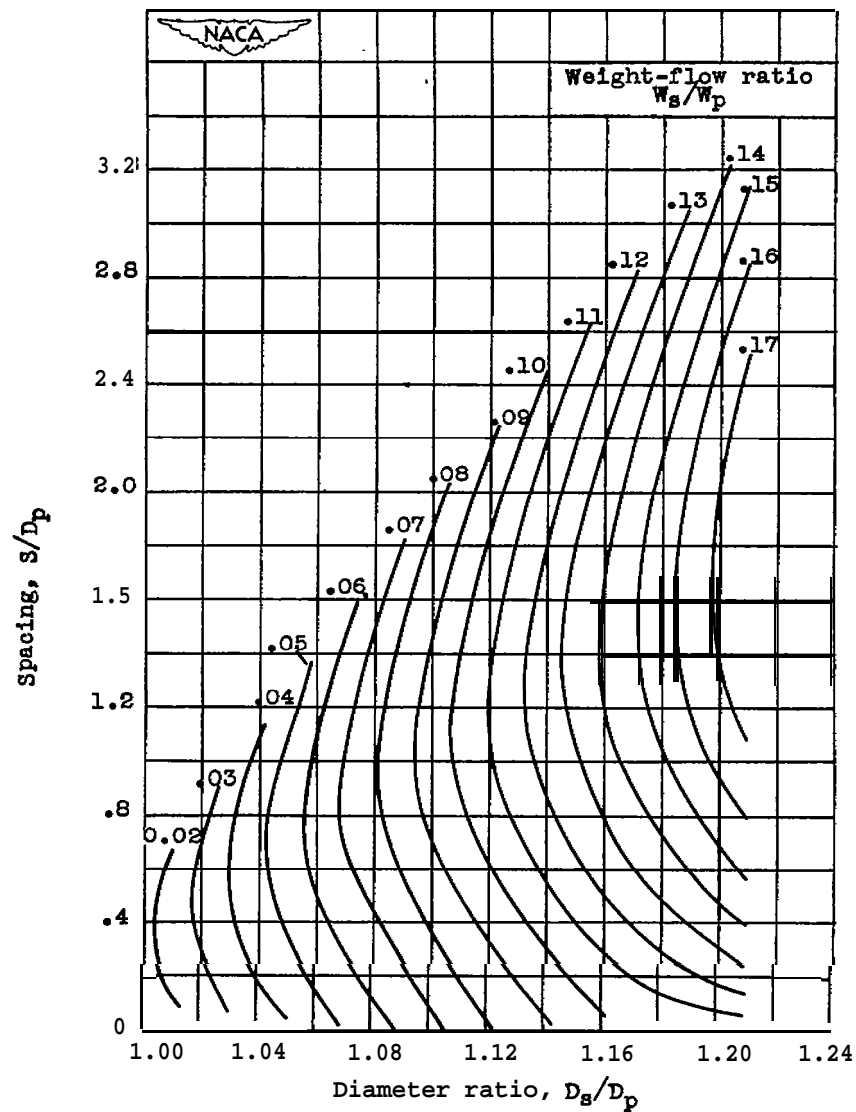
(d) secondary pressure ratio  $P_s/P_0$ , 1.050;  
primary pressure ratio  $P_p/P_0$ , 1.4.

Figure 11. - Continued. Variation of spacing with diameter ratio for constant weight-flow ratios and constant pressure ratios.



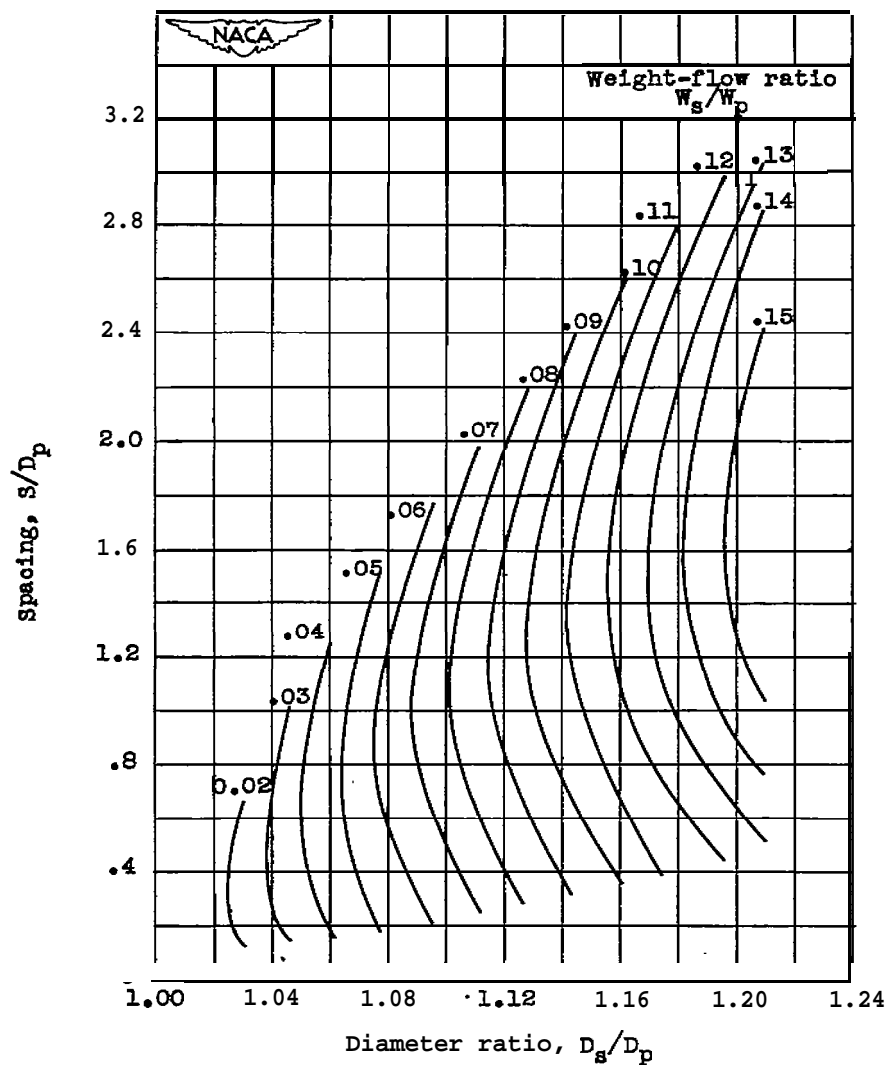
(d) continued. Secondary pressure ratio  $P_s/P_0$ , 1.050; primary pressure ratio  $P_p/P_0$ , 1.6.

Figure 11. - continued. Variation of spacing with diameter ratio for constant weight-flow ratios and constant pressure ratios.



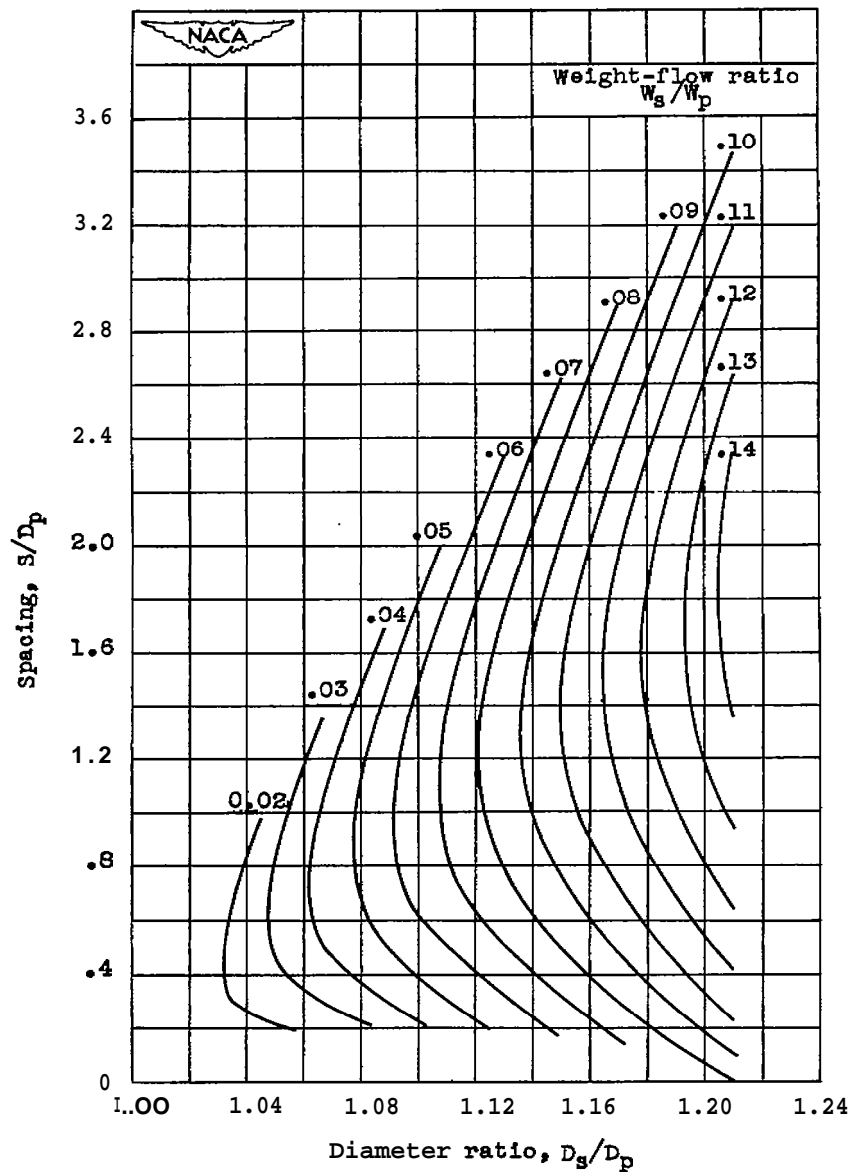
(d) continued. Secondary pressure ratio  
 $P_s/P_0$ , 1.050; primary pressure ratio  
 $P_p/P_0$ , 1.8.

Figure 11. - Continued. Variation of spacing with diameter ratio for constant weight-flow ratios and constant pressure ratios.



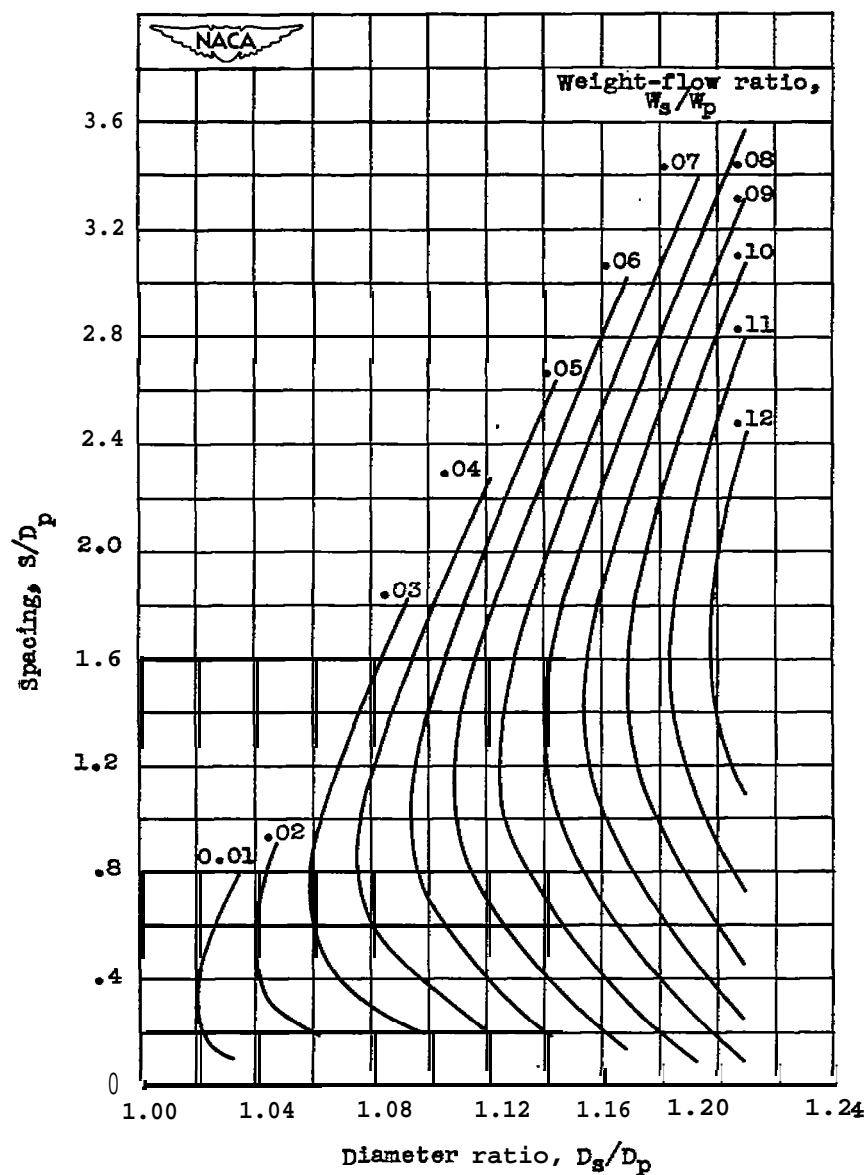
(d) Continued. *secondary pressure ratio*  
 $P_s/P_0$ , 1.050; *primary pressure ratio*  
 $P_p/P_0$ , 2.0.

Figure 11. - Continued. Variation of spacing with diameter ratio for constant weight-flow ratios and constant pressure ratios.



(d) Continued. Secondary pressure ratio  $P_s/P_0$ , 1.050; primary pressure ratio  $P_p/P_0$ , 2.2.

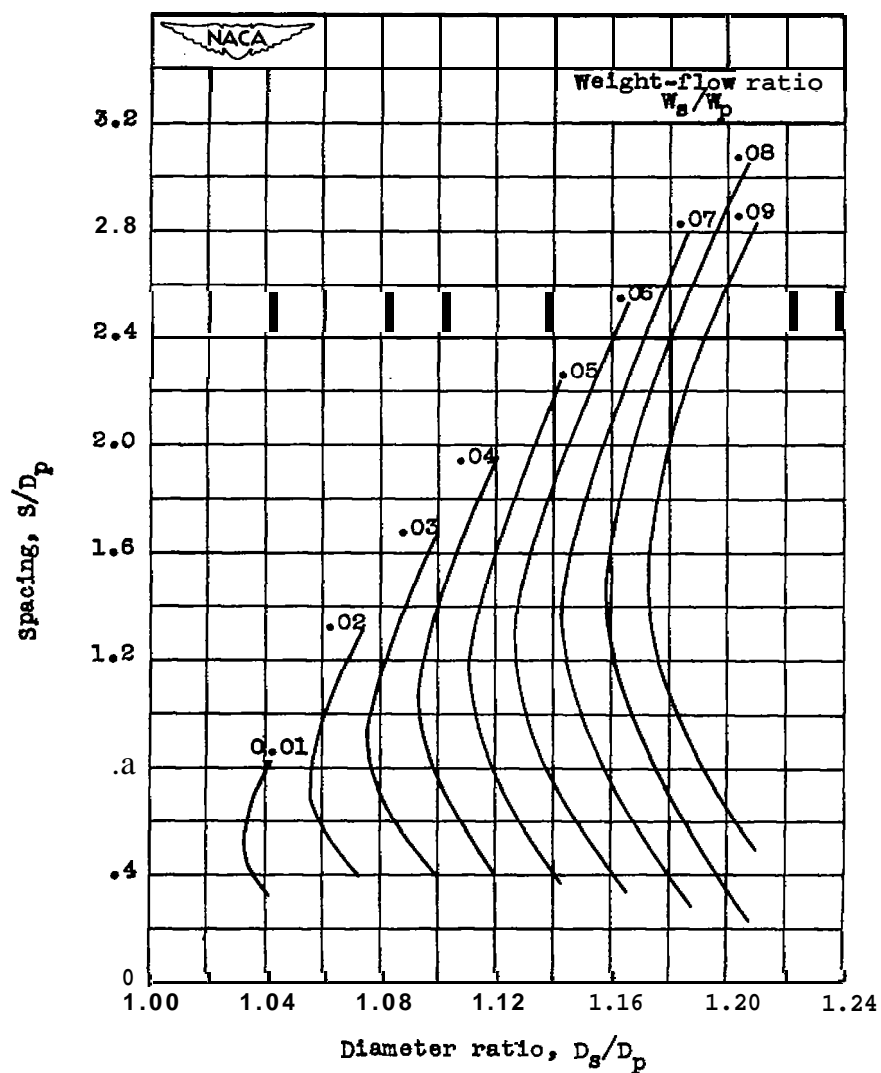
Figure 11. - Continued. variation of spacing with diameter ratio for constant weight-flow ratios and constant pressure ratios.



(d) Continued, Secondary pressure ratio  $P_s/P_0$ , 1.050; primary pressure ratio  $P_p/P_0$ , 2.4.

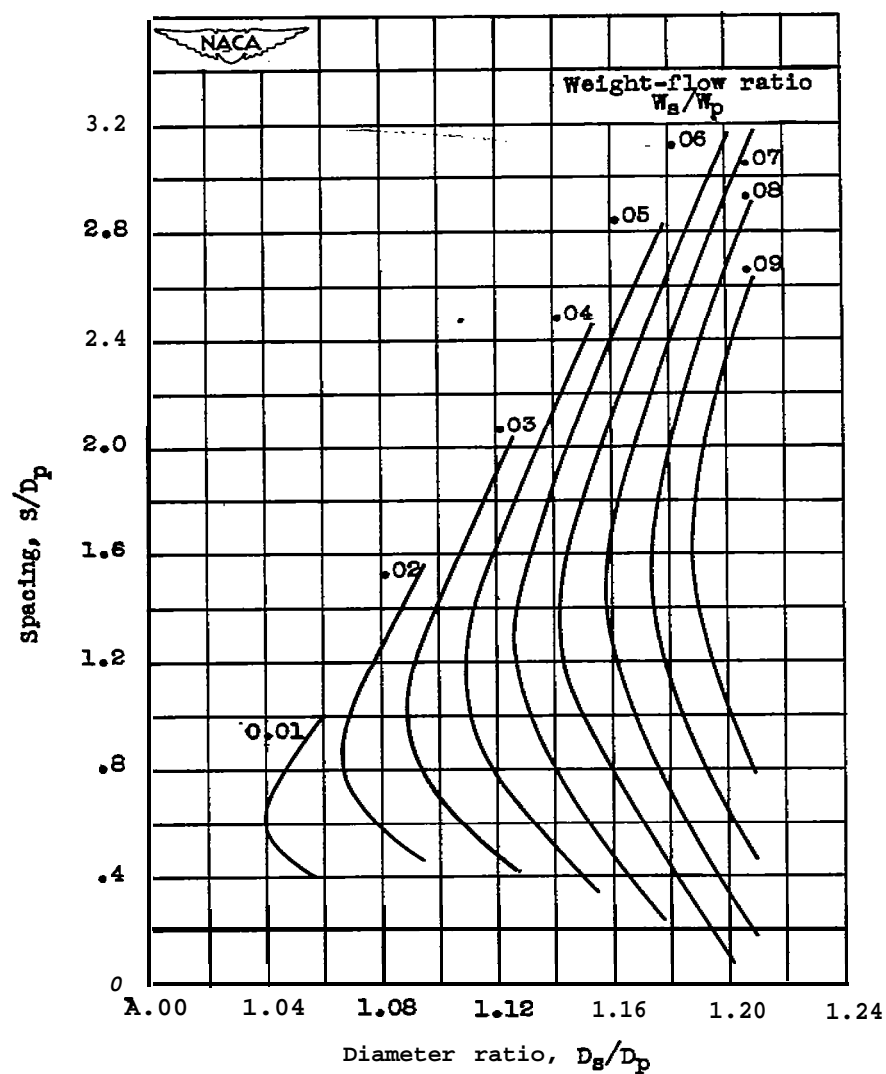
Figure 11. - Continued. variation of spacing with diameter ratio for constant weight-flow ratios and constant pressure ratios.





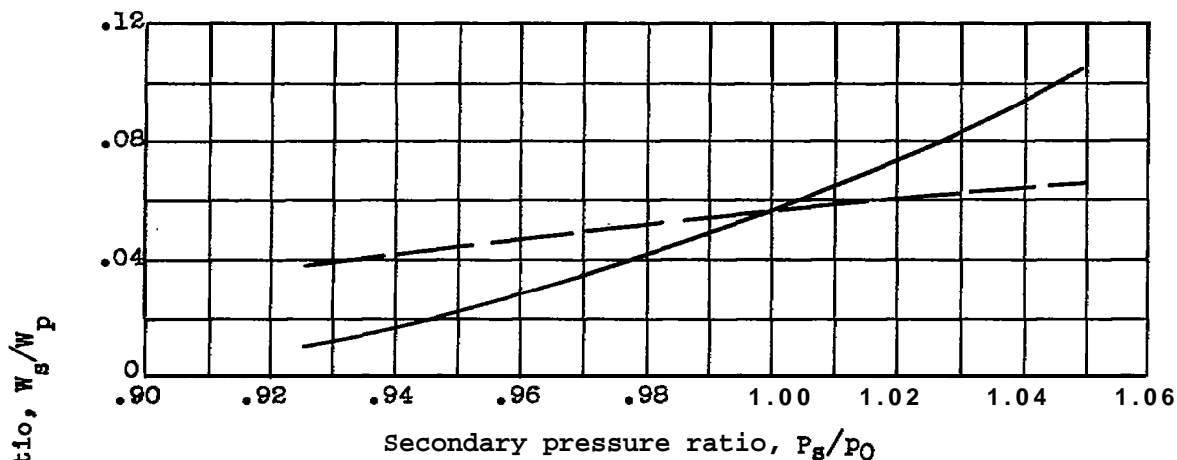
(d) continued. Secondary pressure ratio  $P_s/P_0$ , 1.050; primary pressure ratio  $P_p/P_0$ , 2.6.

Figure 11. - Continued. variation of spacing with diameter ratio for constant weight-flow ratios and constant pressure ratios.

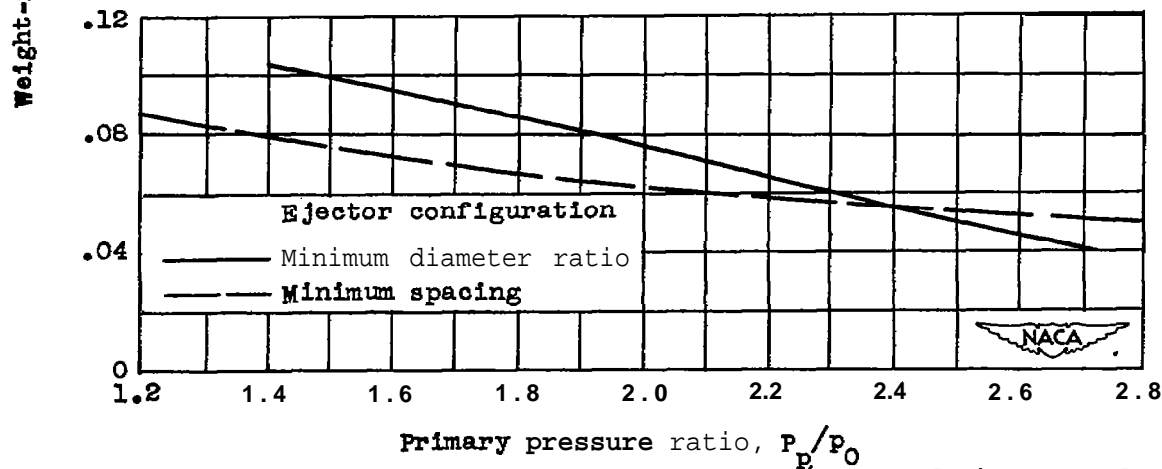


(d) Concluded. Secondary pressure ratio  $P_s/P_0$ , 1.050; primary pressure ratio  $P_p/P_0$ , 2.8.

Figure 11. - Concluded. Variation of spacing with diameter ratio for constant weight-flow ratios and constant pressure ratios.



(a) Variation of weight-flow ratio  $W_s/W_p$  at design primary pressure ratio  $P_p/P_0$  of 2.4.



(b) Variation of weight-flow ratio  $W_s/W_p$  at design secondary pressure ratio  $P_s/P_0$  of 1.0.

Figure 12. - Comparison of performance of minimum-diameter-ratio configuration with minimum-spacing configuration for variation of primary and secondary pressure from design pressure conditions